

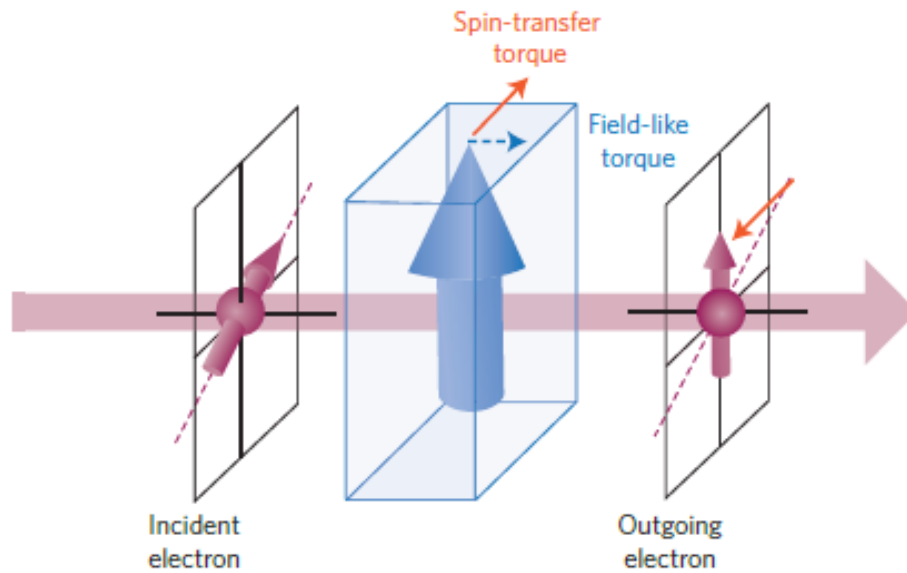
Spin transport in topological insulators

Yu-Ting Fanchiang
Department of Physics,
National Taiwan University

Outline

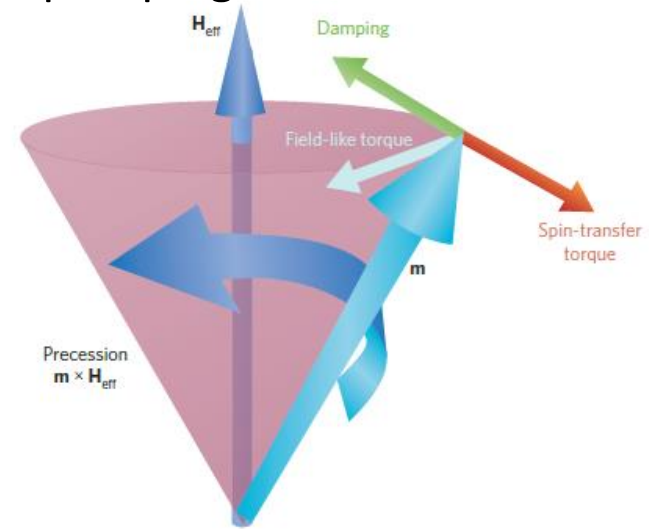
- Introduction to spin current and spin transfer torques
- Measuring spin Hall angle and IEE length
 - Spin pumping
 - Spin-torque ferromagnetic resonance (ST-FMR)
 - Modulation of magnetization damping (MOD)
- Spin transport in TIs: paper review

Spin transfer torques



Ferromagnetic resonance (FMR)

Spin pumping



LLG equation with torque terms:

$$\frac{\partial \mathbf{m}}{\partial t} = -\gamma \mathbf{m} \times H_{eff} + \alpha \mathbf{m} \times \frac{\partial \mathbf{m}}{\partial t} + \boldsymbol{\tau}$$

A. Brataas, et al., Nat. Mater. **11**, 372 (2012)

Damp-like torque:

$$-\frac{\gamma \hbar}{2eM_s V} \mathbf{m} \times (\mathbf{m} \times I_s)$$

Field-like torque:

$$-\frac{\gamma \hbar}{2eM_s V} \mathbf{m} \times I_s$$

Spin current

$$\mathbf{Q} = \mathbf{v} \otimes \mathbf{s}$$

$$= \frac{\hbar^2}{2m} \text{Im} \left(\psi^* \boldsymbol{\sigma} \otimes \nabla \psi \right)$$

For a spinor plane-wave wavefunction in x direction:

$$\psi = \frac{e^{ikx}}{\sqrt{\Omega}} \text{Im} \left(a |\uparrow\rangle + b |\downarrow\rangle \right)$$

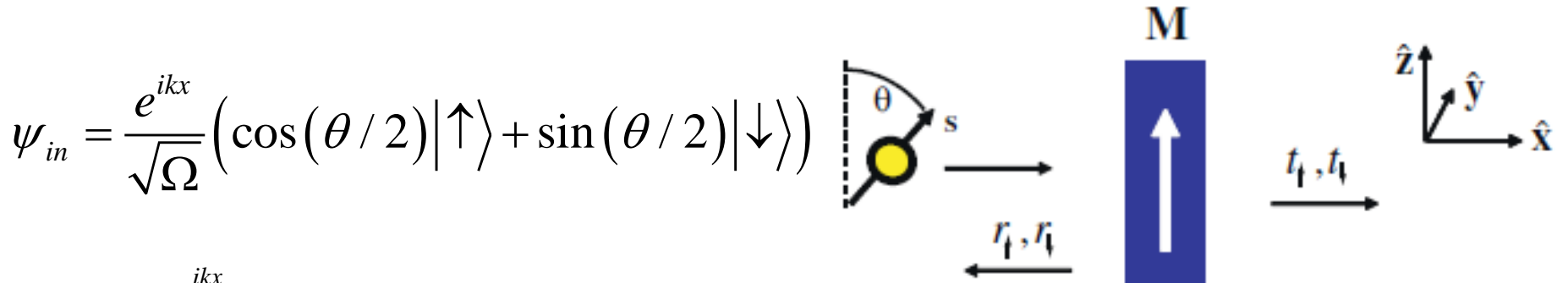
$$Q_{xx} = \frac{\hbar^2 k}{2m\Omega} 2 \text{Re} \left(ab^* \right)$$

$$Q_{xy} = \frac{\hbar^2 k}{2m\Omega} 2 \text{Im} \left(ab^* \right)$$

$$Q_{xz} = \frac{\hbar^2 k}{2m\Omega} 2 \text{Re} \left(|a|^2 - |b|^2 \right)$$

Conservation of angular momentum
Spin transfer torque:

$$\begin{aligned} \mathbf{N}_{st} &= - \int_{pillbox} d^2 R \hat{\mathbf{n}} \cdot \mathbf{Q} \\ &= - \int_{pillbox} d^3 r \nabla \cdot \mathbf{Q} \end{aligned}$$



$$\psi_{in} = \frac{e^{ikx}}{\sqrt{\Omega}} \left(\cos(\theta/2) |\uparrow\rangle + \sin(\theta/2) |\downarrow\rangle \right)$$

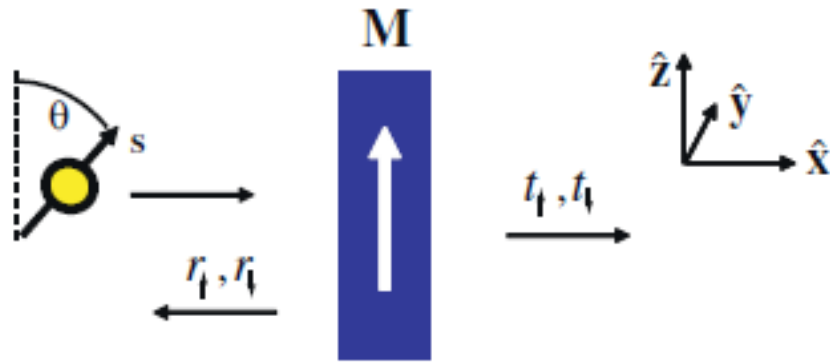
$$\psi_{trans} = \frac{e^{ikx}}{\sqrt{\Omega}} \left(t_{\uparrow} \cos(\theta/2) |\uparrow\rangle + t_{\downarrow} \sin(\theta/2) |\downarrow\rangle \right)$$

$$\psi_{refl} = \frac{e^{-ikx}}{\sqrt{\Omega}} \left(r_{\uparrow} \cos(\theta/2) |\uparrow\rangle + r_{\downarrow} \sin(\theta/2) |\downarrow\rangle \right)$$

$$\mathbf{Q}_{in} = \frac{\hbar^2 k}{2m\Omega} \left[\sin(\theta) \hat{\mathbf{x}} + \cos(\theta) \hat{\mathbf{z}} \right]$$

$$\begin{aligned} \mathbf{Q}_{trans} = & \frac{\hbar^2 k}{2m\Omega} \sin(\theta) \operatorname{Re}(t_{\uparrow} t_{\downarrow}^*) \hat{\mathbf{x}} + \frac{\hbar^2 k}{2m\Omega} \sin(\theta) \operatorname{Im}(t_{\uparrow} t_{\downarrow}^*) \hat{\mathbf{y}} \\ & + \frac{\hbar^2 k}{2m\Omega} \left(|t_{\uparrow}|^2 \cos^2(\theta/2) - |t_{\downarrow}|^2 \sin^2(\theta/2) \right) \hat{\mathbf{z}} \end{aligned}$$

$$\begin{aligned} \mathbf{Q}_{refl} = & -\frac{\hbar^2 k}{2m\Omega} \sin(\theta) \operatorname{Re}(r_{\uparrow} r_{\downarrow}^*) \hat{\mathbf{x}} - \frac{\hbar^2 k}{2m\Omega} \sin(\theta) \operatorname{Im}(r_{\uparrow} r_{\downarrow}^*) \hat{\mathbf{y}} \\ & - \frac{\hbar^2 k}{2m\Omega} \left(|r_{\uparrow}|^2 \cos^2(\theta/2) - |r_{\downarrow}|^2 \sin^2(\theta/2) \right) \hat{\mathbf{z}} \end{aligned}$$



$$\begin{aligned}
 \mathbf{N}_{st} &= A \hat{\mathbf{x}} \cdot (\mathbf{Q}_{in} + \mathbf{Q}_{refl} - \mathbf{Q}_{trans}) \\
 &= \frac{A \hbar^2 k}{2m\Omega} \sin(\theta) \left[1 - \text{Re}(t_{\uparrow} t_{\downarrow}^* + r_{\uparrow} r_{\downarrow}^*) \right] \hat{\mathbf{x}} \\
 &\quad - \frac{A \hbar^2 k}{2m\Omega} \sin(\theta) \left[\text{Im}(t_{\uparrow} t_{\downarrow}^* + r_{\uparrow} r_{\downarrow}^*) \right] \hat{\mathbf{y}}
 \end{aligned}$$

Damp-like torque

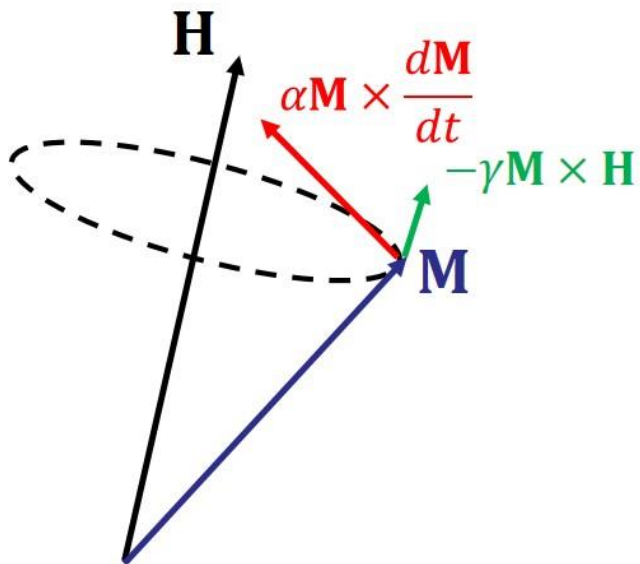
Field-like torque

$$\begin{aligned}
 (|t_{\uparrow}|^2 + |r_{\uparrow}|^2 &= 1 \\
 |t_{\downarrow}|^2 + |r_{\downarrow}|^2 &= 1)
 \end{aligned}$$

Spin mixing conductance

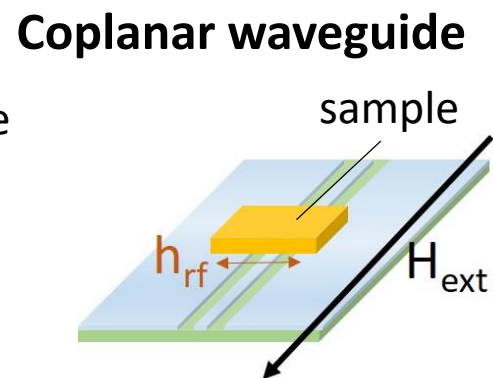
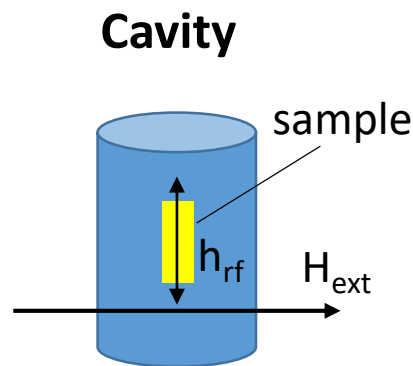
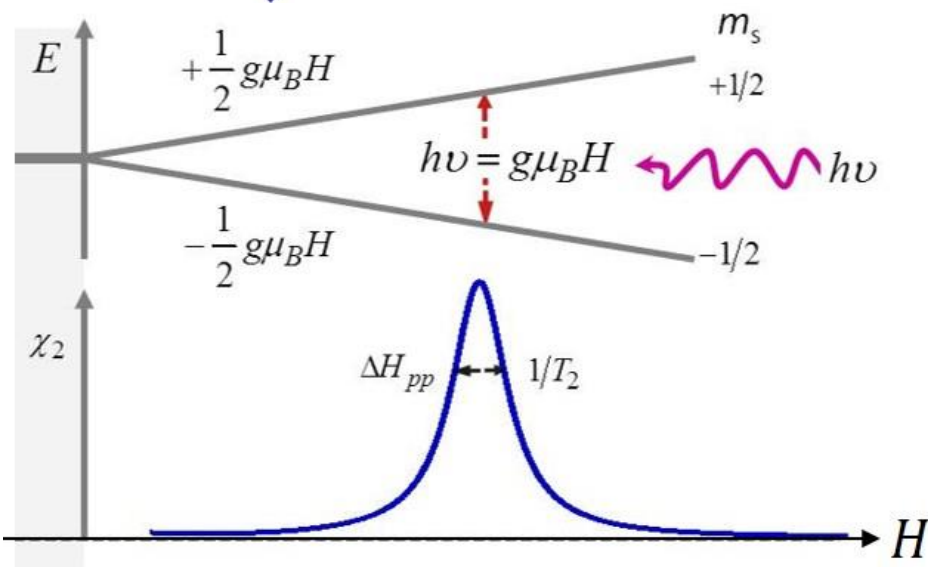
$$\begin{pmatrix} a' \\ b' \end{pmatrix} = \begin{pmatrix} G_{\uparrow\uparrow} & G_{\uparrow\downarrow} \\ G_{\downarrow\uparrow}^* & G_{\downarrow\downarrow} \end{pmatrix} \begin{pmatrix} a \\ b \end{pmatrix} \quad \text{Re}(G_{\uparrow\downarrow}) \gg \text{Im}(G_{\uparrow\downarrow}) \text{ for metals}$$

Ferromagnetic resonance (FMR)



Landau–Lifshitz–Gilbert equation

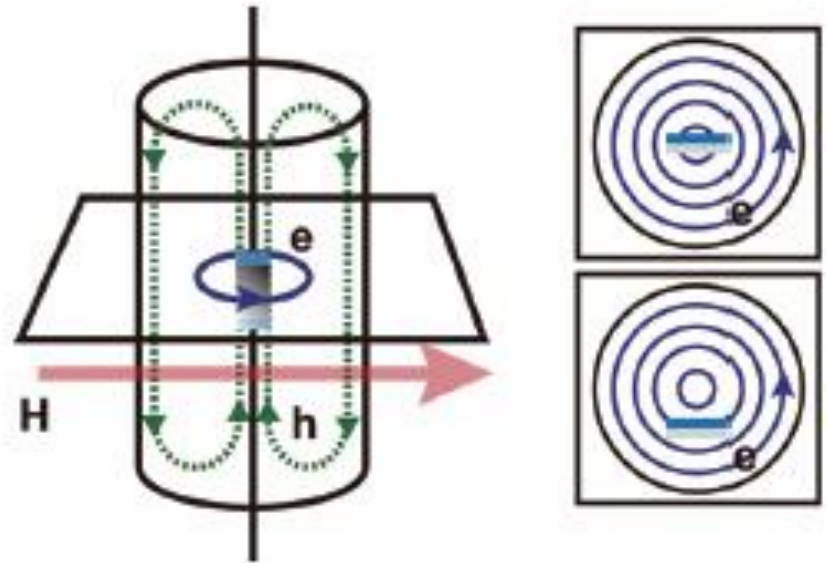
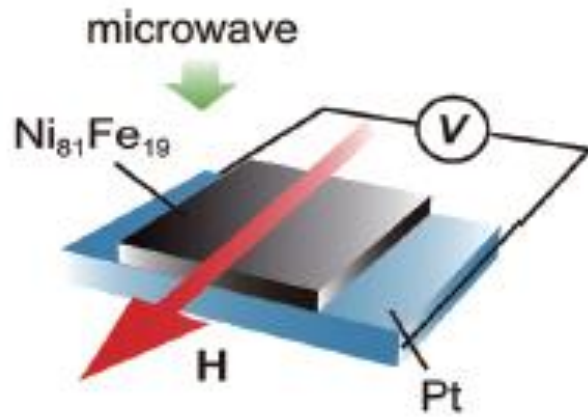
$$\frac{d\mathbf{M}}{dt} = -\gamma\mathbf{M} \times \mathbf{H} + \alpha\mathbf{M} \times \frac{d\mathbf{M}}{dt}$$



Application:

- Measurement of **magnetic anisotropy**
- Measurement of **damping constant α**
- Spin pumping**

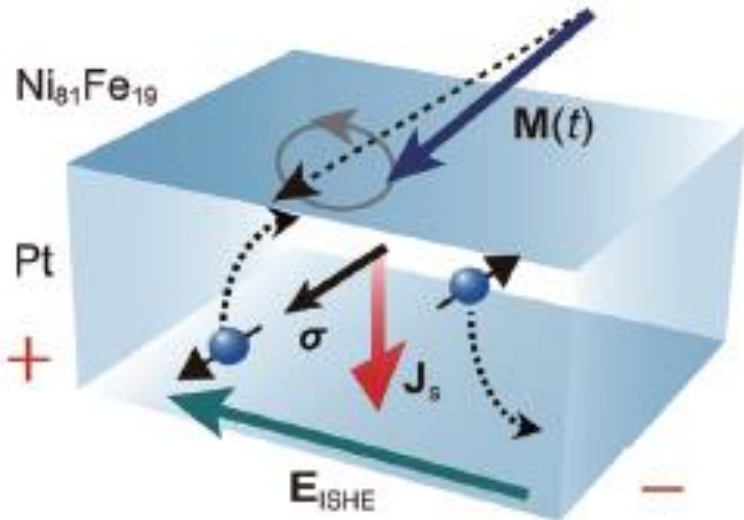
Spin pumping



Spin current projected along H_{ext} :

$$j_s = \frac{\omega}{2\pi} \int_0^{2\pi/\omega} \frac{\hbar}{4\pi} g_r^{\uparrow\downarrow} \frac{1}{M_s^2} \left[\mathbf{M}(t) \times \frac{d\mathbf{M}(t)}{dt} \right]_z dt.$$

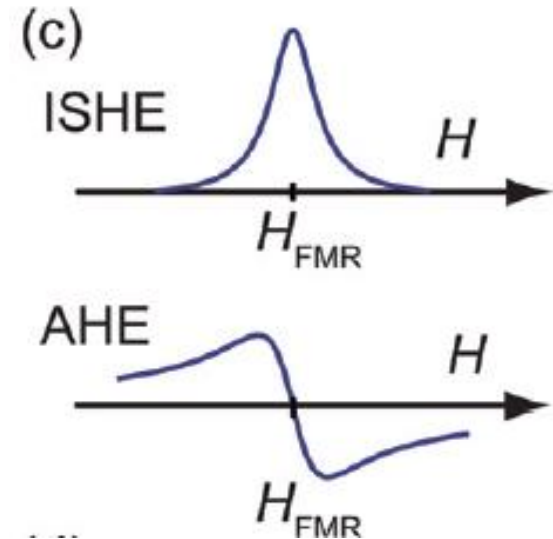
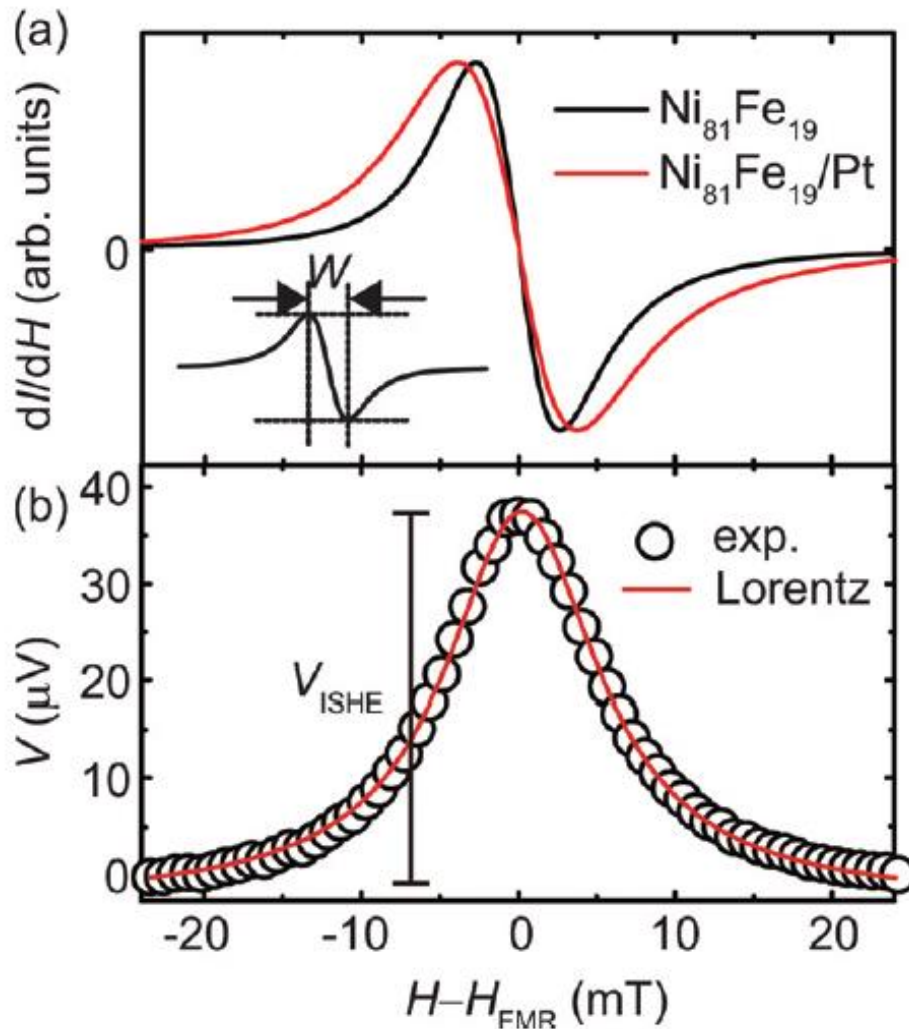
$$V_{\text{ISHE}} \propto \mathbf{J}_e \propto \theta_{\text{SH}} \mathbf{J}_s \times \boldsymbol{\sigma} \propto \theta_{\text{SH}} \mathbf{J}_s \times \mathbf{M} \\ \propto \theta_{\text{SH}} \mathbf{J}_s \times \mathbf{H} \propto \theta_{\text{SH}} \sin \theta_H,$$



E. Saitoh et al., Appl. Phys. Lett. **88**, 182509 (2016)

K. Ando, et al., J. Appl. Phys. **109**, 103913 (2011)

H. Nakayama, et al., Phys. Rev. B **85**, 144408 (2012)



$$V = V_{\text{ISHE}} \frac{\Gamma^2}{(H - H_0)^2 + \Gamma^2} + V_{\text{AHE}} \frac{-2\Gamma(H - H_0)}{(H - H_0)^2 + \Gamma^2}$$

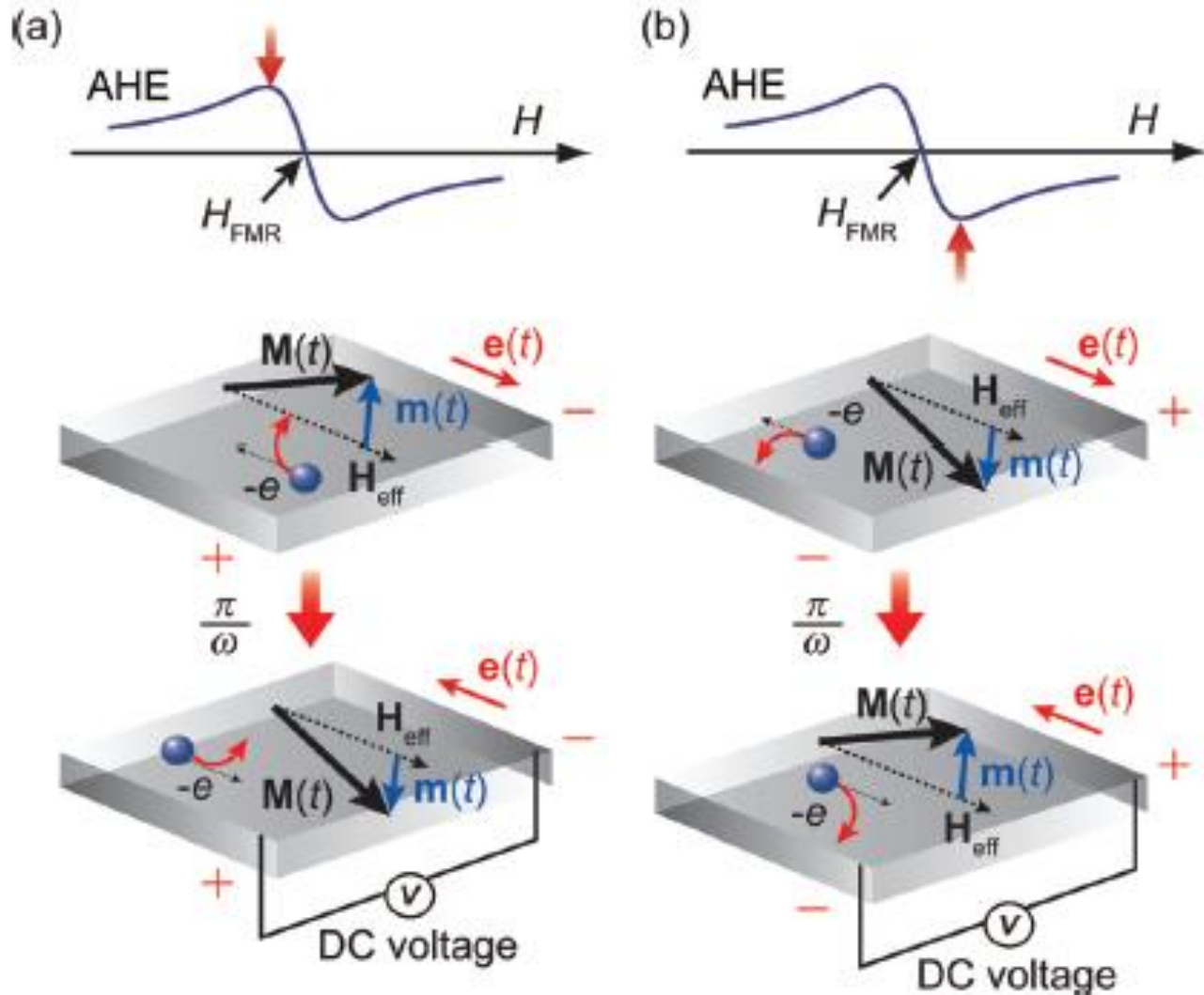
$$g_r^{\uparrow\downarrow} = \frac{2\sqrt{3}\pi M_s \gamma d_F}{g \mu_B \omega} (W_{F/N} - W_F)$$

$$\text{or } g_r^{\uparrow\downarrow} = \frac{4\pi M_s d_F}{g \mu_B} (\alpha_{F/N} - \alpha_F)$$

- E. Saitoh et al., Appl. Phys. Lett. **88**, 182509 (2016)
 K. Ando, et al., J. Appl. Phys. **109**, 103913 (2011)
 H. Nakayama, et al., Phys. Rev. B **85**, 144408 (2012)

A phenomenological model

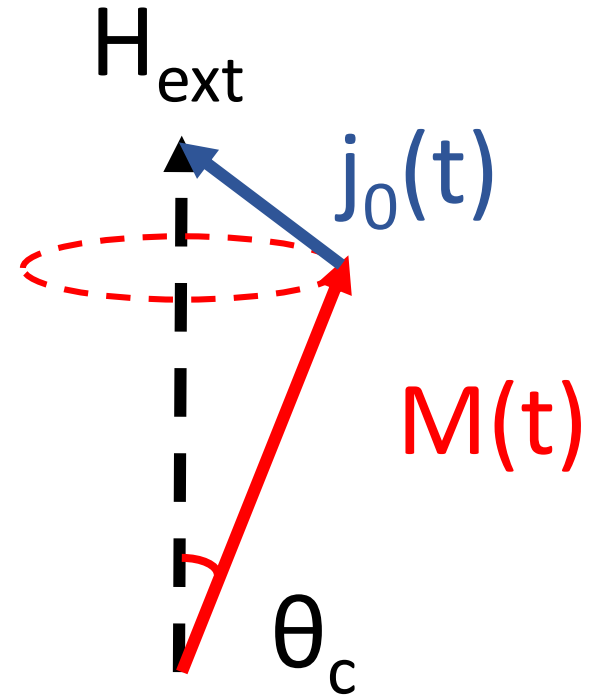
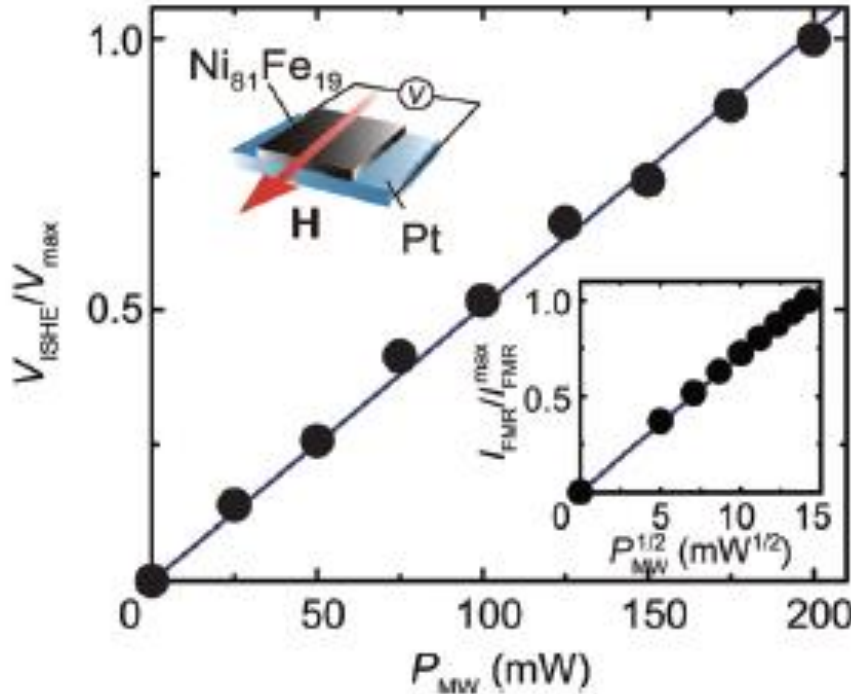
Antisymmetric lineshape from AHE or AMR



Phase shift between the microwave and magnetization determine the polarity.

Small cone angle (linear) regime

Linear power dependence



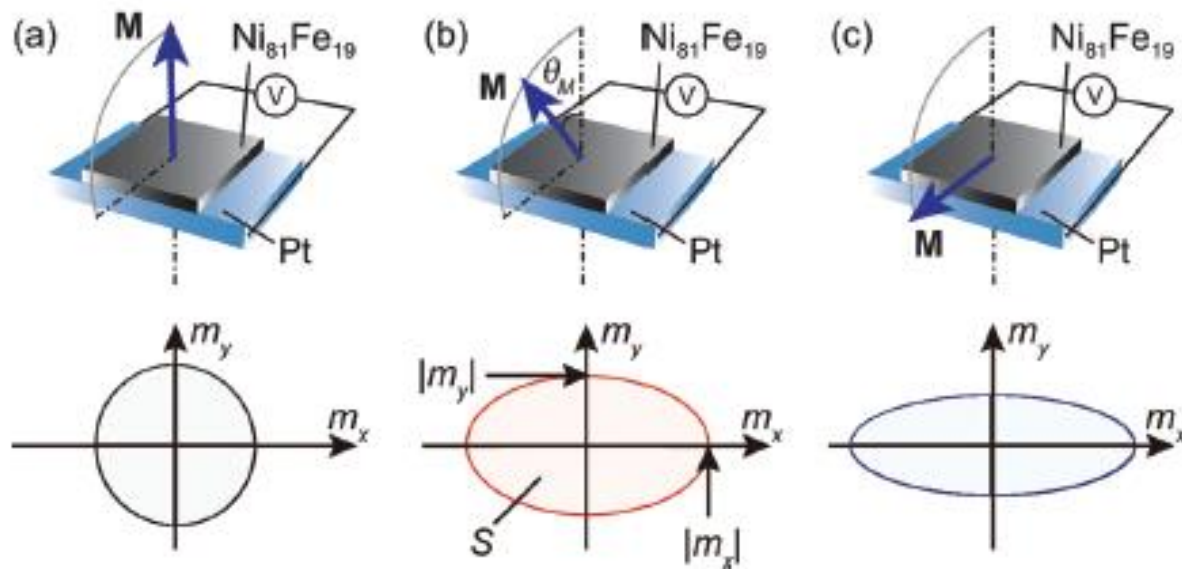
$$j_0 = \frac{g_r^{\uparrow\downarrow} \gamma^2 h_{\text{rf}}^2 \hbar \left[4\pi M_s \gamma + \sqrt{(4\pi M_s)^2 \gamma^2 + 4\omega^2} \right]}{8\pi\alpha^2 \left[(4\pi M_s)^2 \gamma^2 + 4\omega^2 \right]}$$

$$= g_r^{\uparrow\downarrow} fP \left(\frac{\gamma h_{\text{rf}}}{2\alpha\omega} \right)^2 = g_r^{\uparrow\downarrow} fP\theta_c^2, \text{ where } h_{\text{rf}}^2 \propto \text{power}$$

The P factor

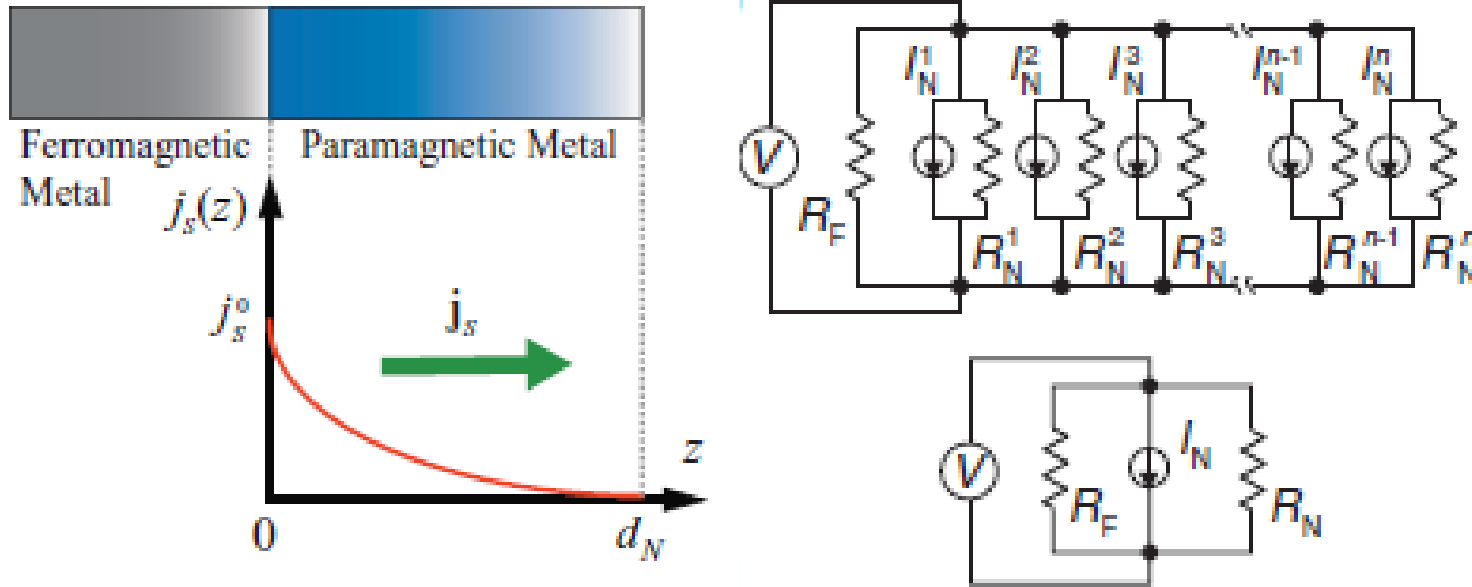
$$P = \frac{2\omega \left[4\pi M_s \gamma + \sqrt{(4\pi M_s)^2 \gamma^2 + 4\omega^2} \right]}{(4\pi M_s)^2 \gamma^2 + 4\omega^2}$$

can be viewed as a correction factor.



The pumped spin current is proportional to the trajectory area. Spin pumping is an adiabatic process. (think about the Carnot engine.)

Spin distribution in normal metals

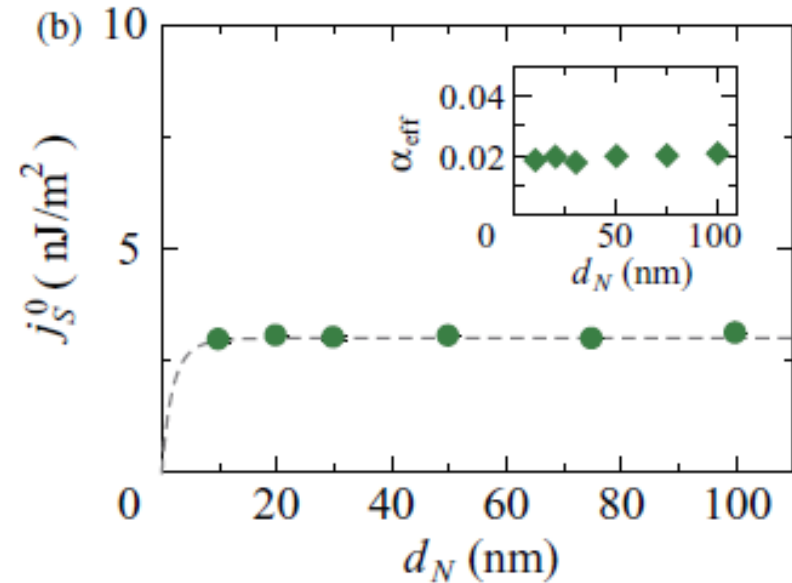
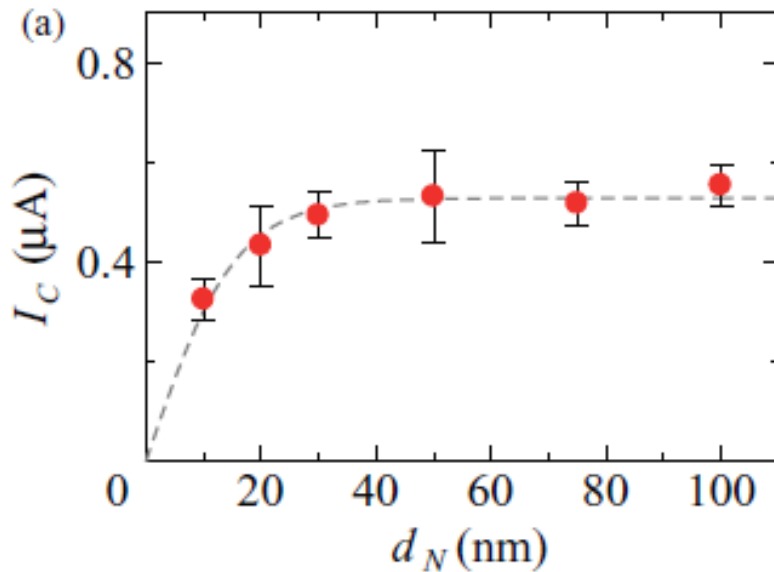


Spin Hall effect acts as a charge current source.

Solving the spin diffusion equation...

$$j_s(z) = \frac{\sinh\left[(d_N - z) / \lambda_N\right]}{\sinh(d_N / \lambda_N)} j_s^0$$

Thickness dependence



Spin backflow depends on the spin diffusion length.

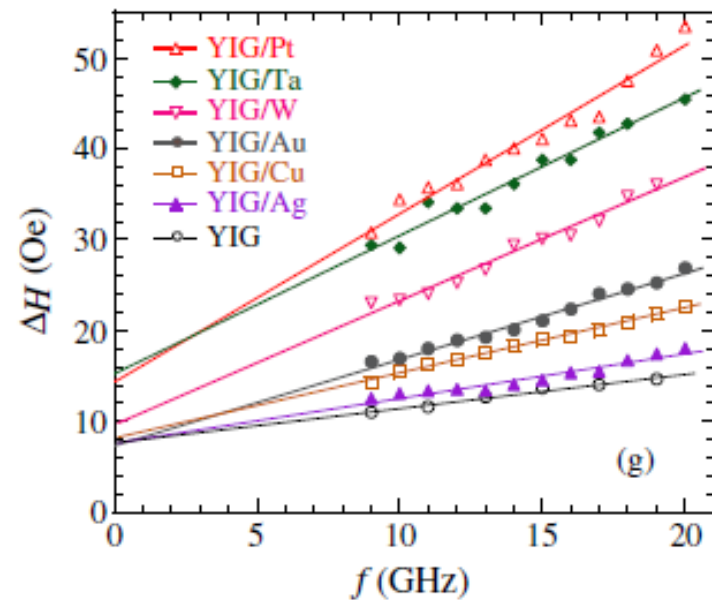
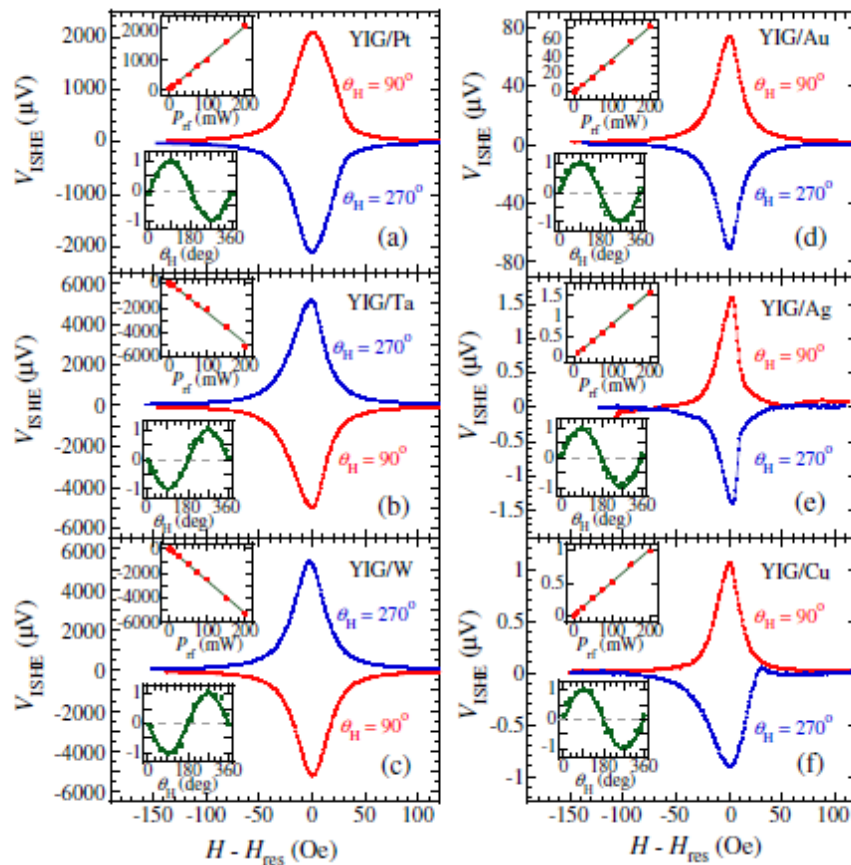
$$\langle j_c \rangle = \frac{1}{d_N} \int_0^{d_N} j_c(y) dy$$

$$= \theta_{SH} \left(\frac{2e}{\hbar} \right) \frac{\lambda_N}{d_N} \tanh \left(\frac{d_N}{2\lambda_N} \right) j_s^0$$

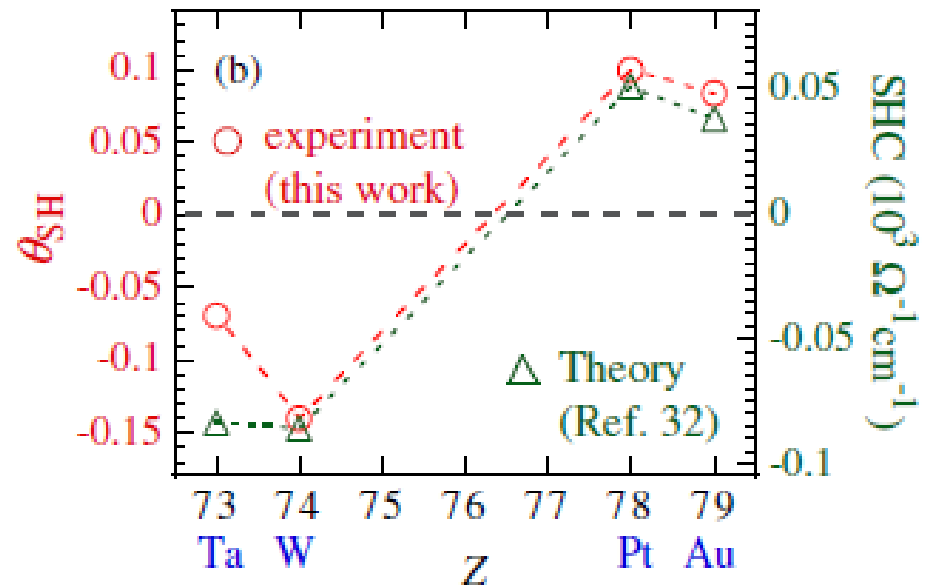
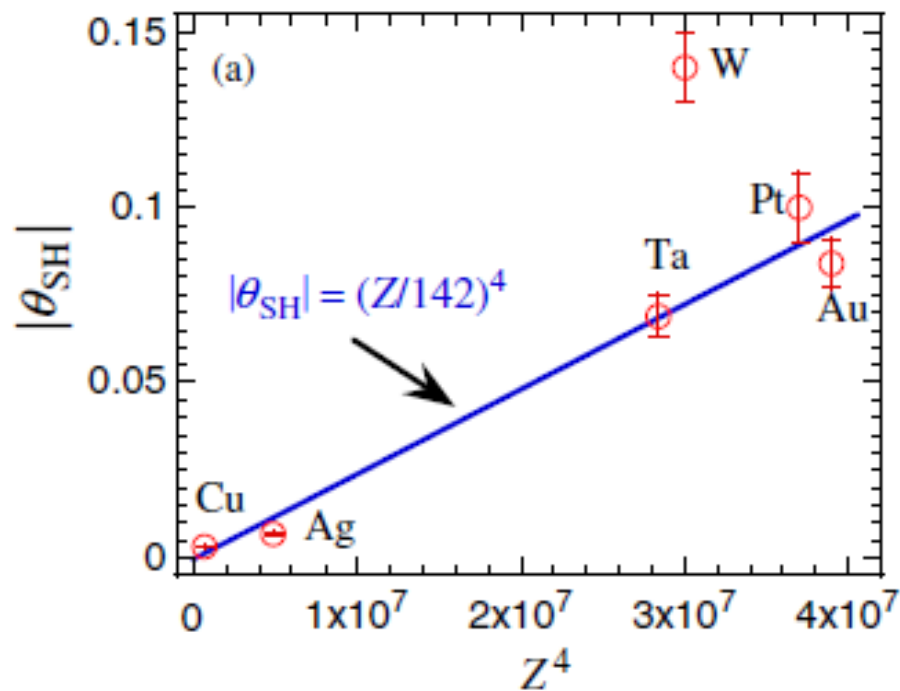
Need to get the thickness dependence data to calculate the spin Hall angle

Scaling of Spin Hall Angle in 3d, 4d, and 5d Metals from $\text{Y}_3\text{Fe}_5\text{O}_{12}$ /Metal Spin PumpingH. L. Wang,¹ C. H. Du,¹ Y. Pu,¹ R. Adur,¹ P. C. Hammel,^{1,*} and F. Y. Yang^{1,†}¹Department of Physics, The Ohio State University, Columbus, Ohio 43210, USA

(Received 23 September 2013; revised manuscript received 24 December 2013; published 15 May 2014)



Bilayer	V_{ISHE}	ΔH change	α_{sp}	$\rho(\Omega m)$	$g_{\uparrow\downarrow}(\text{m}^{-2})$	$\lambda_{\text{SD}}(\text{nm})$	θ_{SH}	$J_s(\text{A}/\text{m}^2)$
YIG/Pt	2.10 mV	24.3 Oe	$(3.6 \pm 0.3) \times 10^{-3}$	4.8×10^{-7}	$(6.9 \pm 0.6) \times 10^{18}$	7.3	0.10 ± 0.01	$(2.0 \pm 0.2) \times 10^7$
YIG/Ta	-5.10 mV	16.5 Oe	$(2.8 \pm 0.2) \times 10^{-3}$	2.9×10^{-6}	$(5.4 \pm 0.5) \times 10^{18}$	1.9	-0.071 ± 0.006	$(1.6 \pm 0.2) \times 10^7$
YIG/W	-5.26 mV	12.3 Oe	$(2.4 \pm 0.2) \times 10^{-3}$	1.8×10^{-6}	$(4.5 \pm 0.4) \times 10^{18}$	2.1	-0.14 ± 0.01	$(1.4 \pm 0.1) \times 10^7$
YIG/Au	$72.6 \mu\text{V}$	5.50 Oe	$(1.4 \pm 0.1) \times 10^{-3}$	4.9×10^{-8}	$(2.7 \pm 0.2) \times 10^{18}$	60	0.084 ± 0.007	$(7.6 \pm 0.7) \times 10^6$
YIG/Ag	$1.49 \mu\text{V}$	1.30 Oe	$(2.7 \pm 0.2) \times 10^{-4}$	6.6×10^{-8}	$(5.2 \pm 0.5) \times 10^{17}$	700	0.0068 ± 0.0007	$(1.5 \pm 0.1) \times 10^6$
YIG/Cu	$0.99 \mu\text{V}$	3.70 Oe	$(8.1 \pm 0.6) \times 10^{-4}$	6.3×10^{-8}	$(1.6 \pm 0.1) \times 10^{18}$	500	0.0032 ± 0.0003	$(4.6 \pm 0.4) \times 10^6$



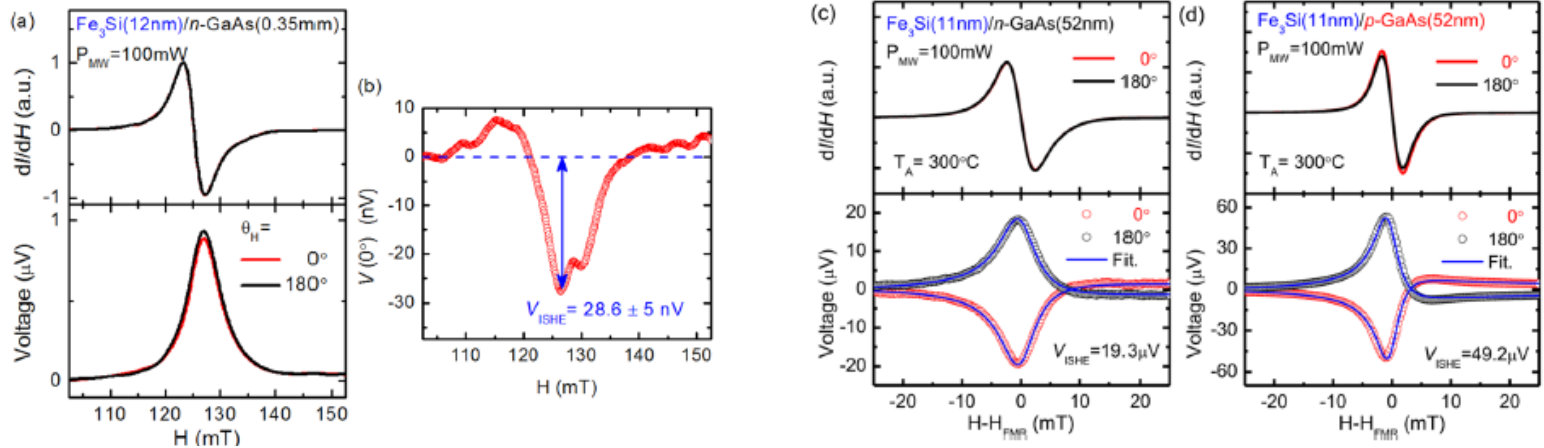
Spin Hall angles strongly depend on the d-electron count.

	T (K)	λ_{sd} (nm)	σ_{NM} (10^6 S/m)	α_{SH} (%)		T (K)	λ_{sd} (nm)	σ_{NM} (10^6 S/m)	α_{SH} (%)
Al	4.2	455 ± 15	10.5	0.032 ± 0.006	Mo	10	10	3.03	-0.20
	4.2	705 ± 30	17	0.016 ± 0.004		10	10	0.667	-0.075
Au	295	86 ± 10	37	11.3	10	8.6 ± 1.3	2.8	$-(0.8 \pm 0.18)$	
	295	83	37	3	295	$35 \pm 3^*$	4.66	$-(0.05 \pm 0.01)$	
	4.5	65^*	48.3	<2.3	Nb	10	5.9 ± 0.3	1.1	$-(0.87 \pm 0.20)$
	295	36^*	25.7	<2.7		Pd	10	13 ± 2	2.2
	295	35 ± 4	28	7.0 ± 0.1	295		9^*	1.97	1.0
	295	27 ± 3	14	7.0 ± 0.3	295		$15 \pm 4^*$	4.0	0.64 ± 0.10
	295	25 ± 3	14.5	12 ± 4	295		5.5 ± 0.5	5	1.2 ± 0.3
	295	50 ± 8	16.7	0.8 ± 0.2	295		2.0 ± 0.1	3.7	0.8 ± 0.20
	<10	40 ± 16	25	1.4 ± 0.4	Pt	295		6.41	0.37
	295	$35 \pm 3^*$	25.2	0.35 ± 0.03		5	8	8.0	0.44
	295	35	20	0.25 ± 0.1		295	7	5.56	0.9
	295	$35 \pm 3^*$	5.25	1.6 ± 0.1		10	11 ± 2	8.1	2.1 ± 0.5
	295	$35 \pm 3^*$	7	0.335 ± 0.006		10	~ 10	8.1	2.4
	295	35^*		1.1 ± 0.3		295	7^*	6.4	8.0
	295	60	20.4	8.4 ± 0.7		295	$10 \pm 2^*$	2.4	1.3 ± 0.2
295	295	1.9	1.75	>10		295	10^*	2	4.0
AuW	295	700	15	0.7 ± 0.1		295	3.7 ± 0.2	2.42	8 ± 1
Ag	295	700	15	0.7 ± 0.1		295	8.3 ± 0.9	4.3 ± 0.2	1.2 ± 0.2
	295	700	15	0.7 ± 0.1	295	7.7 ± 0.7	1.3 ± 0.1	1.3 ± 0.1	
Bi	3	0.3 ± 0.1	-	>0.3	295	$1.5 - 10^*$	2.45 ± 0.1	$3_{-1.5}^{+4}$	
	295	-	2.4 ± 0.3 (I) 50 ± 12 (V)	$-(7.1 \pm 0.8)$ (I) 1.9 ± 0.2 (V)	295	4	4	2.7 ± 0.5	
Cu	295	500	16	0.32 ± 0.03	295	$8 \pm 1^*$	1.02	2.012 ± 0.003	
	295	500	16	0.32 ± 0.03	295	13^*	2.4	2.1 ± 1.5	
CuIr	10	5-30		2.1 ± 0.6	295	1.2		8.6 ± 0.5	
CuMn _x Ty				0.7(Ta); 2.6(Ir)	295	1.4^*		12 ± 4	
				1.35(Au); 1.15(Sb)	295	3.4 ± 0.4	6.0	5.6 ± 0.1	
				-1.2(Lu)	295	7.3	2.1	10 ± 1	
					295	1.2 ± 0.1	3.6	2.2 ± 0.4	

1. The larger spin Hall angles, the shorter spin diffusion lengths.
2. Depending on techniques, materials preparation and geometry, the calculated spin Hall angle can vary by 1 order of magnitude.
3. Rashba effect (broken inversion symmetry) at the interface adds complexity to analyses.

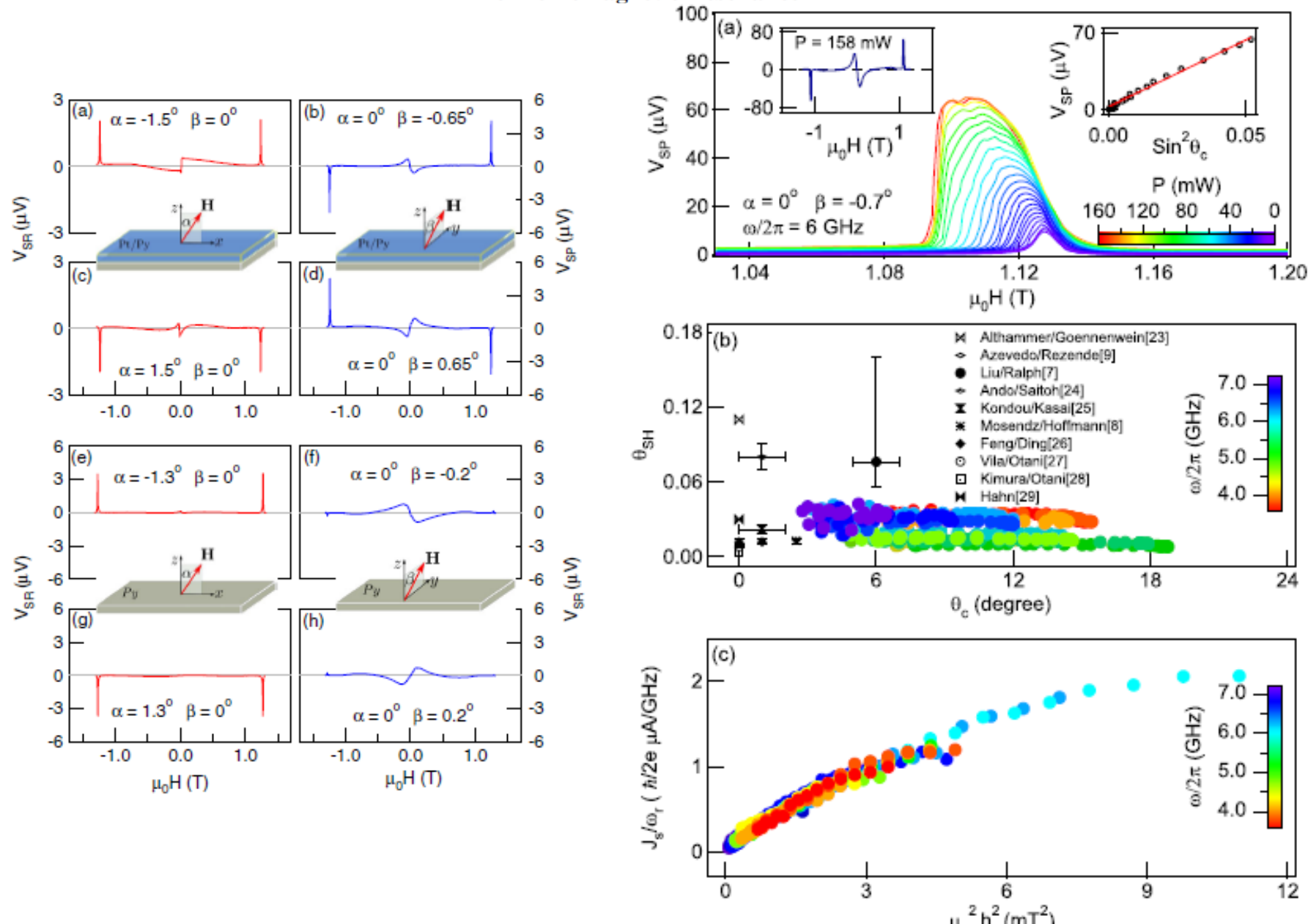
Spurious effects

- Microwave induced Seebeck effect in semiconductor.



- Spin rectification effect. (can be prevented by YIG)
 - the boundary conditions, phase shift between E and B field can strongly affect voltage signals.
- Self-induced ISHE and spin backflow. (can be prevented by YIG)

Universal Method for Separating Spin Pumping from Spin Rectification Voltage of Ferromagnetic Resonance



Spin-torque ferromagnetic resonance (ST-FMR)

PRL 106, 036601 (2011)

PHYSICAL REVIEW LETTERS

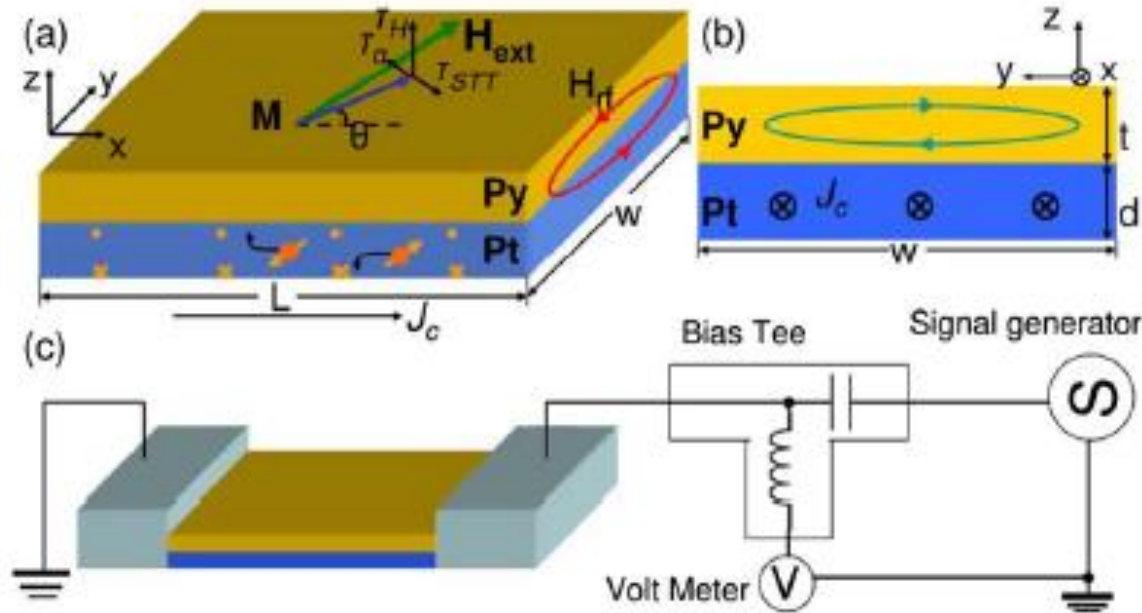
week ending
21 JANUARY 2011

Spin-Torque Ferromagnetic Resonance Induced by the Spin Hall Effect

Luqiao Liu, Takahiro Moriyama, D. C. Ralph, and R. A. Buhrman

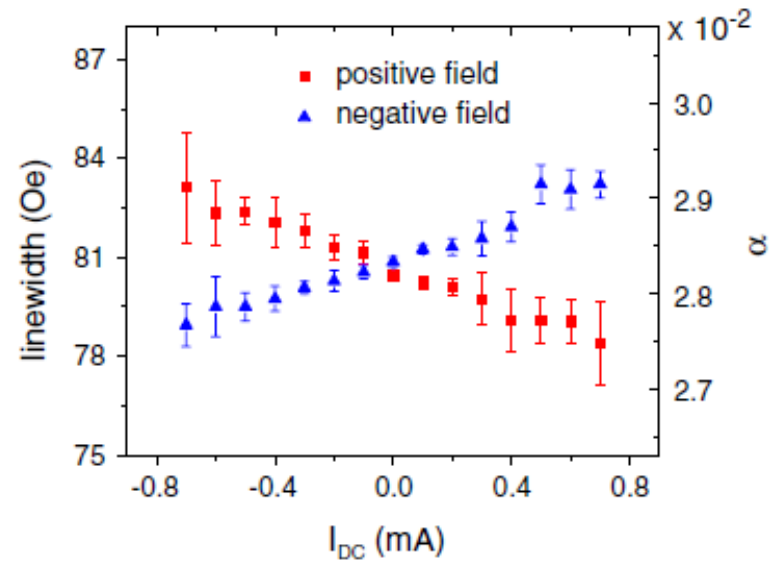
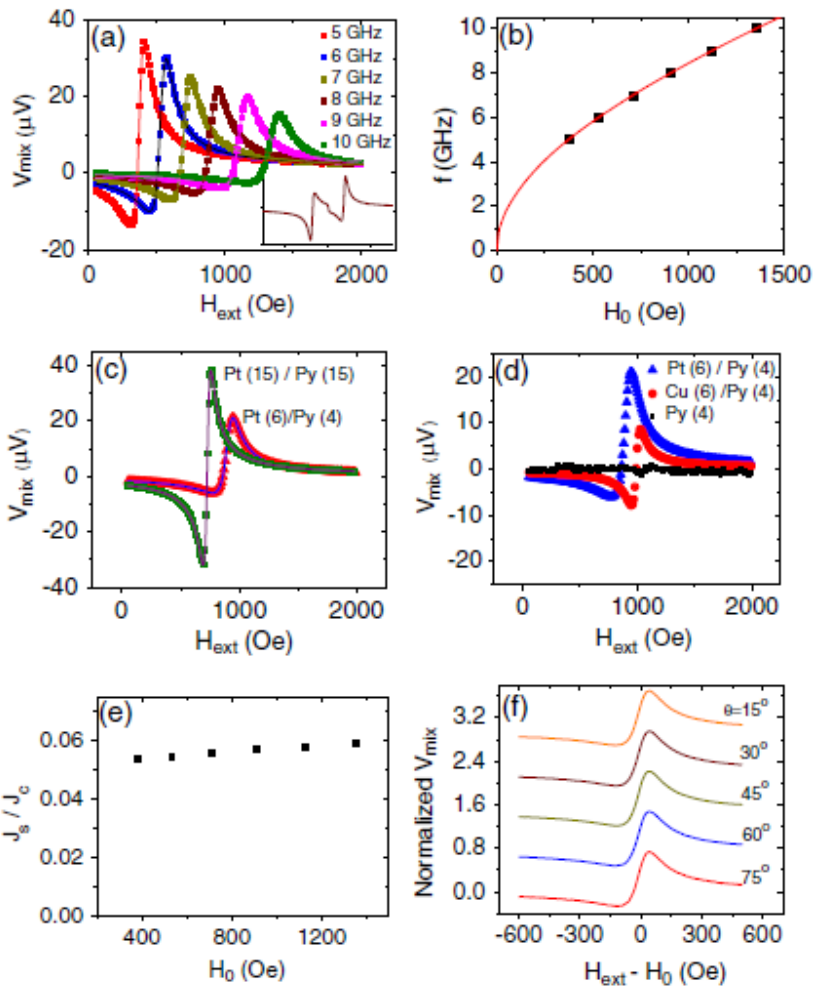
Cornell University, Ithaca, New York, 14853

(Received 12 October 2010; published 20 January 2011)



$$\frac{d\hat{m}}{dt} - \gamma \hat{m} \times \vec{H}_{eff} + \alpha \hat{m} \times \frac{d\hat{m}}{dt} + \gamma \frac{\hbar}{2e\mu_0 M_s t} J_{S,rf} (\hat{m} \times \hat{\sigma} \times \hat{m}) - \gamma \hat{m} \times \vec{H}_{rf}$$

Anti-damp torques



Rely on AMR to generate voltage signals. Not suitable for magnetic insulator.
Special case: Pt/YIG, Ta/YIG...

$$V_{mix} = -\frac{1}{4} \frac{dR}{d\theta} \frac{\gamma I_{rf} \cos \theta}{\Delta 2\pi (df/dH)|_{H_{ext}=H_0}} \left[S \frac{\Delta^2}{\Delta^2 + (H_{ext} - H_0)^2} + A \frac{(H_{ext} - H_0) \Delta}{\Delta^2 + (H_{ext} - H_0)^2} \right]$$

$$\frac{J_{S,rf}}{J_{C,rf}} = \frac{S}{A} \frac{e \mu_0 M_s t d}{\hbar} \left[1 + \left(4\pi M_{eff} / H_{ext} \right) \right]^{1/2}$$

The spin Hall angle can be determined from the relative magnitude of the two components.

Modulation of magnetization damping (MOD)

PRL 101, 036601 (2008)

PHYSICAL REVIEW LETTERS

week ending
18 JULY 2008

Electric Manipulation of Spin Relaxation Using the Spin Hall Effect

K. Ando,^{1,*} S. Takahashi,^{2,3} K. Harii,¹ K. Sasage,¹ J. Ieda,^{2,3} S. Maekawa,^{2,3} and E. Saitoh^{1,4}

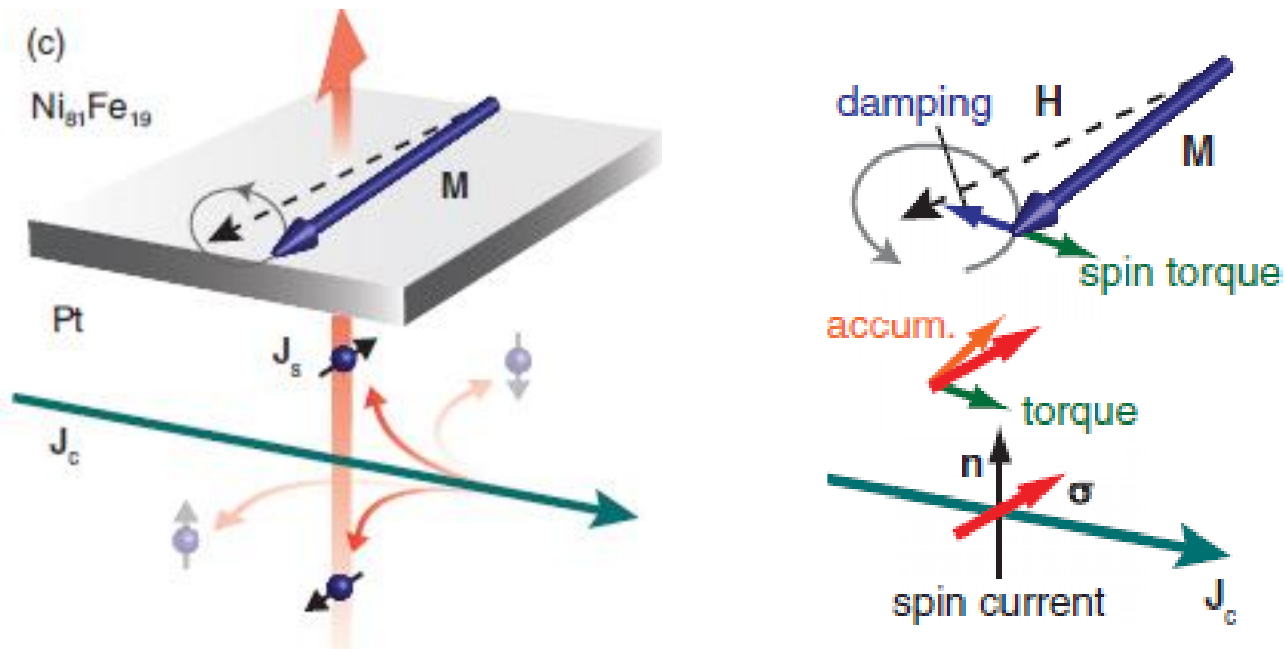
¹Department of Applied Physics and Physico-Informatics, Keio University, Yokohama 223-8522, Japan

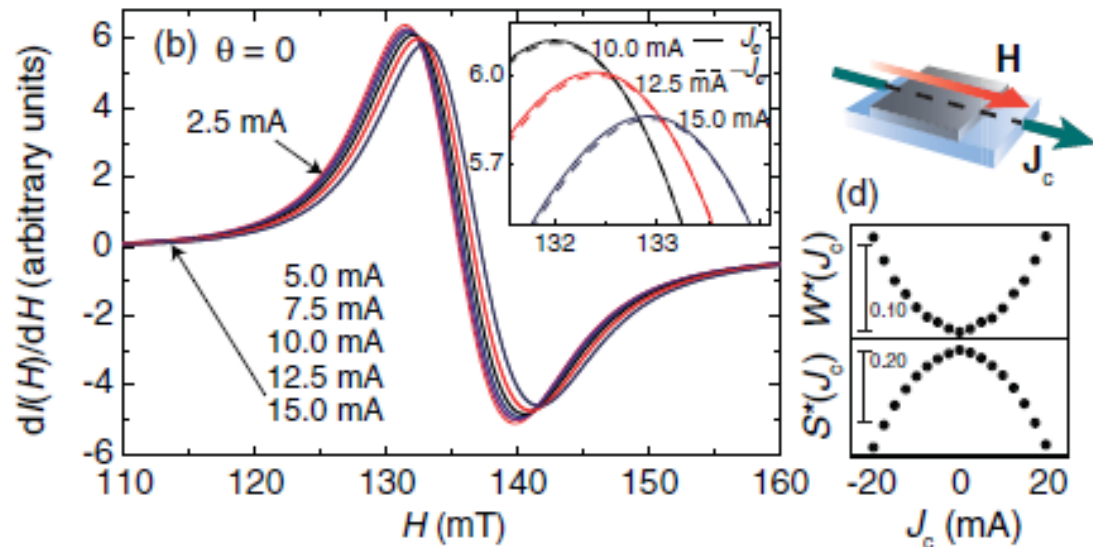
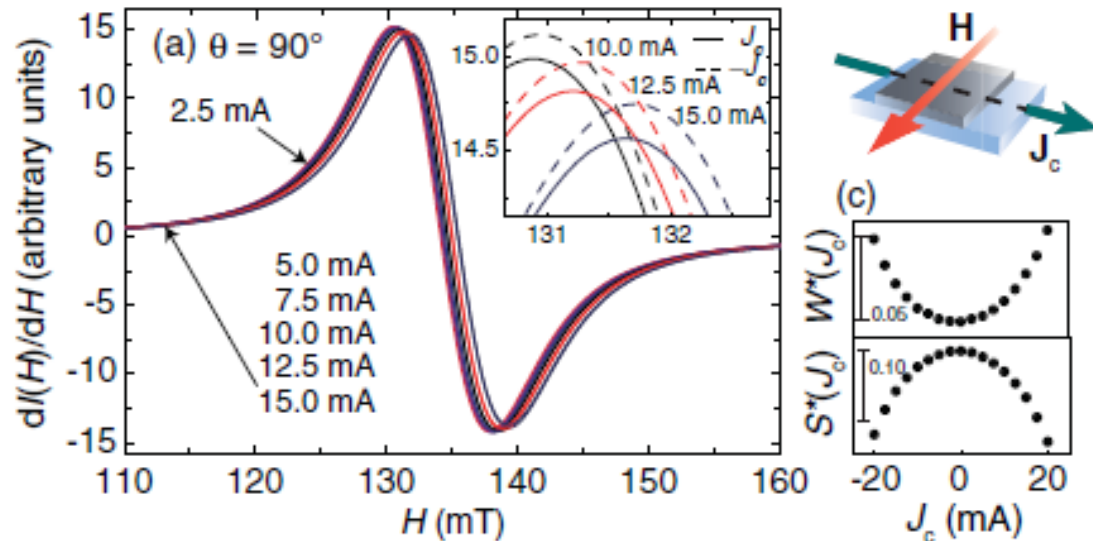
²Institute for Materials Research, Tohoku University, Sendai 980-8577, Japan

³CREST, Japan Science and Technology Agency, Kawaguchi, Saitama 332-0012, Japan

⁴PRESTO, Japan Science and Technology Agency, Kawaguchi, Saitama 332-0012, Japan

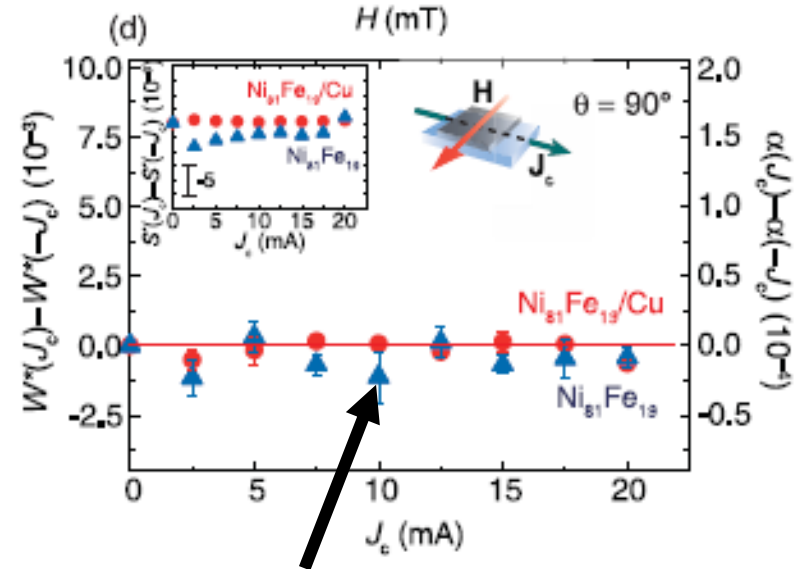
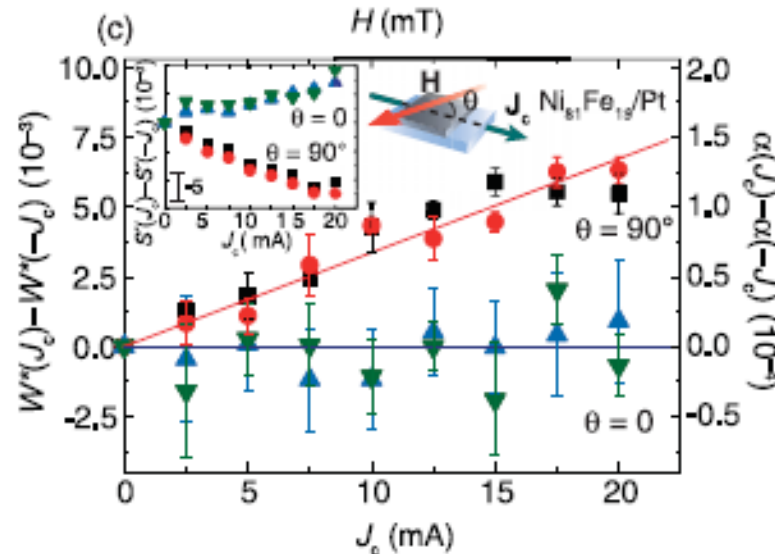
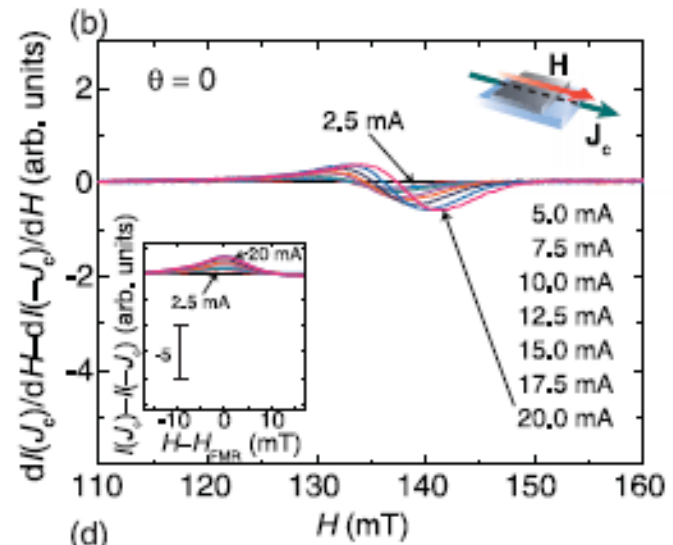
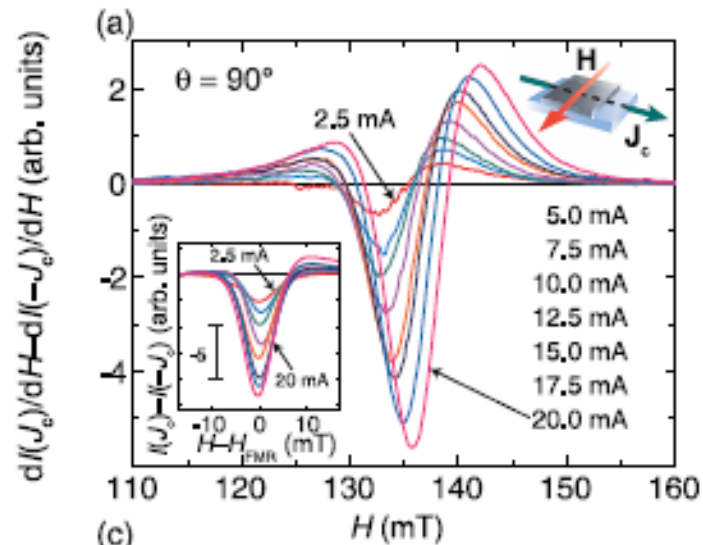
(Received 17 March 2008; published 18 July 2008)





Thermal effects on FMR spectra can be serious.

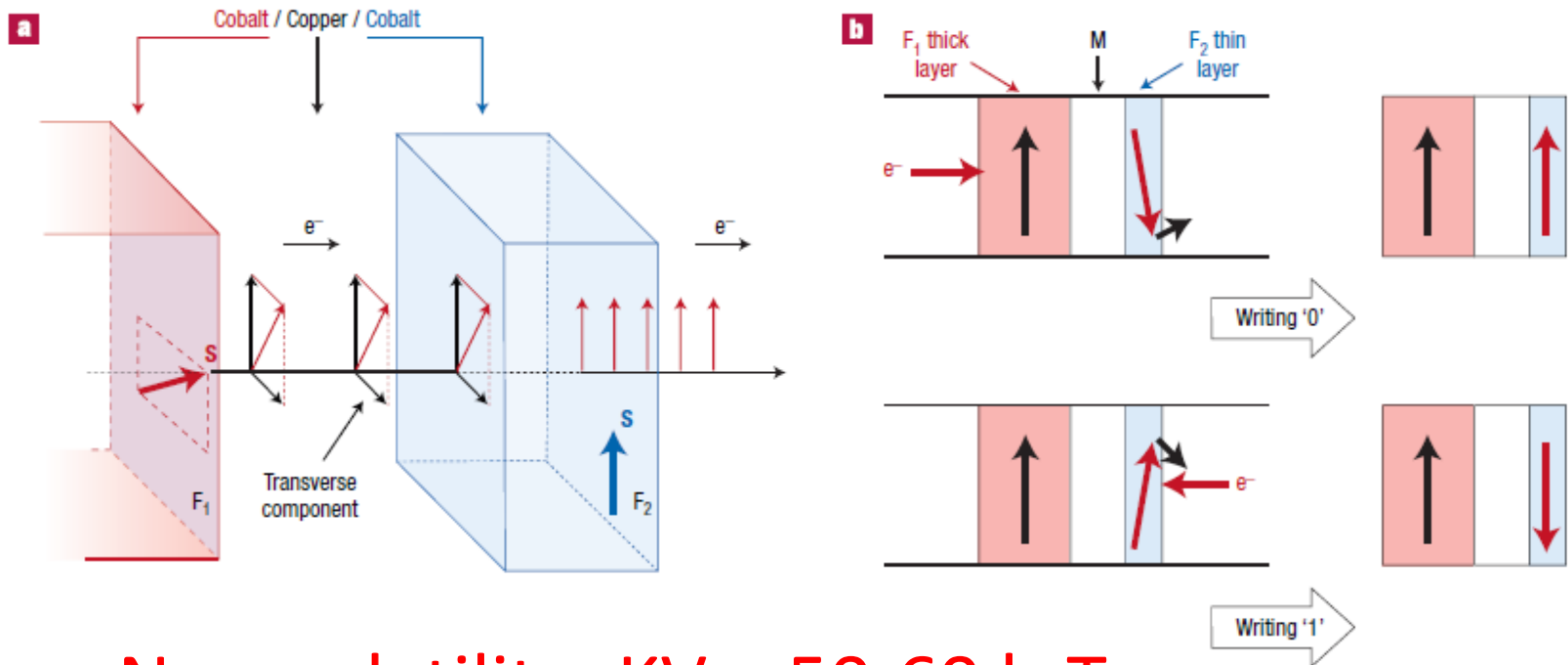
Need to change the in-plane field angle to separate the spin-transfer effect from the thermal effect.



Controlled sample Py/Cu: Cu has small spin Hall angle.

Spin pumping to topological insulators

Application: data storage



Non-volatility: $KV > 50-60 k_B T$

K : magnetic anisotropy constant

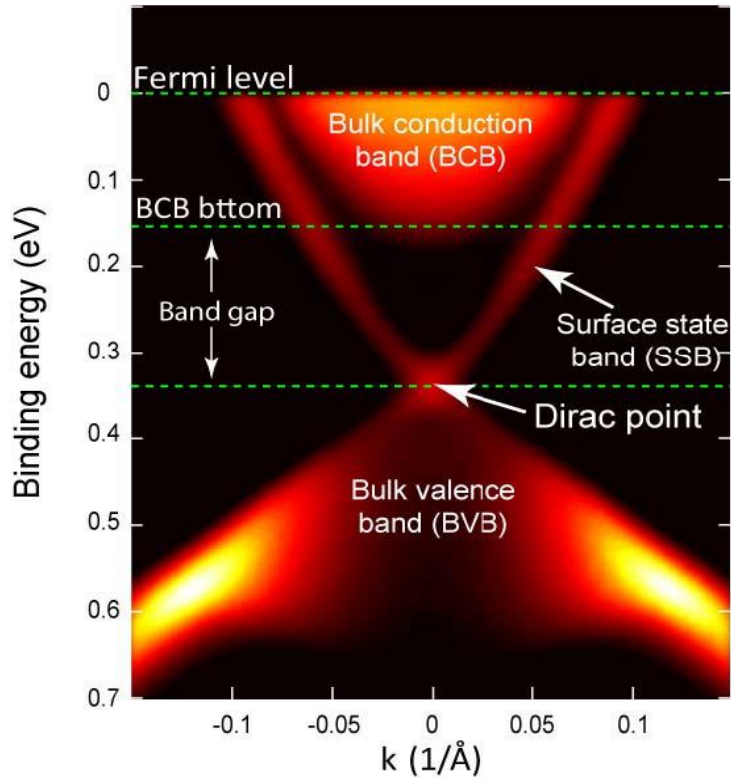
V : volume of nano-particle

k_B : Boltzmann constant

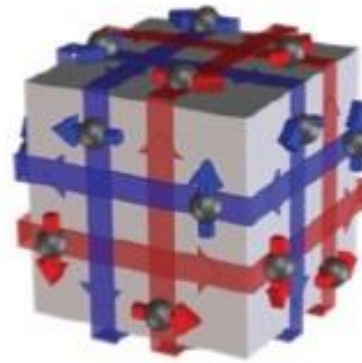
Goal: Find a material that can generate maximum spin torques from a given charge current.

Topological insulators

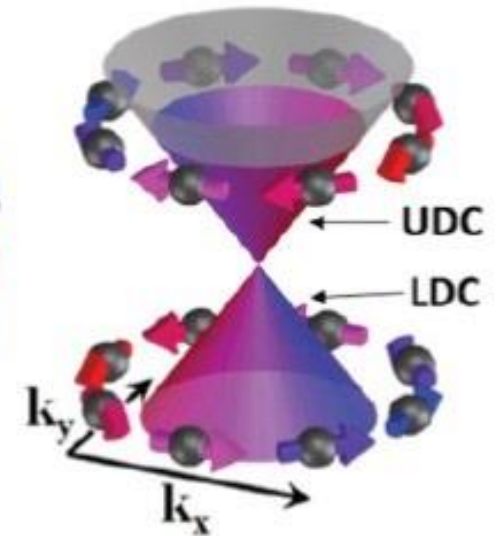
ARPES spectra



real-space



k-space



Nearly 100 % spin polarization.

Spin-momentum locking: the direction of electron motion determines the spin direction.

Challenges

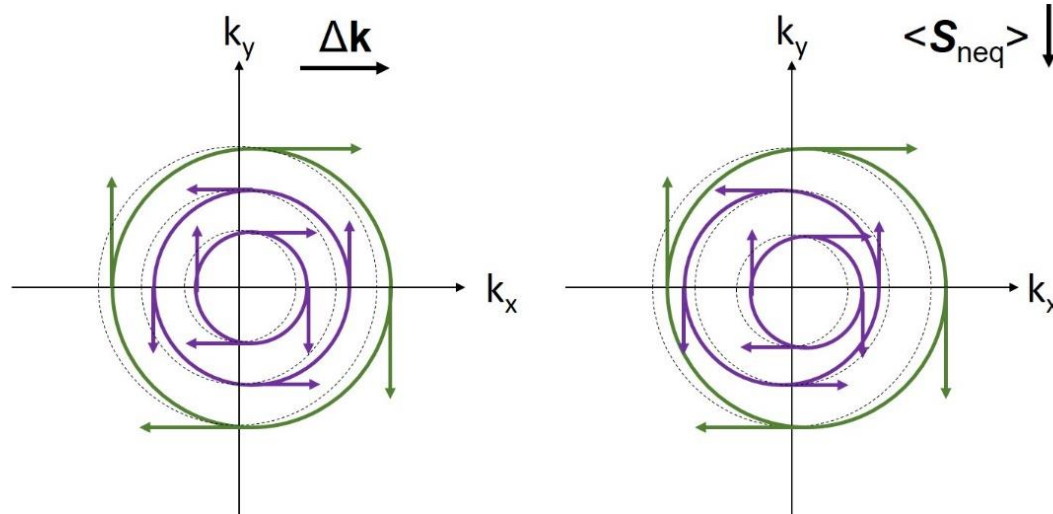
- Bulk conduction of TIs obscures the effect of topological surface states
- Large variation of reported effective spin Hall angle θ_{SH} (or conversion efficiency)
 - **0.022** in $\text{Bi}_2\text{Se}_3/\text{Py}$ at 15 K (Deorani et al. (2014))
 - $\sim 10^{-4}$ in bulk insulating $\text{Bi}_{1.5}\text{Sb}_{0.5}\text{Te}_{1.7}\text{Se}_{1.3}$ at 15 K (Shiomi et al. (2014))
 - **0.021~0.43** in $\text{Bi}_2\text{Se}_3/\text{CoFeB}$ at **RT** (Jamali et al. (2015))
- Current shunting effect by ferromagnetic metals in ST-FMR measurement

Ferrimagnetic insulator YIG with high thermal stability is an ideal spin source.

(b)

Edelstein effect

Inverse Edelstein effect



	Inverse spin Hall effect (ISHE)	Inverse Edelstein effect (IEE)
location	bulk	surface
condition	Spin current normal to the interface	“non-equilibrium” spin density at interface
material	Normal metals and semiconductors including 3D TIs	TIs and Rasba materials possessing k-dependent spin-polarized states

Spin Hall angle and IEE length

$$j_c = \lambda_{IEE} j_s \text{ (definition of IEE length)}$$

$$j_c = \theta_{SH} \lambda_N \tanh\left(\frac{d_N}{2\lambda_N}\right) j_s, \text{ 2D charge current from ISHE}$$

$$\lambda_N \gg d_N, \lambda_{IEE} = \frac{1}{2} d_N \theta_{SH}$$

$$\lambda_N \ll d_N, \lambda_{IEE} = \lambda_N \theta_{SH}$$

Using spin Hall angle to determine conversion ratio of 3D j_c and 2D j_s can lead to “unphysical” value (> 1).

Ex: $\theta_{SH} = 1.6$ for α -Sn if compared with W

Questions

1. Does ferromagnetic metal suppress topological surface states?
2. Can spin pumping distinguish surface and bulk effects (IEE and ISHE) of Bi_2Se_3 ?

Structure		Journal	method	Spin-charge ratio	Importance
Py	Si (001)	Nat. Commun. 4 , 2944 (2013) (A. Fert)	Spin pumping	300K: 0.09 ~ 0.2 0.3 nm	First demonstration of RT IEE with Rasba alloys Ag/Bi
Ag					
Bi					
Py	Al ₂ O ₃	Nature 511 , 449 (2014) (D. Ralph)	ST-FMR	300K: 2 ~ 3.5	Giant RT spin torque ratio of Bi ₂ Se ₃ "Signature" of RT EE
Bi ₂ Se ₃					
Py	Al ₂ O ₃	PRB 90 , 094403 (2014) (S. Oh)	Spin pumping	300K: 0.009 15K: 0.02	ISHE of Bi ₂ Se ₃
Bi ₂ Se ₃					
Py	Bi ₂ Se ₃ , BSTS, and Sn-BTS	PRL 113 , 196601 (2014) (E. Saitoh)	Spin pumping	15K: ~10 ⁻⁴	Low T IEE of TIs (crystal)
Co ₄₀ Fe ₄₀ B ₂₀	Al ₂ O ₃	PRL 114 , 257202 (2015) (S. Oh)	ST-FMR	300K: 0.047 50K: 0.42	Large Low T spin torque ratio of Bi ₂ Se ₃ "Signature" of RT EE
Bi ₂ Se ₃					

Structure		Journal	method	Spin-charge ratio	Importance
Py	Bi ₂ Se ₃	Sci. Rep. 5 , 7907 (2015) (University of Oxford)	Spin pumping	--	Atypical thickness dependence of mixing conductance
	Co ₅₀ Fe ₅₀				
Co ₂₀ Fe ₆₀ B ₂₀	Bi ₂ Se ₃	Nano Lett. 15 , 7126 (2015) (Jian-Ping Wang, University of Minnesota)	Spin pumping	300K: 0.43	Giant RT ISHE of Bi ₂ Se ₃
	InP				
Fe	Ag	PRL 116 , 096602 (2016) (A. Fert)	Spin pumping	300K: 0.62 ~ 1.5 2.1 nm	Giant RT IEE of TI Sn
	Sn				
	InSb (001)				
Py	Bi ₂ Te ₃	PRB 92 , 241304(R) (2015) (S. F. Lee)	Spin pumping	5 K: 0.003 ~ 0.0062	“Signature” of low T IEE of Bi ₂ Te ₃ Low T ISHE of Bi ₂ Te ₃
	Al ₂ O ₃				
	Bi ₂ Se ₃	PRL 117 , 076601 (2018) (N. Samarth)	Spin pumping	300 K IEE length: 0.04 nm	First study on FI/TI
	YIG				

Structure	Journal	method	Spin-charge ratio	Importance
Py	PRB 90 , 094403 (2014) (S. Oh)	Spin pumping	300K: 0.009 15K: 0.02	ISHE of Bi ₂ Se ₃
Bi ₂ Se ₃				
Al ₂ O ₃				

PHYSICAL REVIEW B **90**, 094403 (2014)

Observation of inverse spin Hall effect Nothing new. in bismuth selenide

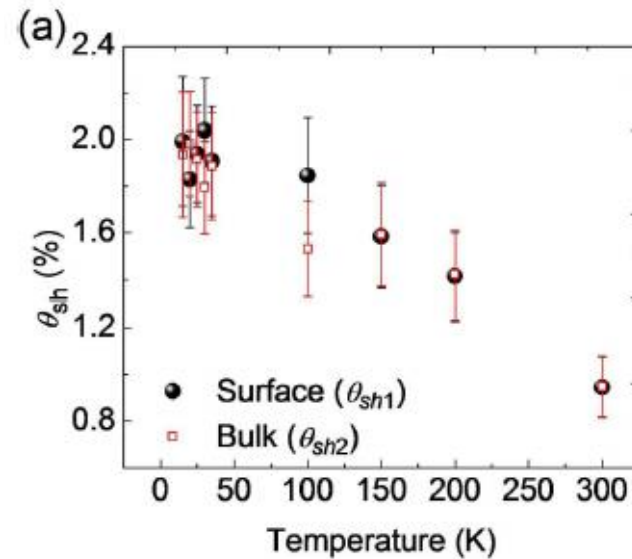
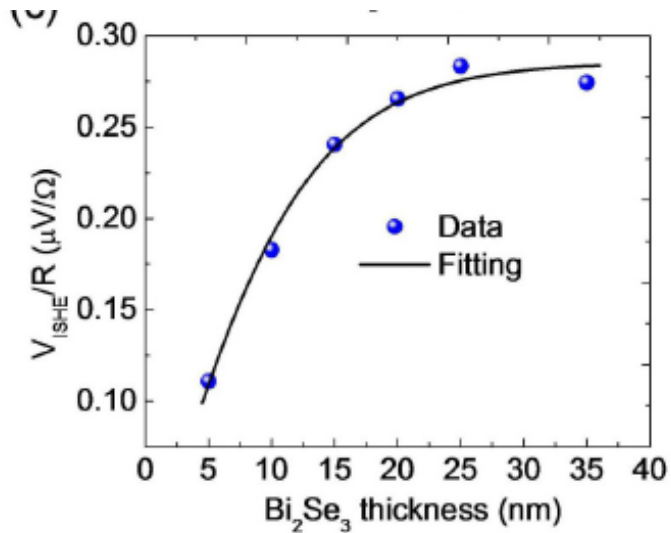
Praveen Deorani,¹ Jaesung Son,¹ Karan Banerjee,¹ Nikesh Koirala,² Matthew Brahlek,² Seongshik Oh,² and Hyunsoo Yang^{1,*}

¹*Department of Electrical and Computer Engineering, National University of Singapore, 117576, Singapore*

²*Department of Physics & Astronomy, Rutgers Center for Emergent Materials, Institute for Advanced Materials, Devices and Nanotechnology, The State University of New Jersey, New Jersey 08854, USA*

(Received 19 April 2014; revised manuscript received 20 August 2014; published 3 September 2014)

Bismuth Selenide (Bi₂Se₃) is a topological insulator exhibiting helical spin polarization and strong spin-orbit coupling. The spin-orbit coupling links the charge current to spin current via the spin Hall effect (SHE). We demonstrate a Bi₂Se₃ spin detector by injecting the pure spin current from a magnetic permalloy layer to a Bi₂Se₃ thin film and detect the inverse SHE in Bi₂Se₃. The spin Hall angle of Bi₂Se₃ is found to be 0.0093 ± 0.0013 and the spin diffusion length in Bi₂Se₃ to be 6.2 ± 0.15 nm at room temperature. Our results suggest that topological insulators with strong spin-orbit coupling can be used in functional spintronic devices.



was taken to be of opposite signs. Fitting the measured data, we obtain $\theta_{\text{sh}1}$ at surface and $\theta_{\text{sh}2}$ at bulk for each temperature as shown in Fig. 4(a), which does not show any clear distinction between the surface and bulk value. Figure 4(b) shows the λ_{sf}

In order to distinguish the surface and bulk contributions, they assumed a spin Hall angle $\theta_{\text{sh}1}$ for TSS, believing that TSS would give far larger spin Hall angle than the bulk. However, the fitting results show that $\theta_{\text{sh}1} \approx \theta_{\text{sh}2}$. That is, no TSS features were revealed in this work.

Structure	Journal	method	Spin-charge ratio	Importance
Py Bi ₂ Se ₃ , BSTS, and Sn-BTS	PRL 113 , 196601 (2014) (E. Saitoh)	Spin pumping	15K: $\sim 10^{-4}$	Low T IEE of TIs (crystal)

PRL 113, 196601 (2014)

PHYSICAL REVIEW LETTERS

week ending
7 NOVEMBER 2014

Spin-Electricity Conversion Induced by Spin Injection into Topological Insulators

Y. Shiomi,¹ K. Nomura,¹ Y. Kajiwara,¹ K. Eto,² M. Novak,² Kouji Segawa,² Yoichi Ando,² and E. Saitoh^{1,3,4,5}

¹*Institute for Materials Research, Tohoku University, Sendai 980-8577, Japan*

²*Institute of Scientific and Industrial Research, Osaka University, Ibaraki, Osaka 567-0047, Japan*

³*WPI Advanced Institute for Materials Research, Tohoku University, Sendai 980-8577, Japan*

⁴*CREST, Japan Science and Technology Agency, Tokyo 102-0076, Japan*

⁵*Advanced Science Research Center, Japan Atomic Energy Agency, Tokai 319-1195, Japan*

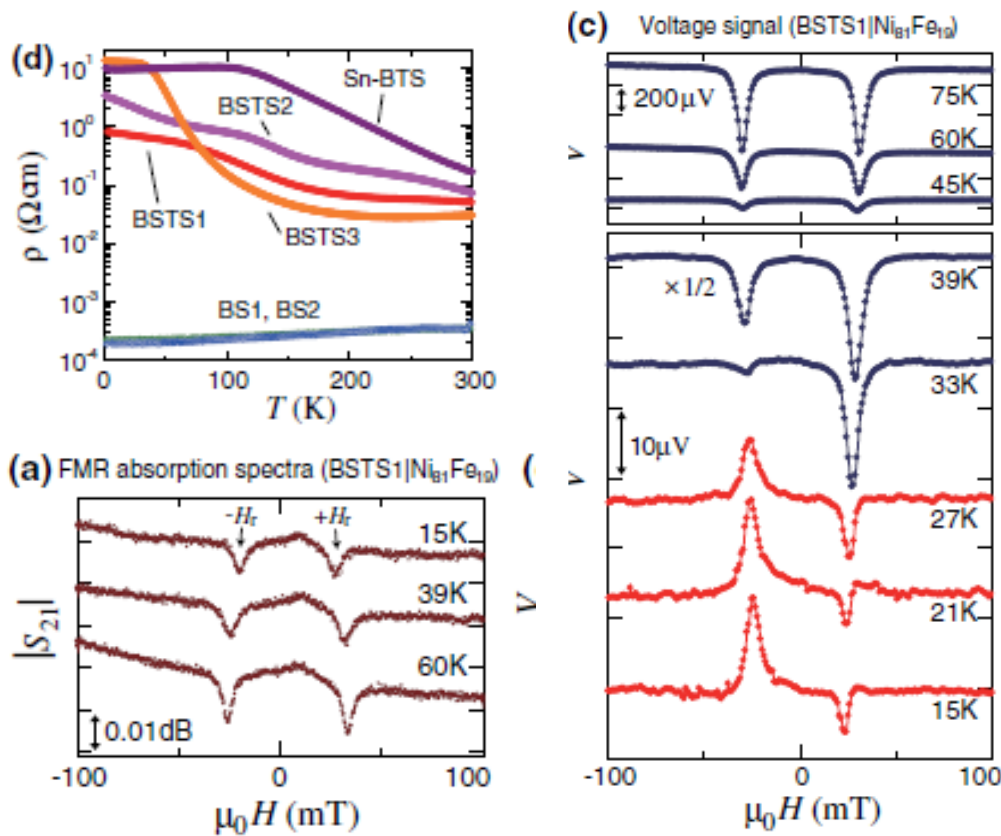
(Received 11 May 2014; published 3 November 2014)

We report successful spin injection into the surface states of topological insulators by using a spin pumping technique. By measuring the voltage that shows up across the samples as a result of spin pumping, we demonstrate that a spin-electricity conversion effect takes place in the surface states of bulk-insulating topological insulators Bi_{1.5}Sb_{0.5}Te_{1.7}Se_{1.3} and Sn-doped Bi₂Te₂Se. In this process, the injected spins are converted into a charge current along the Hall direction due to the spin-momentum locking on the surface state.

DOI: 10.1103/PhysRevLett.113.196601

PACS numbers: 72.25.Pn, 72.25.Dc, 73.20.-r, 75.76.+j

Obviously, they have realized the difficulties of separating surface and bulk effects. So they choose bulk-insulating BSTS to rule out ISHE. However, the very small spin-charge ratio is very puzzling. (Question 1)



The data show negative field shifts as T became lower, similar to Faris' data. However, they did not mention this.

unit vector perpendicular to the plane. Here, due to the strictly 2D nature, spins do not “flow” along the z direction within the surface state and the converted charge current J_c has the 2D nature. Hence, the mechanism of this spin-electricity conversion is different from that in the inverse spin Hall effect, where a spin current flowing within a finite thickness of a sample is converted into a 3D charge current along the Hall direction. samples [Fig. 3(a)]. It is worth mentioning that the present spin-electricity conversion effect is rather similar to that reported in Rashba-split systems [31,32], but the efficiency is, in principle, much higher in TIs than that in the Rashba-split system [33]. The spin-momentum locking on a single Dirac cone predicts efficient spin-electricity conversion in TIs even at room temperature as long as the surface state is robust, while in the Rashba-split systems where a pair of bands exist, one of the bands counteracts the effect of the other.

The thing is, are TSS still “robust” in this structure?

to the spin-momentum locking. Though the efficiency of the spin-electricity conversion in the present work is as small as $\eta \sim 10^{-4}$, the spin-momentum locking on topological surface states can, in principle, lead to efficient conversion between spin and electricity.

Structure	Journal	method	Spin-charge ratio	Importance
Co ₂₀ Fe ₆₀ B ₂₀	Nano Lett. 15 , 7126 (2015) (Jian-Ping Wang, University of Minnesota)	Spin pumping	300K: 0.015 ~ 0.43	Giant RT ISHE of Bi ₂ Se ₃
Bi ₂ Se ₃				
InP				

NANO LETTERS

Letter

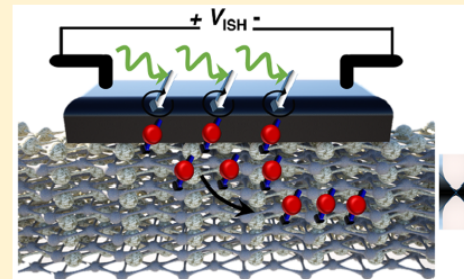
pubs.acs.org/NanoLett

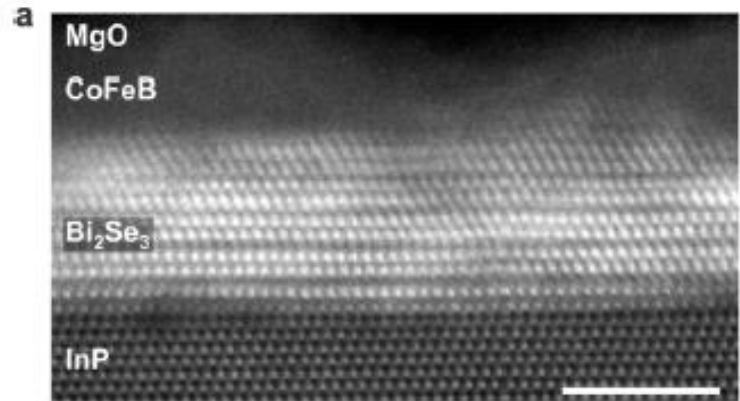
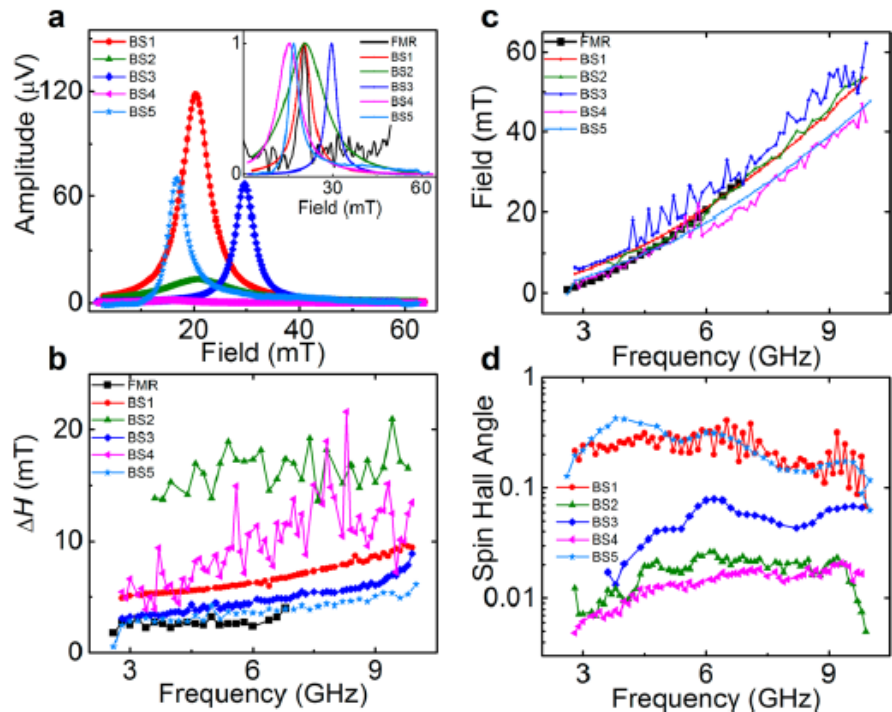
Nothing new in physics again.

Giant Spin Pumping and Inverse Spin Hall Effect in the Presence of Surface and Bulk Spin–Orbit Coupling of Topological Insulator Bi₂Se₃

Mahdi Jamali,[†] Joon Sue Lee,[‡] Jong Seok Jeong,[§] Farzad Mahfouzi,^{||} Yang Lv,[†] Zhengyang Zhao,[†] Branislav K. Nikolić,[⊥] K. Andre Mkhoyan,[§] Nitin Samarth,^{*,‡} and Jian-Ping Wang^{*,†}

ABSTRACT: Three-dimensional (3D) topological insulators are known for their strong spin–orbit coupling (SOC) and the existence of spin-textured surface states that might be potentially exploited for “topological spintronics.” Here, we use spin pumping and the inverse spin Hall effect to demonstrate successful spin injection at room temperature from a metallic ferromagnet (CoFeB) into the prototypical 3D topological insulator Bi₂Se₃. The spin pumping process, driven by the magnetization dynamics of the metallic ferromagnet, introduces a spin current into the topological insulator layer, resulting in a broadening of the ferromagnetic resonance (FMR) line width. Theoretical modeling of spin pumping through the surface of Bi₂Se₃, as well as of the measured angular dependence of spin-charge conversion signal, suggests that pumped spin current is first greatly enhanced by the surface SOC and then converted into a dc-voltage signal primarily by the inverse spin Hall effect due to SOC of the bulk of Bi₂Se₃. We find that the FMR line width broadens significantly (more than a factor of 5) and we deduce a spin Hall angle as large as 0.43 in the Bi₂Se₃ layer.





The wide fluctuation of spin pumping signals from sample to sample could be explained based on the nonuniform composition of Bi_2Se_3 at its interface with the magnetic layer. Recently, it has been shown that surfaces of TIs are very nonuniform in terms of chemical potential and position of Dirac point.⁵³ Because the $\text{Bi}_2\text{Se}_3/\text{CoFeB}$ interface plays the major role in the spin injection, the large variations of the spin pumping characteristics could be associated with nonuniform Bi_2Se_3 surface. Moreover, the decapping process could also be responsible for modification of the TI surface considering Bi_2Se_3 has strong thermoelectric properties.⁵⁴ Comparing the samples BS1–4 with BS5, BS5 is not involved in any high-temperature decapping process and we obtain the maximum spin Hall angle in this sample. This suggests that heat treatment temperature and a large spin Hall angle. In highly bulk-conductive Bi_2Se_3 TIs, the inverse Hall effect of the bulk seems to dominate over the inverse Edelstein effect of the surface state, at least in spin pumping experiments. Moreover, we find

(Question 2??)

The samples had severely degraded. All of the curves should be smooth, so the calculated spin Hall angles are questionable.

Structure		Journal	method	Spin-charge ratio	Importance
Fe		PRL 116 ,096602 (2016) (A. Fert)	Spin pumping	300K: 0.62 ~ 1.5	Giant RT IEE of TI Sn
Ag					
Sn					
InSb (001)					

Spin-pumping into surface states of topological insulator α -Sn, spin to charge conversion

at room temperature

J.-C. Rojas-Sánchez^{1,2*}, S. Oyarzun^{3,4}, Y. Fu^{3,4}, A. Marty^{3,4}, C. Vergnaud^{3,4}, S. Gambarelli^{3,4}, L. Vila^{3,4},
M. Jamet^{3,4}, Y. Ohtsubo^{5,6}, A. Taleb-Ibrahimi^{7,8}, P. Le Fèvre⁸, F. Bertran⁸, N. Reyren^{1,2*}, J.-M. George^{1,2} and
A. Fert^{1,2}

1 Unité Mixte de Physique CNRS/Thales, 91767 Palaiseau, France

2 Université Paris-Sud, Université Paris-Saclay, UMR137, 91767 Palaiseau, France

3 Université Grenoble Alpes, INAC-SP2M, F-38000 Grenoble, France

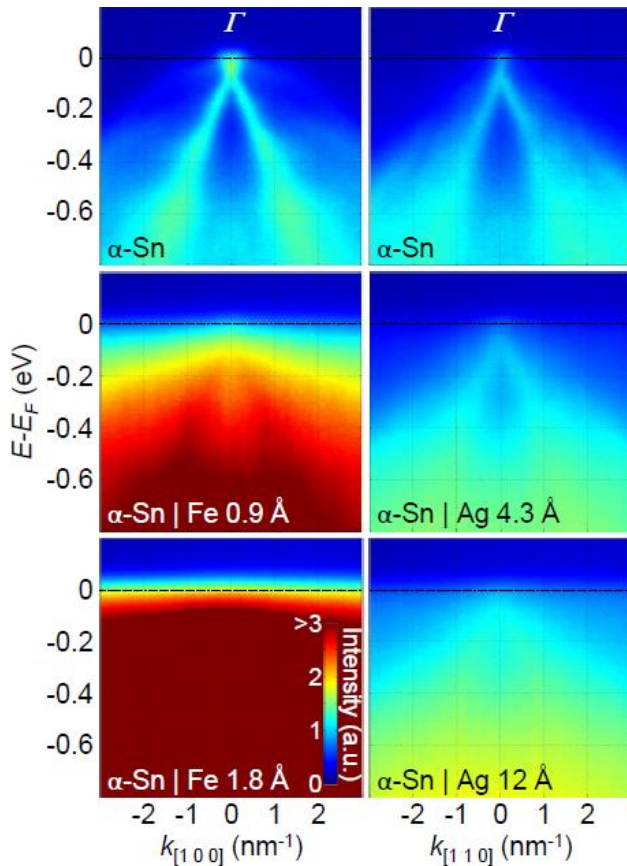
4 CEA, Institut Nanosciences et Cryogénie, F-38000 Grenoble, France

5 Graduate School of Frontier Biosciences, Osaka University, Suita 565-0871, Japan

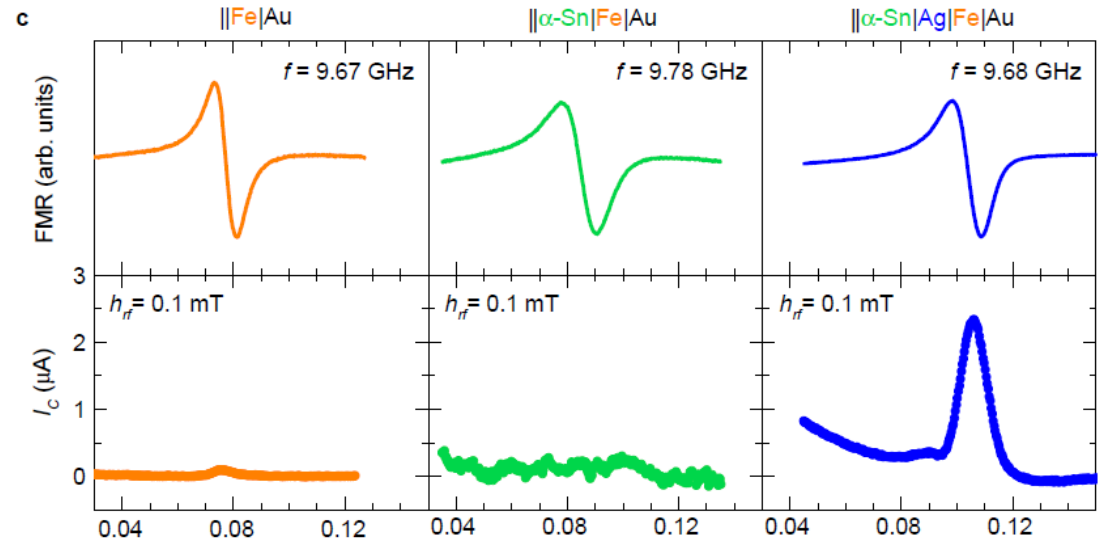
6 Graduate School of Science, Osaka University, Toyonaka 560-0043, Japan

7 UR1 CNRS, Synchrotron SOLEIL, Saint-Aubin, 91192 Gif sur Yvette, France

8 Synchrotron SOLEIL, Saint-Aubin, 91192 Gif sur Yvette, France



Fermi level is very closed to the Dirac point of Sn. TSS disappeared when Fe was deposited on top. (Question 1)



surfaces” of TI²². We believe that the long relaxation time on free topological surfaces characterizes the slow relaxation inside the 2D topological states whereas, by interfacing the TI (or Rashba) surface with a metal as Ag, we introduce a faster additional relaxation mechanism provided by exchanges of electrons with the adjacent 3D metal. We conclude that the best conditions for the exploitation of topological states of TI in spintronics should be with TI interfaced with (trivial) insulators instead of metals, for example in experiments of spin-pumping or thermal²³ spin injection from an insulating ferromagnet. If one remarks that $v_F \tau$ is also the critical length for

Could this explain the small spin-charge ratio from the Japanese group’s work?

Structure	Journal	method	Spin-charge ratio	Importance
Bi ₂ Se ₃ YIG	PRL 117 , 076601 (2018) (N. Samarth)	Spin pumping	300 K IEE length: 0.04 nm	First study on FI/TI

Surface-State-Dominated Spin-Charge Current Conversion in Topological-Insulator–Ferromagnetic-Insulator Heterostructures

Hailong Wang,¹ James Kally,¹ Joon Sue Lee,¹ Tao Liu,² Houchen Chang,² Danielle Reifsnnyder Hickey,³
K. Andre Mkhoyan,³ Mingzhong Wu,² Anthony Richardella,¹ and Nitin Samarth^{1,*}

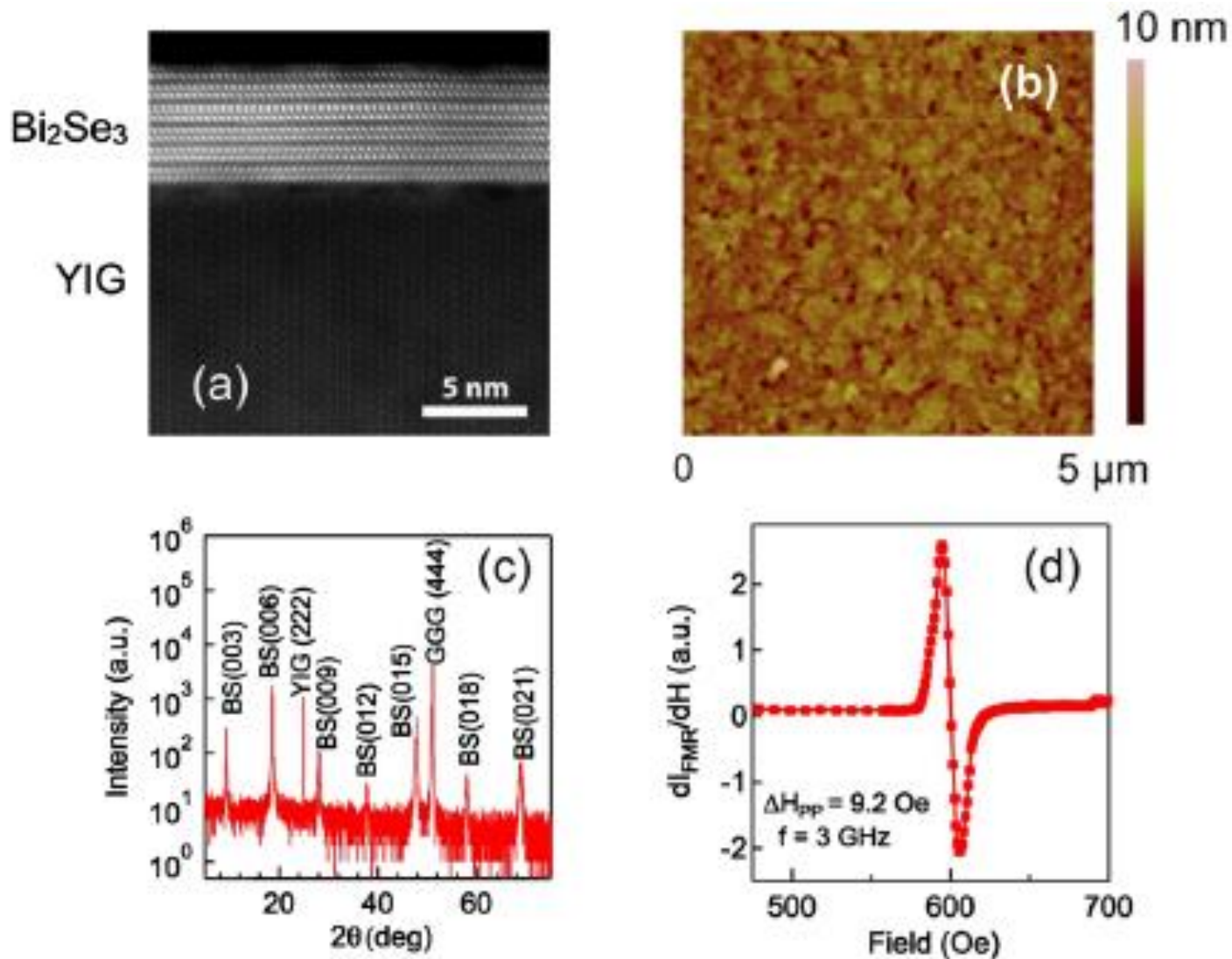
¹*Department of Physics, The Pennsylvania State University, University Park, Pennsylvania 16802, USA*

²*Department of Physics, Colorado State University, Fort Collins, Colorado 80523, USA*

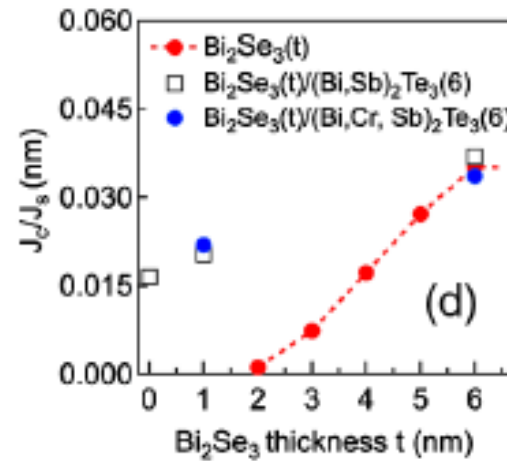
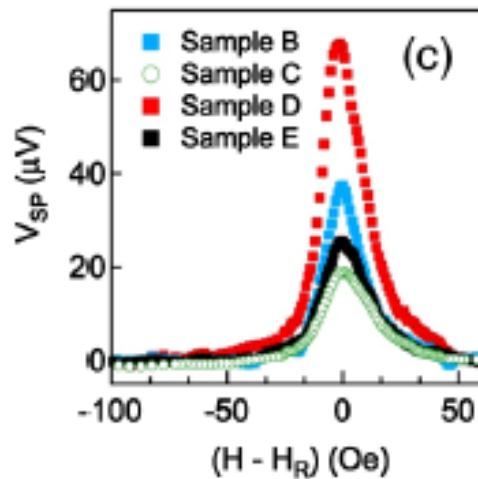
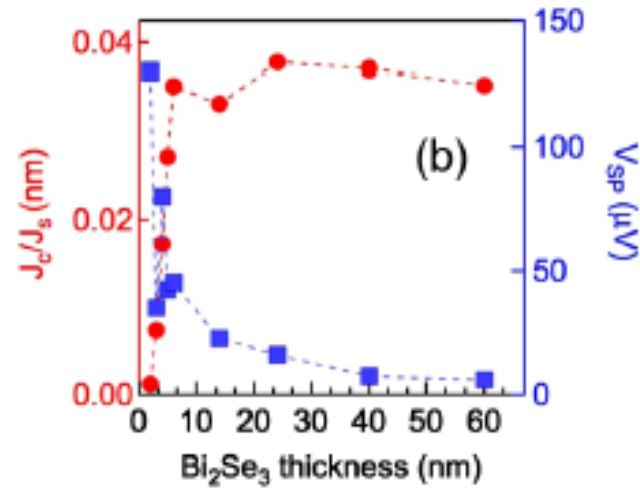
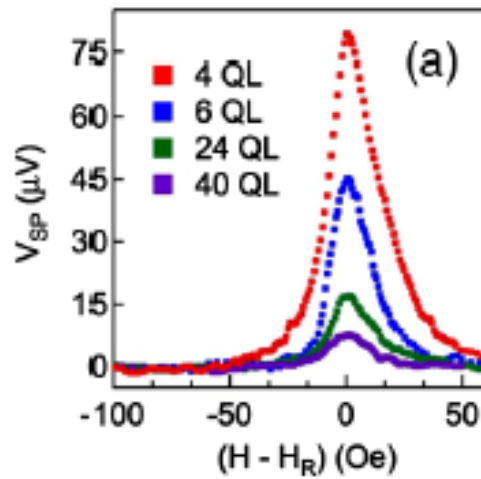
³*Department of Chemical Engineering and Materials Science, University of Minnesota, Minneapolis, Minnesota 55455, USA*

(Received 8 February 2016; revised manuscript received 19 May 2016; published 11 August 2016)

We report the observation of ferromagnetic resonance-driven spin pumping signals at room temperature in three-dimensional topological insulator thin films—Bi₂Se₃ and (Bi, Sb)₂Te₃—deposited by molecular beam epitaxy on Y₃Fe₅O₁₂ thin films. By systematically varying the Bi₂Se₃ film thickness, we show that the spin-charge conversion efficiency, characterized by the inverse Rashba-Edelstein effect length (λ_{IREE}), increases dramatically as the film thickness is increased from two quintuple layers, saturating above six quintuple layers. This suggests a dominant role of surface states in spin and charge interconversion in topological-insulator–ferromagnet heterostructures. Our conclusion is further corroborated by studying a series of Y₃Fe₅O₁₂/(Bi, Sb)₂Te₃ heterostructures. Finally, we use the ferromagnetic resonance linewidth broadening and the inverse Rashba-Edelstein signals to determine the effective interfacial spin mixing conductance and λ_{IREE} .



There is an amorphous interlayer between Bi_2Se_3 and YIG, which prevent a direct coupling between Bi_2Se_3 and YIG.



Surface-state-dominated spin-to-charge conversion is confirmed by:

1. Unique Bi_2Se_3 thickness dependence, in which a maximum SCC occurs at the 2D limit of Bi_2Se_3 .
2. Changing the bulk band of TIs while preserving the Bi_2Se_3 surface states does not affect SCC much (questionable).

Structure	Journal	method	Spin-charge ratio	Importance
Py Bi ₂ Se ₃ Al ₂ O ₃	Nature 511 , 449 (2014) (D. Ralph)	ST-FMR	300K: 2 ~ 3.5	Giant RT spin torque ratio of Bi ₂ Se ₃ “Signature” of RT EE

LETTER

doi:10.1038/nature13534

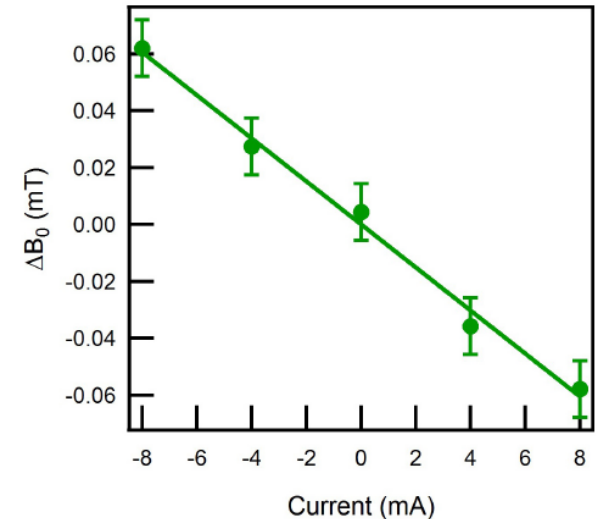
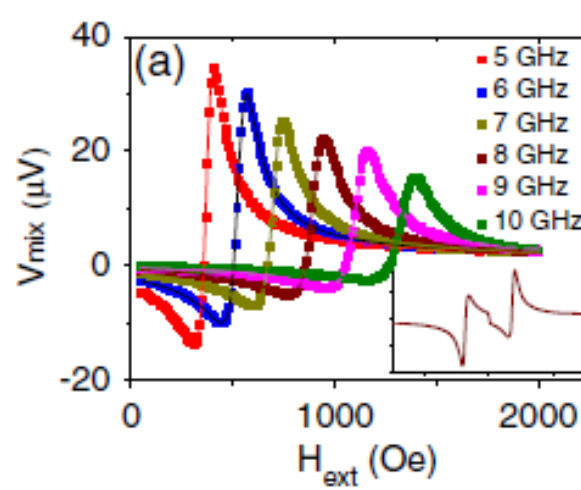
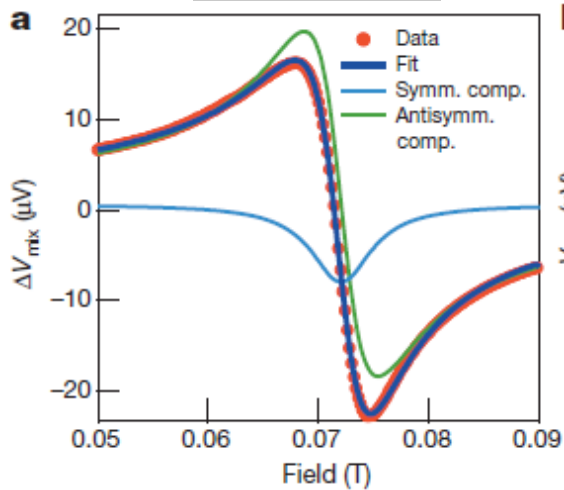
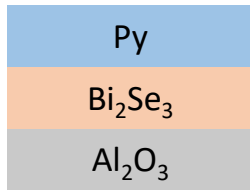
Spin-transfer torque generated by a topological insulator

A. R. Mellnik¹, J. S. Lee², A. Richardella², J. L. Grab¹, P. J. Mintun¹, M. H. Fischer^{1,3}, A. Vaezi¹, A. Manchon⁴, E.-A. Kim¹, N. Samarth² & D. C. Ralph^{1,5}

Signatures of Edelstein effect (EE):

1. Large anti-symmetric component of voltage signals.
2. Resonance field shifts.

The two features result from **non-equilibrium spin density** at TSS.



Large antisymmetric component for Bi₂Se₃/Py. In contrast, symmetric signals dominate for Pt/Py (without EE).

The resonance field shifted when applying dc current. From the shifts, magnitude of field-like torques can be determined.

any previously measured spin current source material. However, as noted above, for practical applications the specific layer structure of our devices (topological insulator/metallic magnet) does not make good use of this high intrinsic spin Hall effect through the generation of spin currents. They did not do Bi₂Se₃ thickness dependence measurement, so it's still hard to extract the EE. require coupling to metallic magnets so that the majority of the current will flow in the topological

insulator. Using insulating magnets may also have the advantage of providing much less Gilbert damping than do metallic magnets²⁹, which is present for magnetic bilayers. Additionally, the use of insulating bilayers eliminates any deleterious effects of bulk conduction. Our results therefore point towards

Structure	Journal	method	Spin-charge ratio	Importance
<div style="background-color: #ADD8E6; padding: 2px; text-align: center;">$\text{Co}_{40}\text{Fe}_{40}\text{B}_{20}$</div> <div style="background-color: #FFDAB9; padding: 2px; text-align: center;">Bi_2Se_3</div> <div style="background-color: #A9A9A9; padding: 2px; text-align: center;">Al_2O_3</div>	PRL 114 , 257202 (2015) (S. Oh)	ST-FMR	300K: 0.047 50K: 0.42	Large Low T spin torque ratio of Bi_2Se_3 “Signature” of RT EE

PRL **114**, 257202 (2015)

PHYSICAL REVIEW LETTERS

week ending
26 JUNE 2015

Topological Surface States Originated Spin-Orbit Torques in Bi_2Se_3

Yi Wang,¹ Praveen Deorani,¹ Karan Banerjee,¹ Nikesh Koirala,² Matthew Brahlek,² Seongshik Oh,² and Hyunsoo Yang^{1,*}

¹*Department of Electrical and Computer Engineering, National University of Singapore, 117576 Singapore, Singapore*

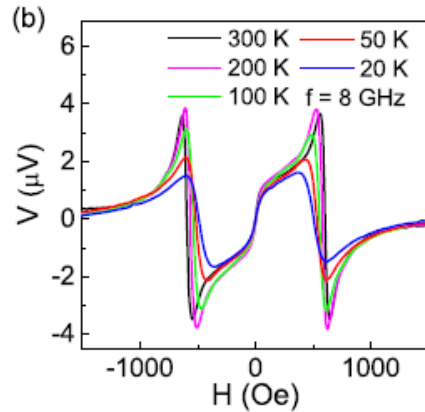
²*Department of Physics and Astronomy, Rutgers, The State University of New Jersey, Piscataway, New Jersey 08854, USA*

(Received 4 February 2015; revised manuscript received 27 April 2015; published 24 June 2015)

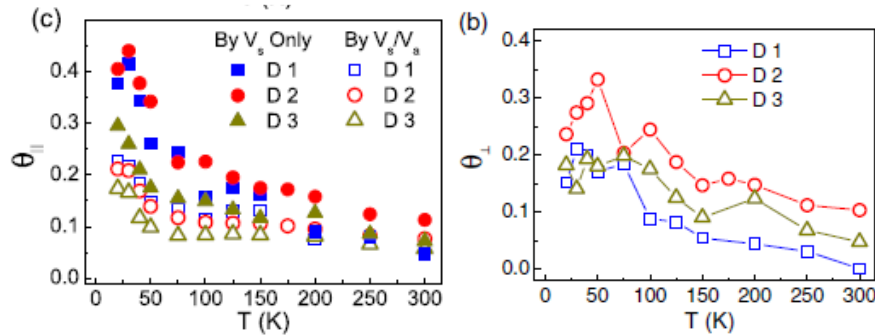
The three dimensional topological insulator bismuth selenide (Bi_2Se_3) is expected to possess strong spin-orbit coupling and spin-textured topological surface states and, thus, exhibit a high charge to spin current conversion efficiency. We evaluate spin-orbit torques in $\text{Bi}_2\text{Se}_3/\text{Co}_{40}\text{Fe}_{40}\text{B}_{20}$ devices at different temperatures by spin torque ferromagnetic resonance measurements. As the temperature decreases, the spin-orbit torque ratio increases from ~ 0.047 at 300 K to ~ 0.42 below 50 K. Moreover, we observe a significant out-of-plane torque at low temperatures. Detailed analysis indicates that the origin of the observed spin-orbit torques is topological surface states in Bi_2Se_3 . Our results suggest that topological insulators with strong spin-orbit coupling could be promising candidates as highly efficient spin current sources for exploring the next generation of spintronic applications.

DOI: 10.1103/PhysRevLett.114.257202

PACS numbers: 75.76.+j, 72.25.Dc, 73.20.-r, 85.75.-d



Large antisymmetric component of voltage.



Spin-charge ratio was greatly enhanced at low T. But the RT values are two order of magnitudes smaller than that from the Cornell group.

On the other hand, a possible out-of-plane spin polarization in the TSS has been theoretically predicted [55,56] and experimentally observed in Bi_2Se_3 [57,58], which is attributed to the hexagonal warping effect in the Fermi surface [55,59]. This out-of-plane spin polarization in the TSS can account for the observed $\Delta\tau$ especially in the low temperature range (<50 K), and the $\Delta\tau$ adds to the τ_{Oe} [27,31]. Moreover, as shown in Figs. 3(a) and 4(a), the out-of-plane torque ($\Delta\tau$) has the same order of magnitude comparable to the in-plane torque (τ_{\parallel}) below 50 K ($\Delta\tau/\tau_{\parallel} \sim 60\%$) [37], which is in agreement with the behavior of hexagonal TSS in TI [55,56]. With the analysis from different aspects, our findings especially in the low temperature range (<50 K) indicate a TSS origin of spin-orbit torques in Bi_2Se_3 and CFB.

They explained the origin of field-like torques with spin texture only qualitatively. They did not resort to the model proposed by the Cornell group.

Questions

1. Does ferromagnetic metal suppress topological surface states?

Yes. (A. Fert and E. Saitoh)

2. Can spin pumping distinguish surface and bulk effects (IEE and ISHE) of Bi_2Se_3 ?

It's difficult for TI/FM, but how about FI/TI?

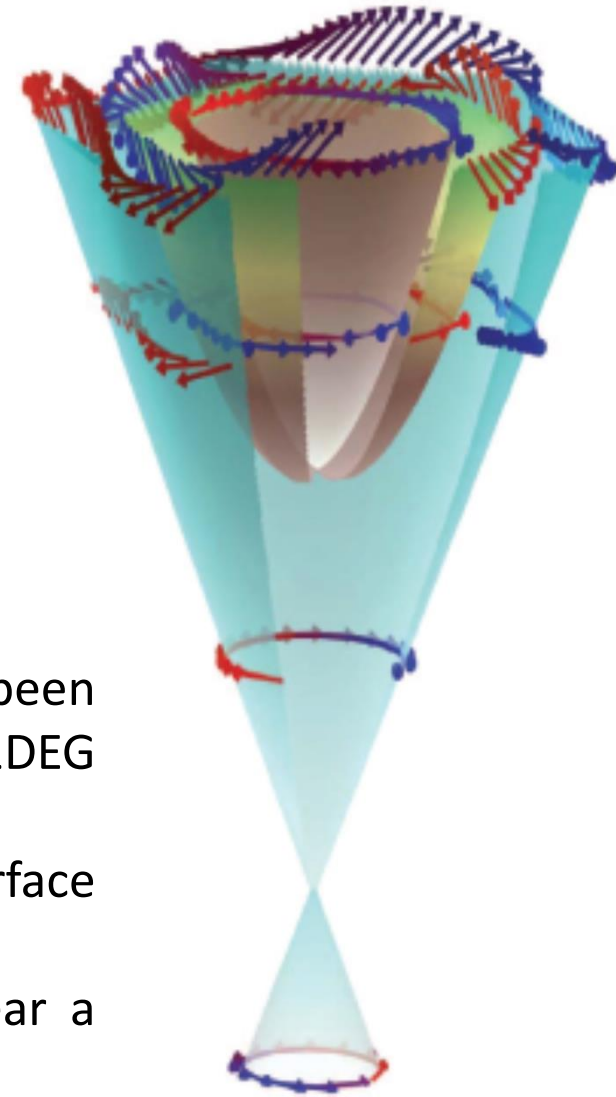
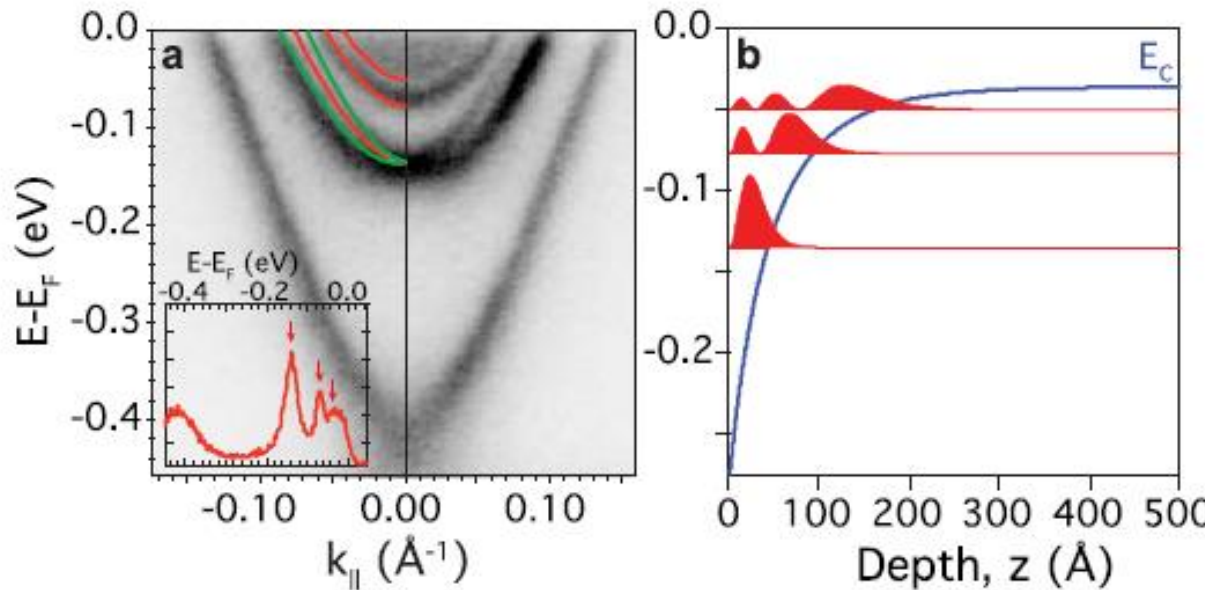
3. Now that ST-FMR have shown the signature of EE with large field-like torques, which come from non-equilibrium spin density, is it possible to observe similar effect (IEE) with spin pumping?

Note that in A. Fert's work they did not deposit Fe directly on Sn. A Ag layer may weaken the effect of non-equilibrium spin density, which is localized, on Fe. That is, the Ag layer separate Fe and Sn out of the range of exchange coupling. Therefore, "signatures (negative field shift)" of IEE were not observed.

More questions

- How does the ac component of the pumped spin current affect the TSS?
- How does spin canting of TSS affect the spin transport properties?

Spin texture of Bi_2Se_3



- Large Rashba splitting of 2DEG in Bi_2Se_3 has been confirmed by ARPES. The interplay between TSS and 2DEG leads to intricate spin texture.
- The spin pumping effect strongly depends on the interface electronic structure and spin texture.
- The spin transport of topological interface state near a magnetic layer is of further interest to investigate.

King et. al., PRL **107**, 096802 (2011)

Bahramy et. al., Nat. Commun. **3**, 1159 (2012)



Spin transport and interfacial exchange coupling in topological insulator/magnetic insulator heterostructure

Yu-Ting Fanchiang, Y. H. Lin, K. Y. Lin, C. K. Cheng, M. Hong

Department of Physics, National Taiwan University

H. Y. Hung, C. N. Wu, Y. C. Liu, H. Y. Lin, K. H. Chen, C. C. Tseng, C. C. Chen, S. R. Yang, S. W. Huang, J. Kwo

Department of Physics, National Tsing-Hua University

S. F. Lee

Institute of Physics, Academia Sinica

J. G. Lin

Center for Condensed Matter Sciences, National Taiwan University

Outline

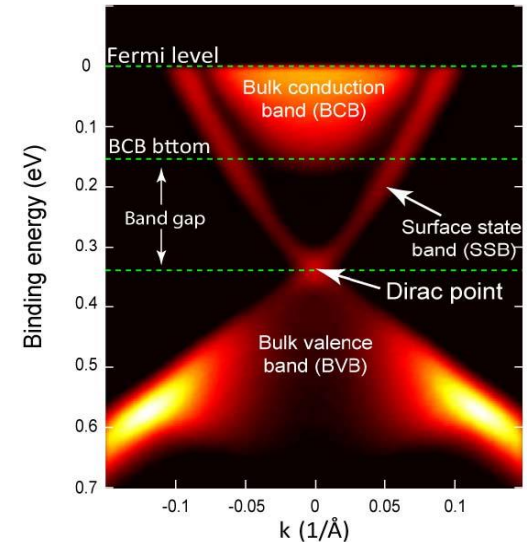
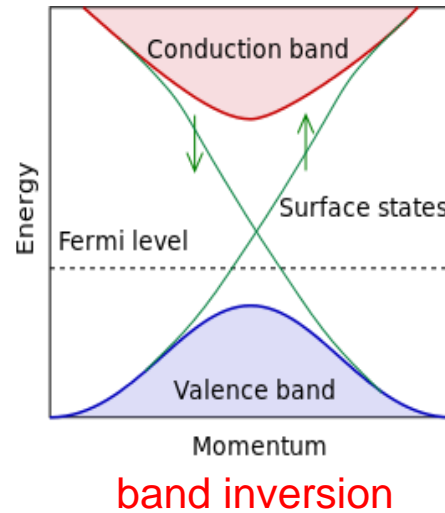
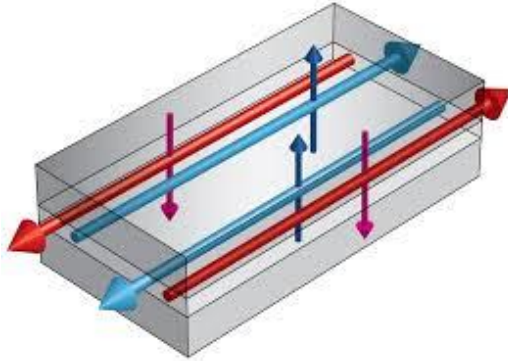
Introduction

- Spin pumping in topological insulators (TIs)
- Magnetic proximity effect (MPE) in TI/magnetic insulator heterostructures

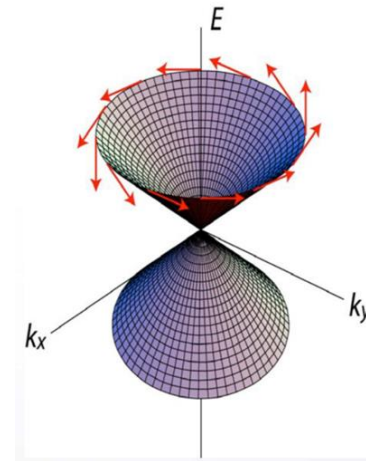
Experimental results

- Spin pumping and spin-to-charge conversion (SCC) in TI/ferromagnetic metals
- Surface-state-modulated magnetization dynamics in $\text{Bi}_2\text{Se}_3/\text{YIG}$
- Spin pumping in transferred- $\text{Bi}_2\text{Se}_3/\text{YIG}$ and $\text{Bi}_2\text{Se}_3/\text{Au}/\text{YIG}$ trilayer
- Evidence for exchange Dirac gap in magneto-transport of topological insulator-magnetic insulator heterostructures

Topological insulators (TI)



Electronic band structure along K- Γ -K of undoped **Bi₂Se₃** by ARPES, Y. L. Chen et al, Science, (2010).



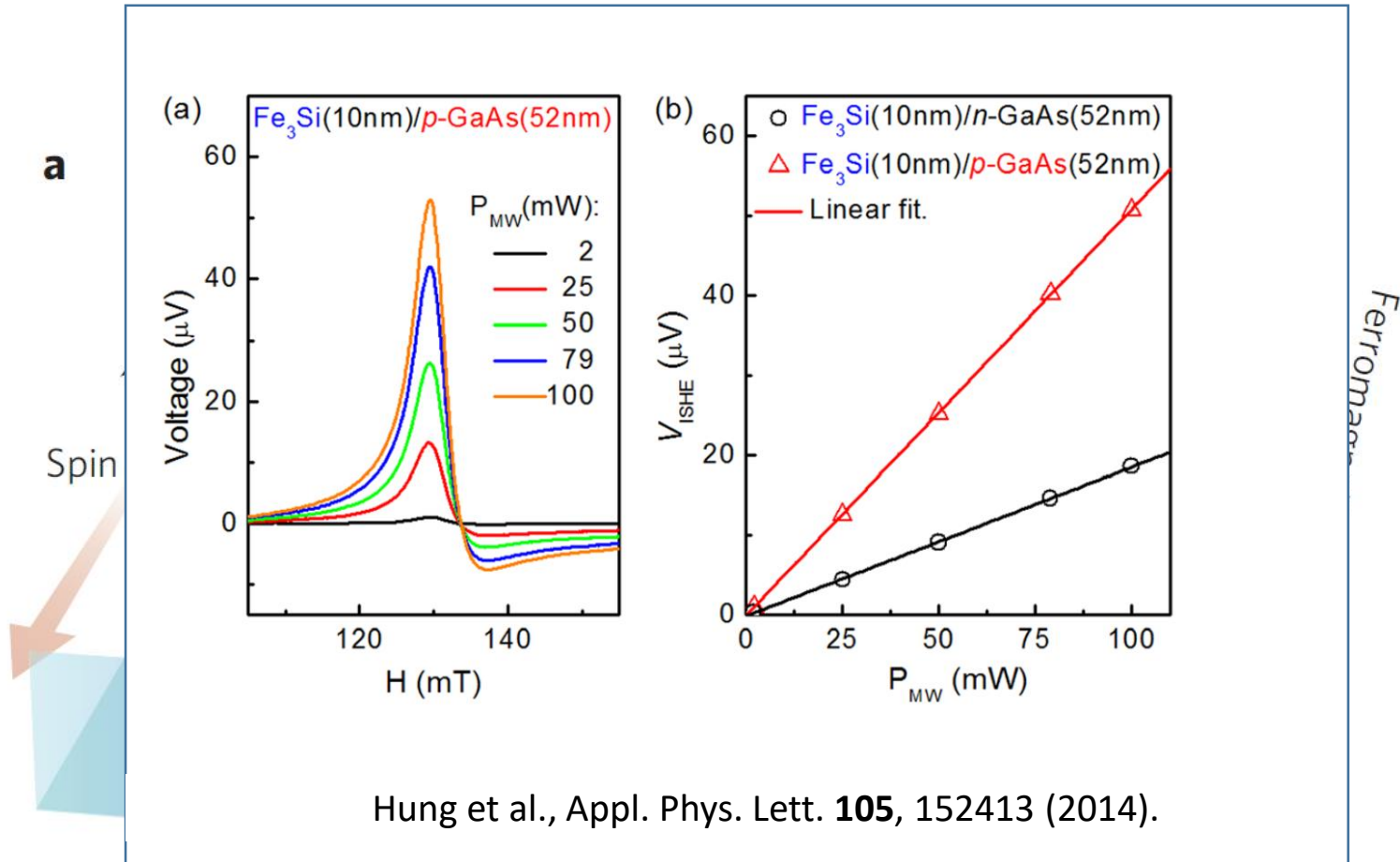
■ Extraordinary physical properties

- Quantum spin Hall state
- Spin-momentum locking

■ Applications

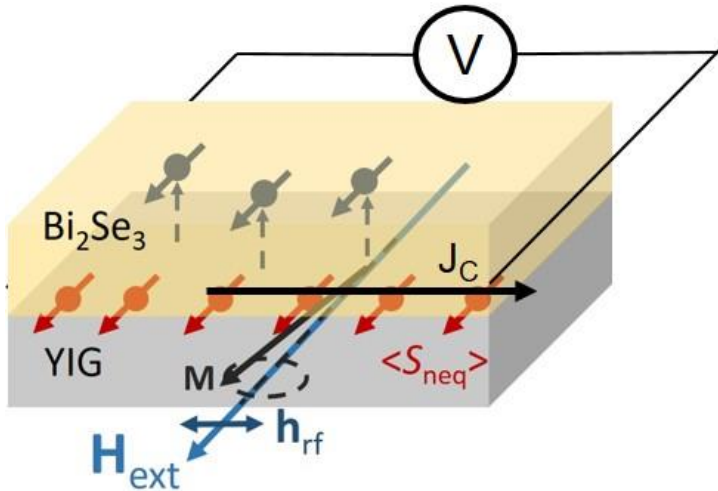
- Low dissipation spintronics and spin-caloritronics
- High spin-charge conversion device, such as a “spin battery”.
- Interface of TI and superconductor - Majorana fermion, quantum computation

Spin pumping: a solution to impedance mismatch problem



Ando et al., Nat. Mater. **10**, 655 (2013).

Spin pumping as an effective way to probe the spin-momentum locking



Spin pumping: a widely used spin injection method
FMR in the magnetic layer

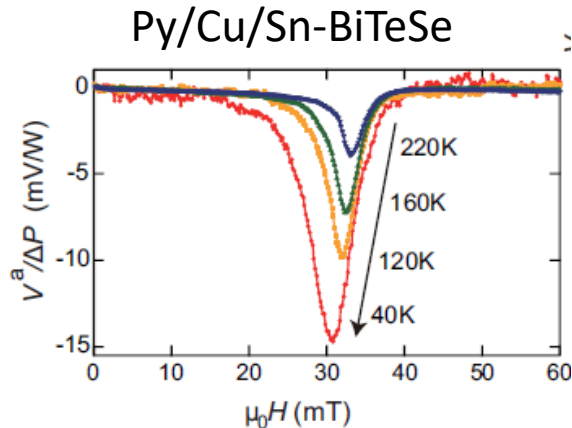
→ Exchange interaction at the interface: **transfer of spin angular momentum**

→ Spin accumulation at the interface

→ **Charge current generated via spin-momentum locking**

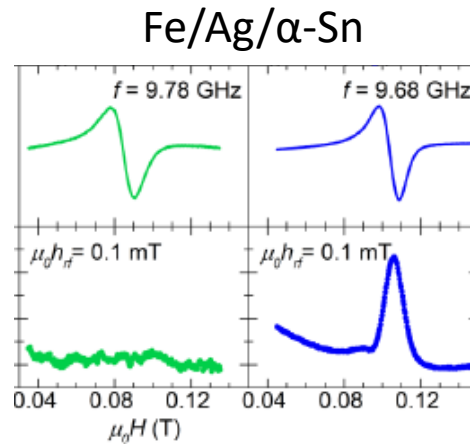
Various material systems and experimental configurations have been reported.

E. Saitoh group



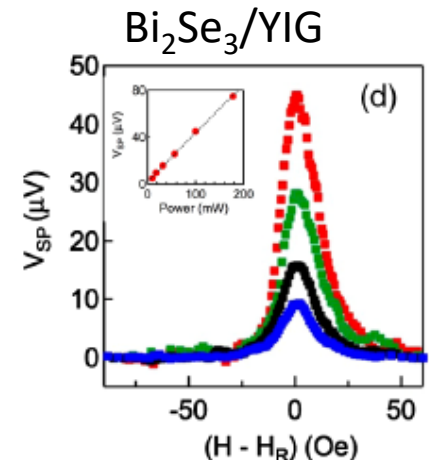
PRB **94**, 204404 (2016).

A. Fert group



PRL **116**, 096602 (2016).

N. Samarth group



PRL **117**, 076601 (2016).

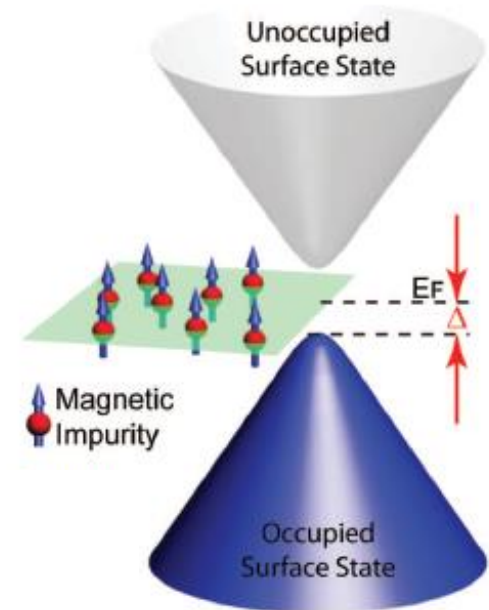
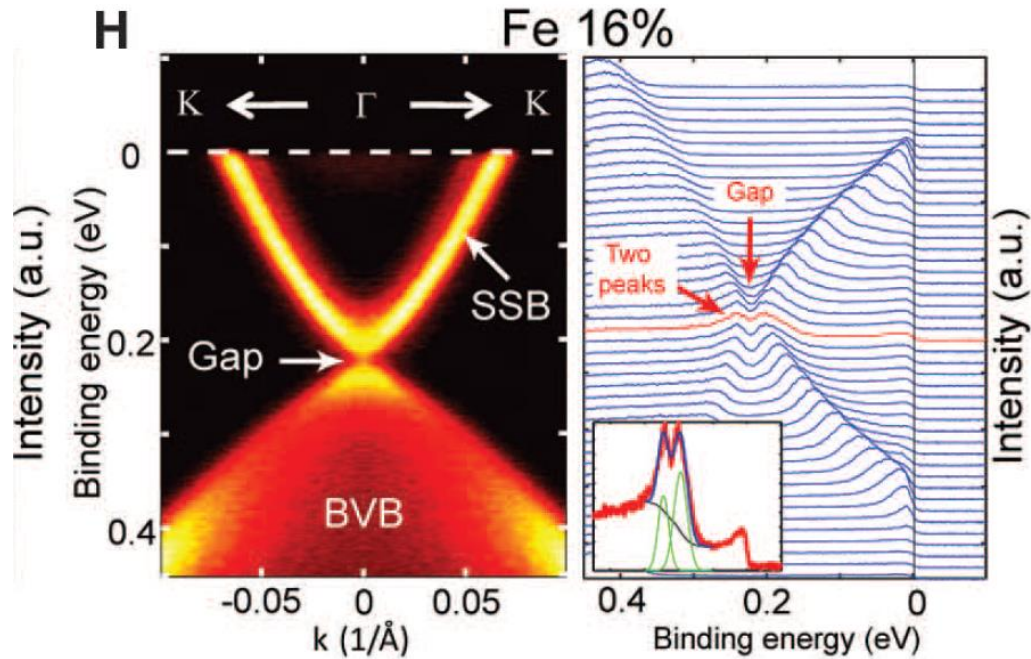
Challenges of spin pumping into TIs

- Bulk conduction of TIs obscures the effect of topological surface states
- Large variation in reported effective spin Hall angle θ_{SH}
 - **0.022** in Bi₂Se₃/Py at 15 K (Deorani et al. (2014))
 - **~10⁻⁴** in bulk insulating Bi_{1.5}Sb_{0.5}Te_{1.7}Se_{1.3} at 15 K (Shiomi et al. (2014))
 - **0.021-0.43** in Bi₂Se₃/CoFeB at RT (Jamali et al. (2015))
 - **0.27-0.62** in Fe/Ag/ α -Sn at RT (Rojas-Sánchez et al. (2016))
 - **~0.02** in Bi₂Se₃/YIG at RT (Wang et al. (2016))
- Current shunting effect by ferromagnetic metals in ST-FMR measurement
Ferrimagnetic insulator YIG with high thermal stability is an ideal spin source.

Breaking the time-reversal-symmetry of TI surface state

Experimental observations

1. Gap opening of TI surface states
2. Quantum anomalous Hall effect (QAHE)
3. Topological magnetoelectric effect



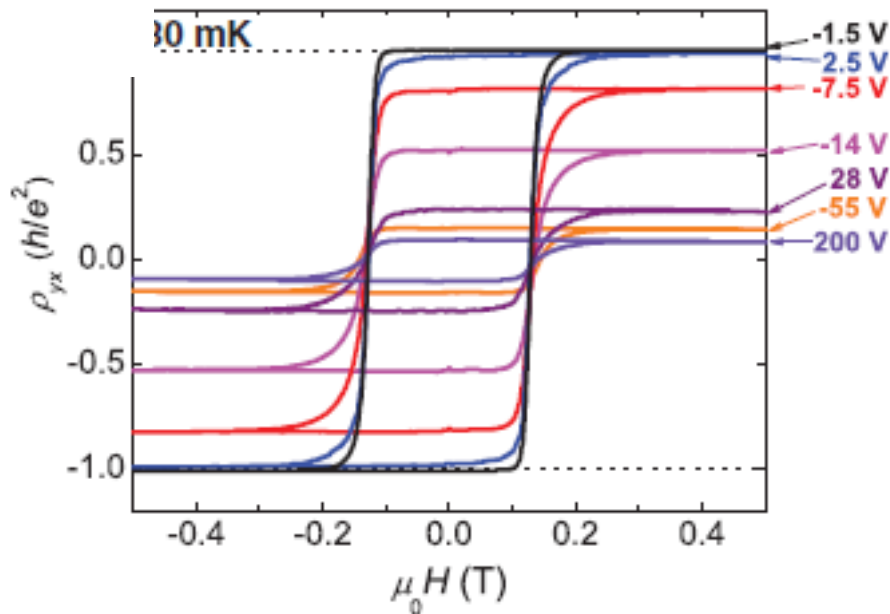
Chen et al., Science **329**, 659 (2010).

Breaking the time-reversal-symmetry of TI surface state

Experimental observations:

1. Gap opening of TI surface states
2. Quantum anomalous Hall effect (QAHE)
3. Topological magnetoelectric effect

Cr_{0.15}(Bi_{0.58}Sb_{0.12})_{1.85}Te_{3.7} at 30 mK



Quantum Hall effect without an external field!

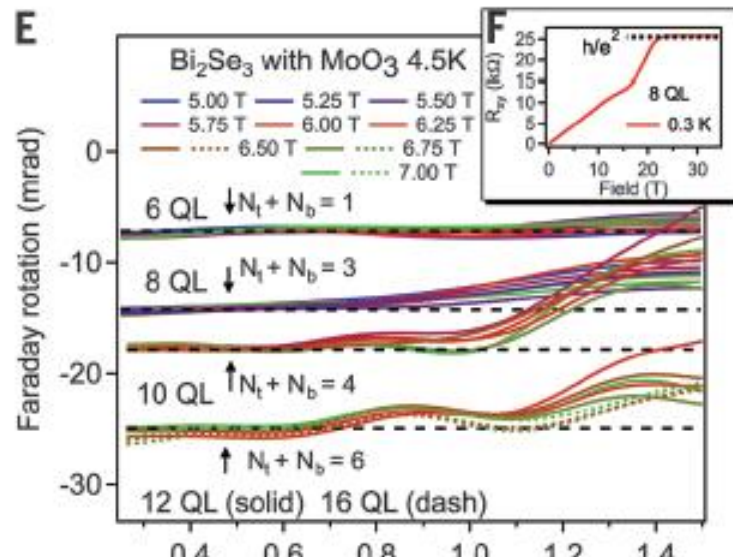
Chang et al., Science **340**, 167 (2013).

Breaking the time-reversal-symmetry of TI surface state

Experimental observations:

1. Gap opening of TI surface states
2. Quantum anomalous Hall effect (QAHE)
3. Topological magnetoelectric effect

Bi₂Se₃ at above 5 T field



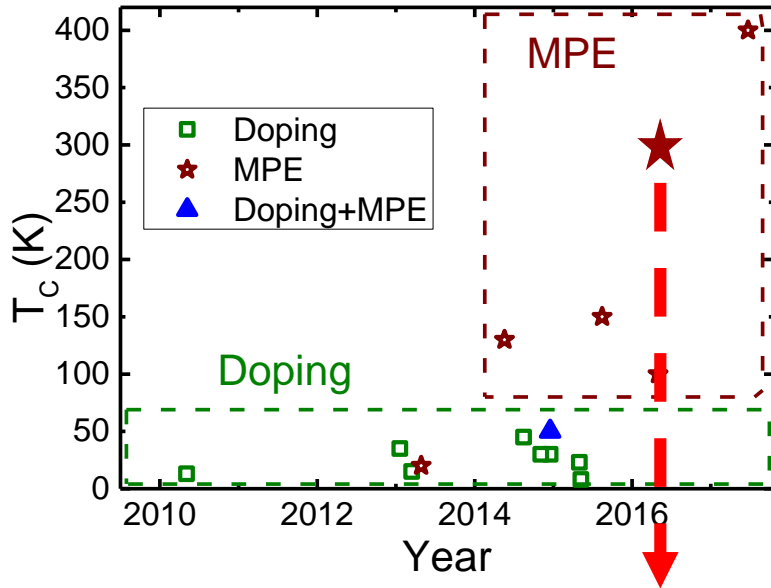
Wu et al., Science **354**, 1124 (2016).

Quantized Faraday rotation.

Other effective ways of breaking TRS aside from magnetic doping and high external field?

Magnetic proximity effect

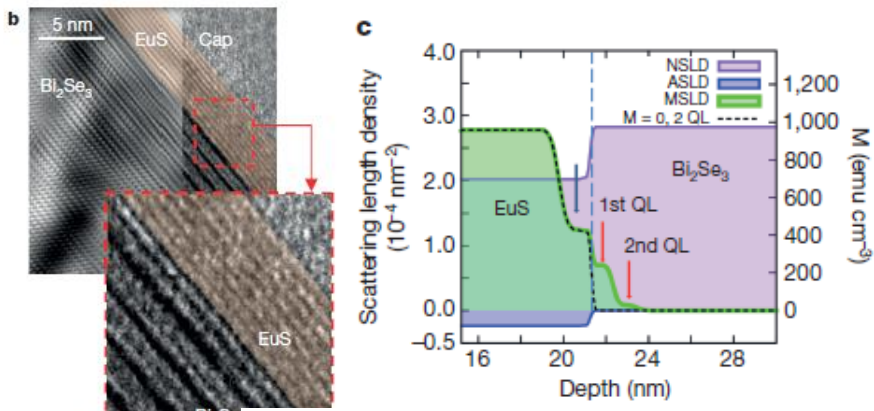
Magnetic proximity effect (MPE) in TI/magnetic layer heterostructures



Advantages of using the MPE to break time reversal symmetry:

- Higher T_C than that of magnetic doping
- No crystal defects
- Uniform magnetization

Discovery of RT MPE in EuS/Bi₂Se₃, exhibiting an interfacial PMA.



Katmis *et al.*, Nature **533**, 513 (2016).

How about MPE and the interfacial magnetic anisotropy in Bi₂Se₃/YIG?

High T IMA and low T PMA!

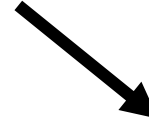
Our progress of spin pumping into TIs project (Mar. 2014 -)

Material development: FM/TI ($\text{Fe}_3\text{Si}/\text{TI}$, and Py/TI)
(2014. Mar. - Dec. 2014)

- Serious interdiffusion problem.
- Properties of FM is greatly altered.



Material development & optimization: TI/FI
(TI/YIG and TI/TmIG) (Jan. 2015 -)
Interdiffusion problem is relieved.



Results I and II

Magnetic anisotropy and proximity effect (Feb. 2016 -)

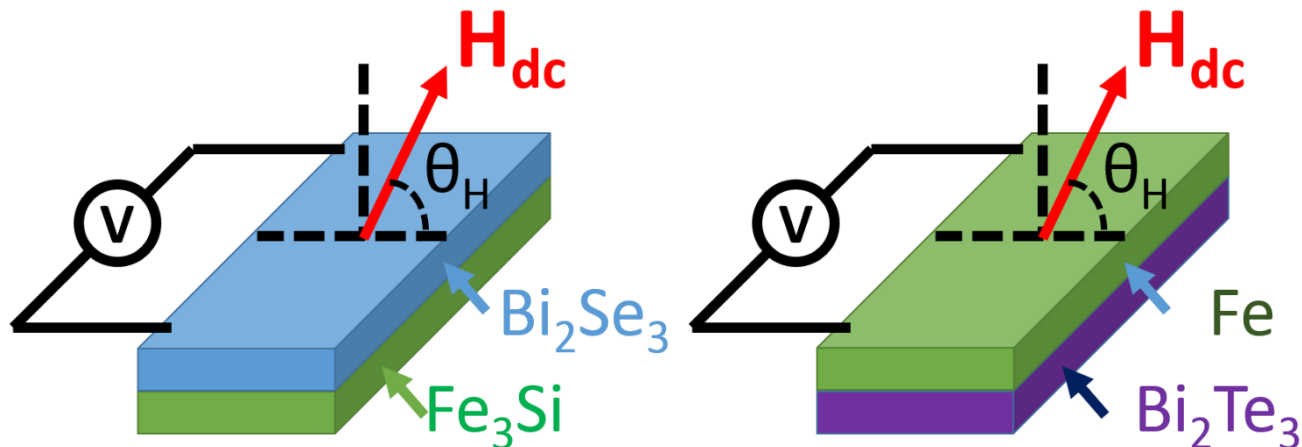
- Large in-plane magnetic anisotropy and large spin mixing conductance due to TSS
- Possible signature of MPE
- Enhanced exchange effect field at low T

Results I and III

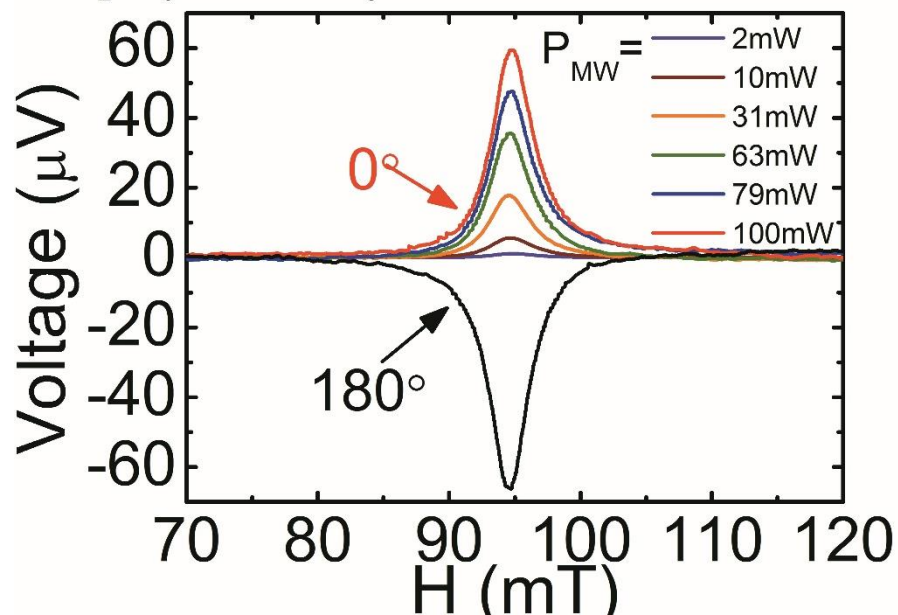
Spin pumping in to TIs (Jan. 2015 -)

Observed spin-to-charge conversion is small. **Goal: obtained sizable and more reliable voltage signals.**

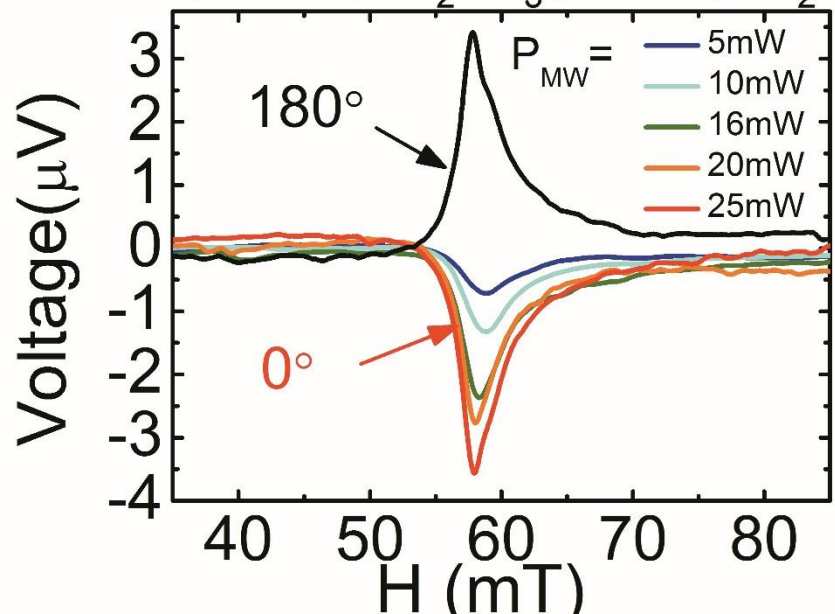
Spin Pumping in $\text{Bi}_2\text{Se}_3/\text{Fe}_3\text{Si}$ and $\text{Fe}/\text{Bi}_2\text{Te}_3$ Structures



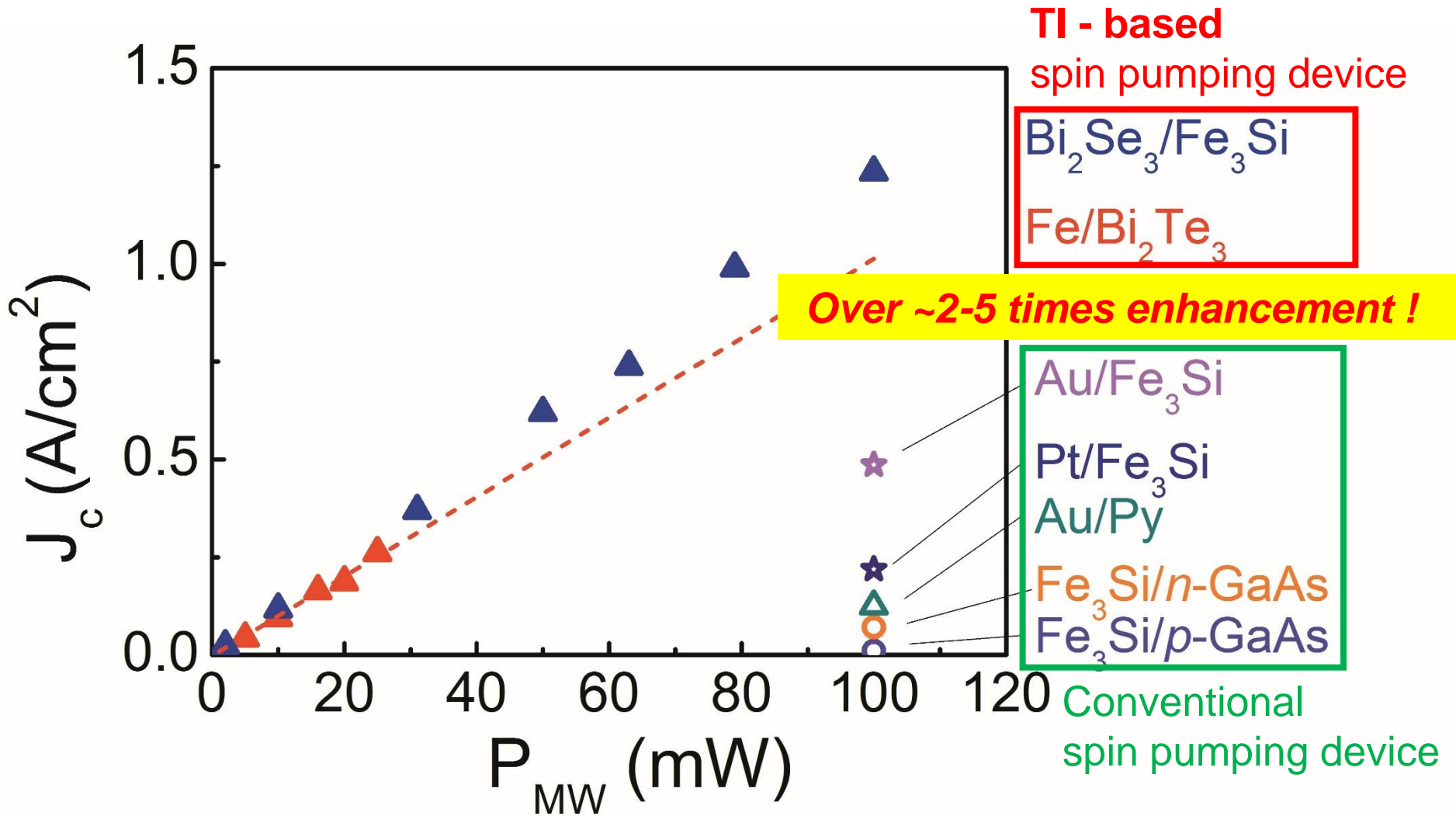
$\text{Bi}_2\text{Se}_3(10\text{nm})/\text{Fe}_3\text{Si}(10\text{nm})/\text{GaAs-S.I. (111)A}$



$\text{Fe}(10\text{nm})/\text{Bi}_2\text{Te}_3(10\text{nm})/\text{Al}_2\text{O}_3$



Potential Spin Battery Candidates: Converted Charge Current Density Comparison

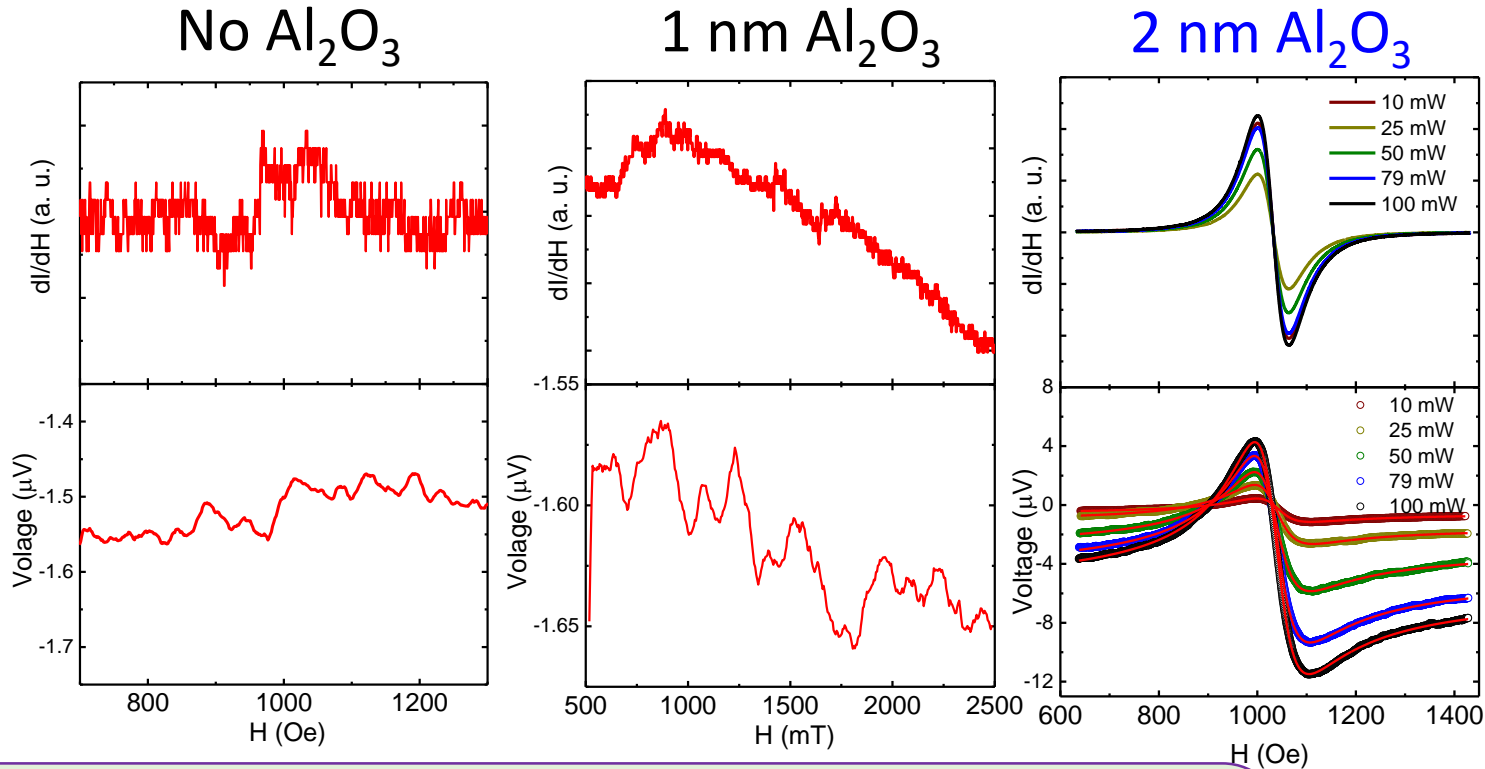


Comparison of θ_{ISHE}

NM (FM)	Spin mixing conductance (m^{-2})	Spin current density (Jm^{-2})	Spin Hall Angle θ_{ISHE}	J_c (A/cm^2)
Bi ₂ Se ₃ (Fe ₃ Si)	6.66×10^{18}	1.98×10^{-9}	0.0053 ± 0.002	1.32
Bi ₂ Te ₃ (Fe)	2.36×10^{18}	1.15×10^{-9}	0.0068 ± 0.003	1.00
<i>p</i> -GaAs(Fe ₃ Si)	5.89×10^{18}	8.91×10^{-10}	0.00019	0.0087
<i>n</i> -GaAs(Fe ₃ Si)	1.46×10^{19}	1.53×10^{-9}	0.000028	0.061
Au (Fe ₃ Si)	4.24×10^{18}	6.48×10^{-10}	0.00505	0.49

- ◆ Much larger spin current density and θ_{ISHE} than conventional spin pumping devices
- ◆ Comparable to $\theta_{ISHE} \sim 0.009$ from S. Oh et al
- ◆ Strong spin-charge conversion efficiency

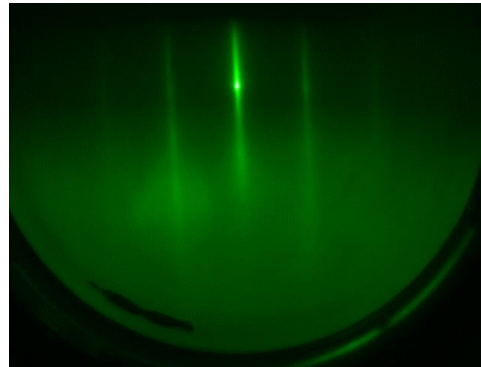
Using Al_2O_3 as a barrier layer to prevent interdiffusion



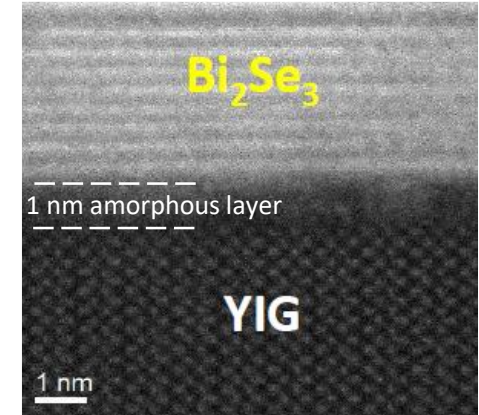
- ◆ Much larger spin current density and θ_{ISHE} than conventional spin pumping devices
- ◆ Comparable to $\theta_{\text{ISHE}} \sim 0.009$ from S. Oh et al
- ◆ Strong spin-charge conversion efficiency

Growth and structural characterization of $\text{Bi}_2\text{Se}_3/\text{YIG}$

◆ Streaky RHEED pattern

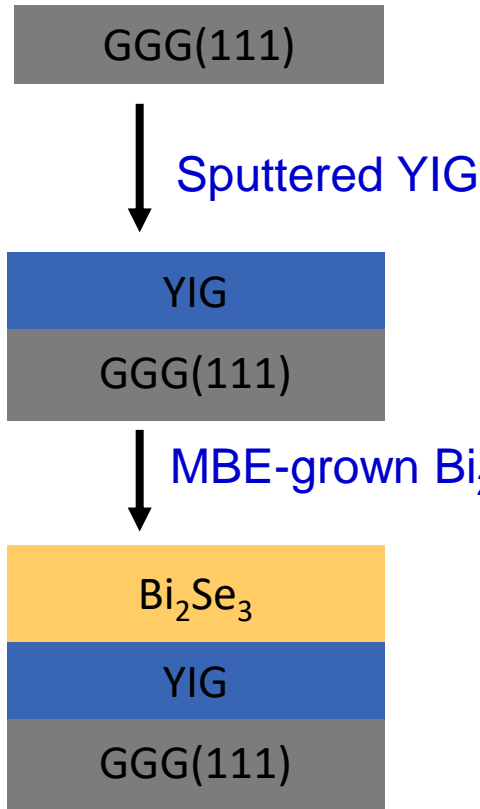
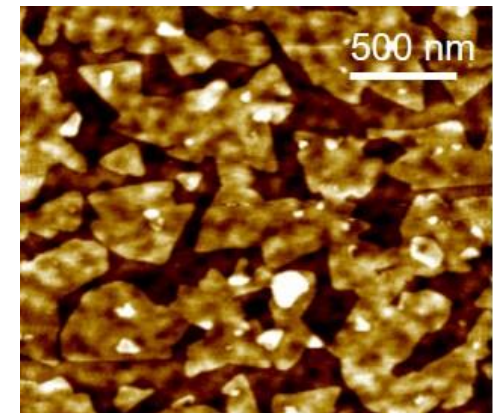
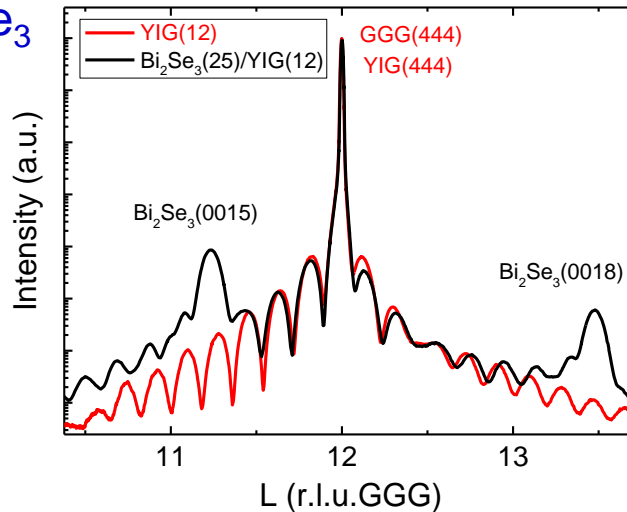


◆ 1 nm interlayer



◆ Excellent crystallinity

◆ High quality layer-by-layer growth

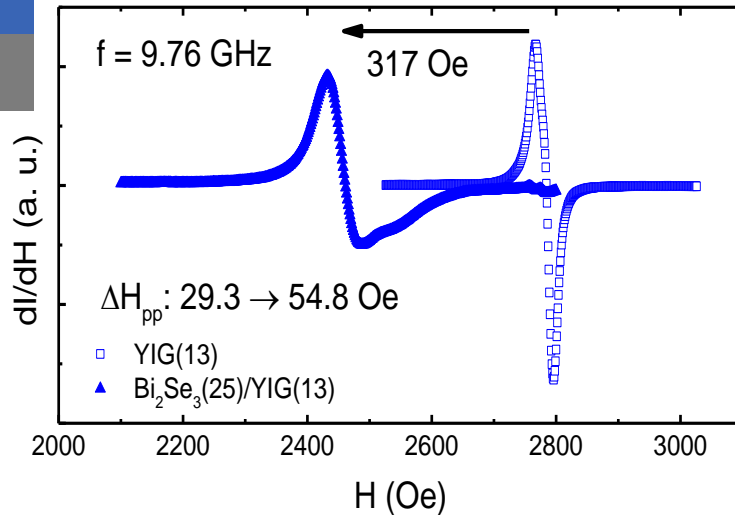


Magnetic anisotropy in $\text{Bi}_2\text{Se}_3/\text{YIG}$

25 nm Bi_2Se_3

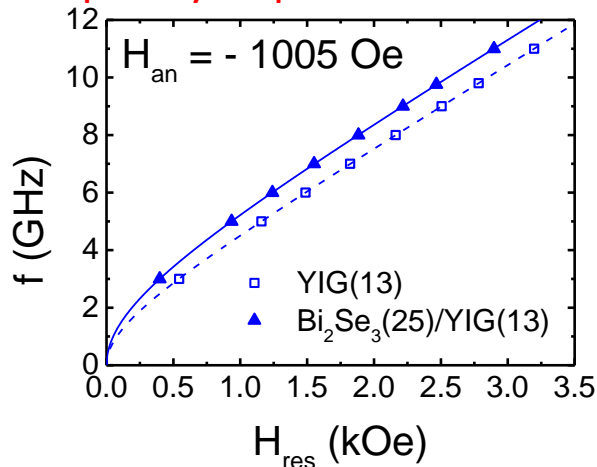
13 nm YIG

GGG(111)

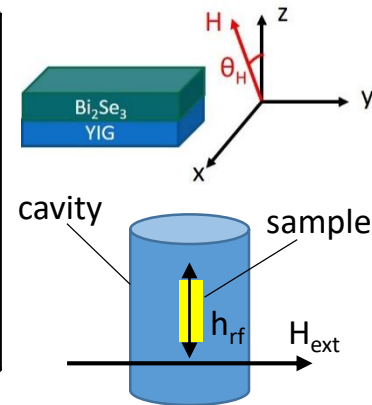
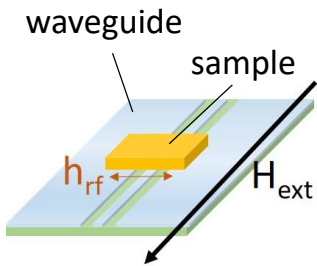
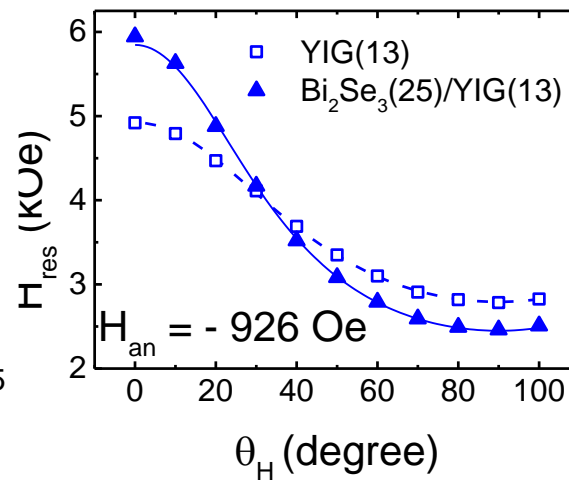


- Large H_{res} shift is observed after growing Bi_2Se_3 on YIG, due to change of magnetic anisotropy.
- Angle- and frequency-dependent FMR show an enhanced in-plane anisotropy introduced by Bi_2Se_3 .

Frequency-dependent FMR



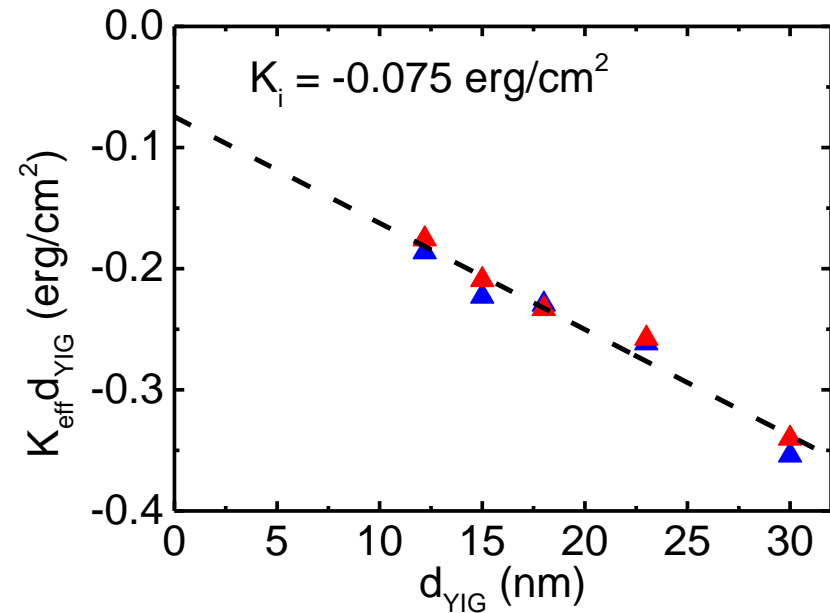
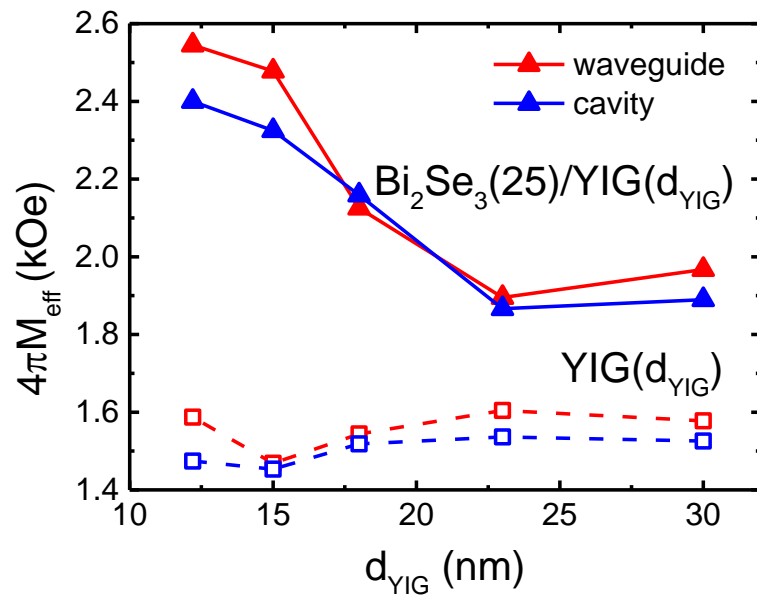
Angle-dependent FMR



Dr. S. F. Lee's lab
in Academia Sinica

Dr. J. G. Lin's lab
In NTU/CCMS

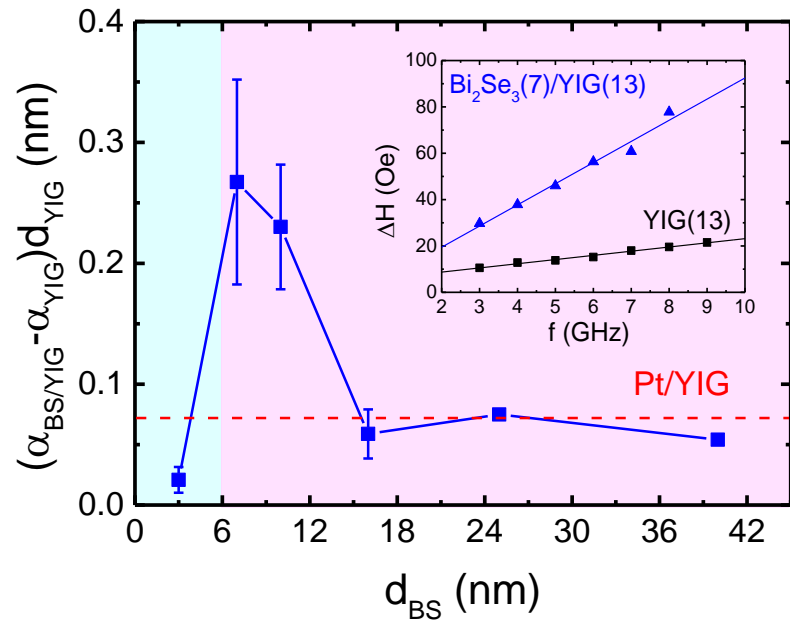
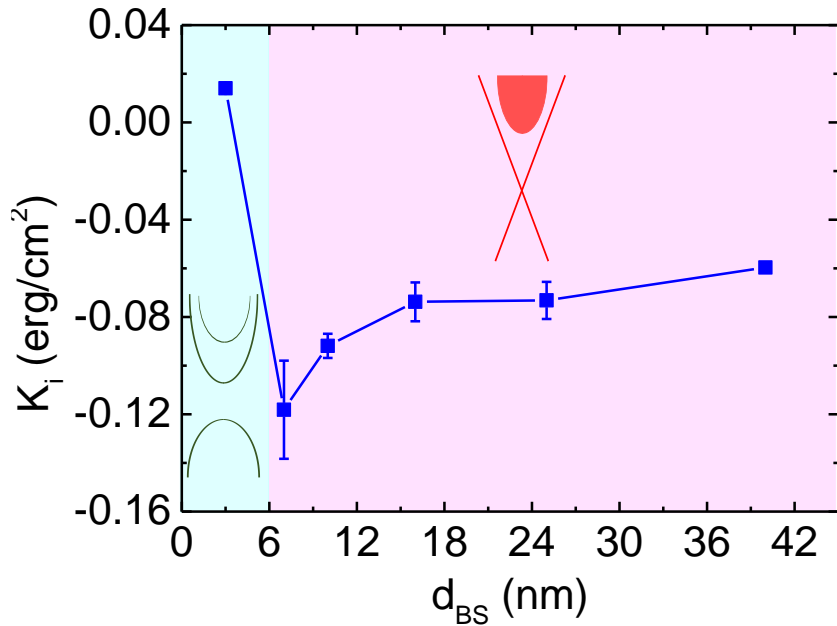
Interfacial magnetic anisotropy favoring in-plane direction



- The effective magnetization M_{eff} is larger in thinner YIG samples, which implies the change of anisotropy occurring at TI/YIG interfaces.

$$\begin{aligned}
 & 4\pi \left(M_{\text{eff}} (\text{Bi}_2\text{Se}_3/\text{YIG}) - M_{\text{eff}} (\text{YIG}) \right) \\
 &= -\frac{2}{M_S} \left(K_{\text{eff}} (\text{Bi}_2\text{Se}_3/\text{YIG}) - K_{\text{eff}} (\text{YIG}) \right) \\
 &= -H_{\text{an}} \\
 &\Rightarrow \frac{2K_i}{M_S} \left(\frac{1}{d_{\text{YIG}}} \right) = H_{\text{an}}
 \end{aligned}$$

Bi₂Se₃ thickness dependence of K_i and damping enhancement



- A. TSS can strongly enhance the magnetic anisotropy of the magnetic layer. (Kim *et al.*, Phys. Rev. Lett. **119**, 027201 (2017))
- B. Such unconventional thickness dependence might be related to the **topological surface states** of Bi₂Se₃.
- C. The normalized damping enhancement peaks near the **2D limit (6 nm)** of Bi₂Se₃, which is **3 times larger than that of Pt/YIG**.

Surface-state-mediated exchange coupling: theoretical aspect

PRL **119**, 027201 (2017)

PHYSICAL REVIEW LETTERS

week ending
14 JULY 2017

Understanding the Giant Enhancement of Exchange Interaction in Bi_2Se_3 -EuS Heterostructures

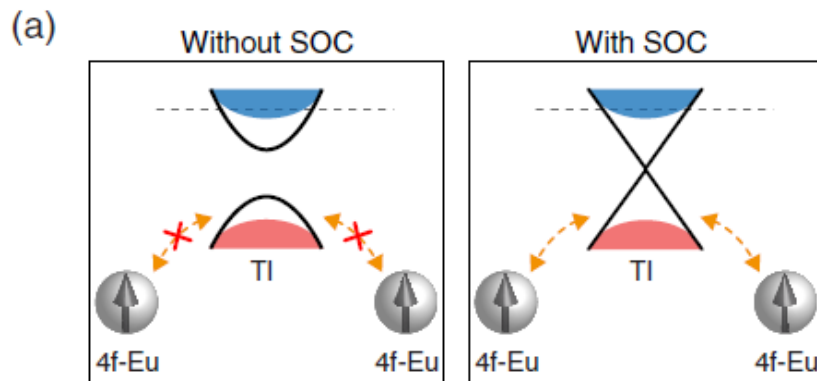
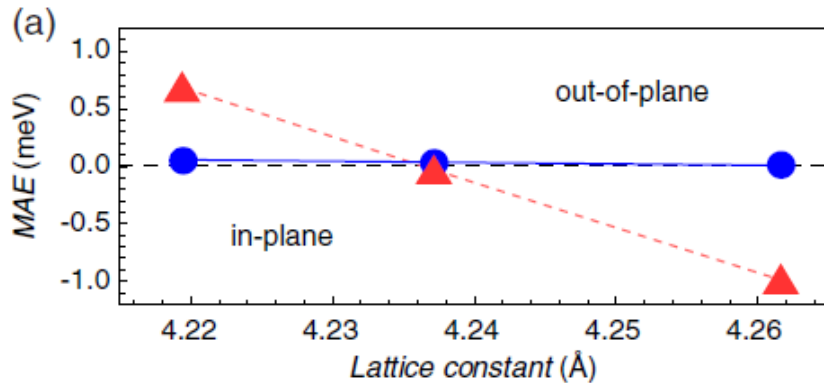
Jeongwoo Kim,¹ Kyoung-Wan Kim,² Hui Wang,¹ Jairo Sinova,^{2,3} and Ruqian Wu^{1,*}

¹Department of Physics and Astronomy, University of California, Irvine, California 92697, USA

²Institut für Physik, Johannes Gutenberg Universität Mainz, Mainz, 55128, Germany

³Institute of Physics, Academy of Sciences of the Czech Republic, Cukrovarnická 10, 162 53 Praha 6, Czech Republic

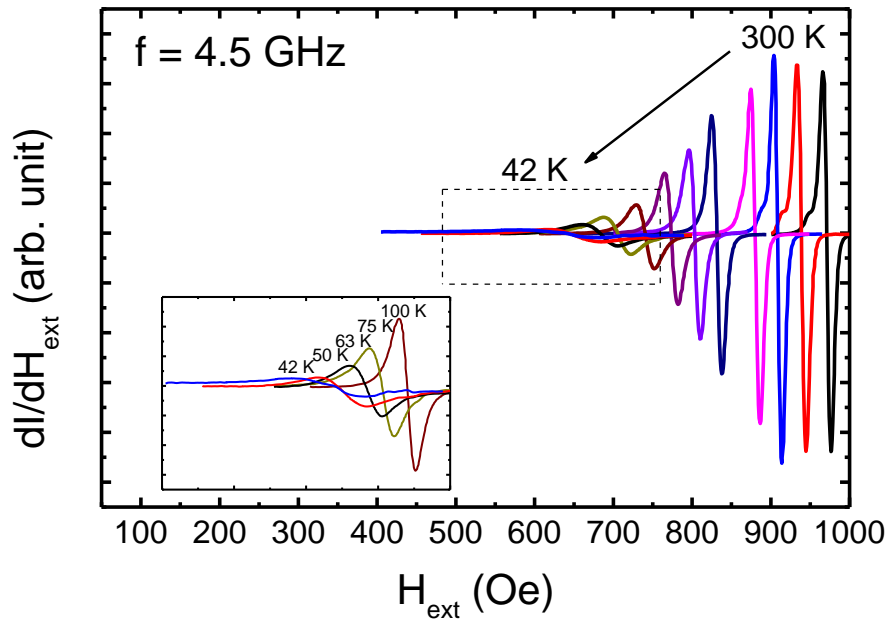
(Received 21 December 2016; revised manuscript received 22 March 2017; published 13 July 2017)



- A. The strong SOC of TI can enhance the magnetic anisotropy of the magnetic insulator.
- B. The sign of anisotropy may depend on **atomic structure at the interface**.
- C. The TI surface state **mediates the exchange coupling** of the magnetic ion of the magnetic layer.

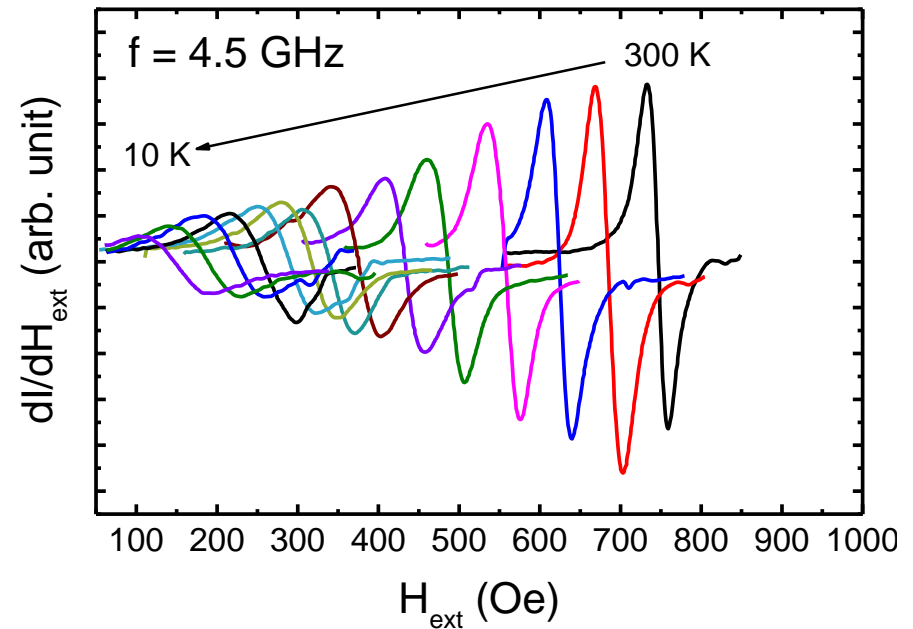
Temperature-dependent FMR of YIG and Bi₂Se₃/YIG

23 nm YIG



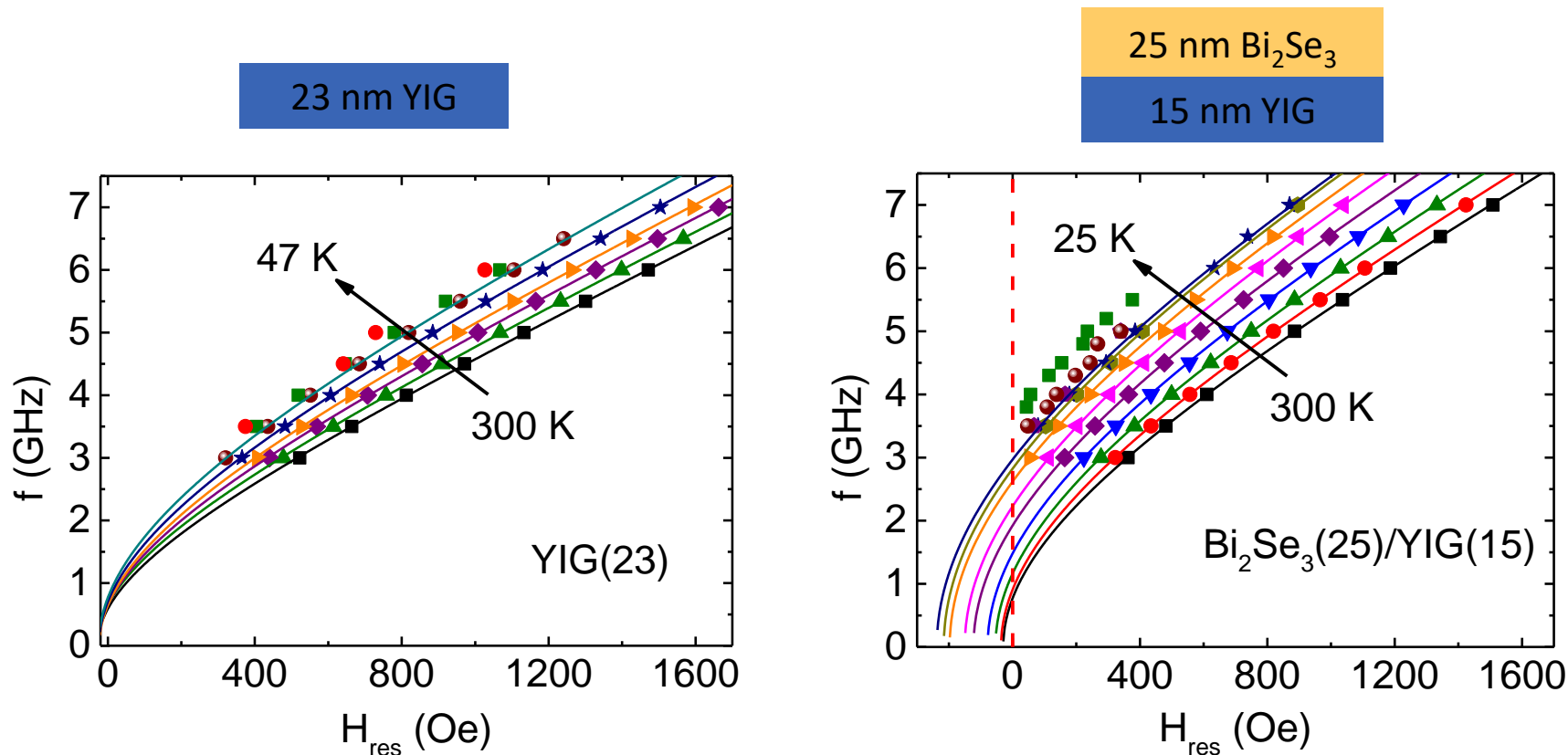
25 nm Bi₂Se₃

15 nm YIG



- Larger linewidth and damping \rightarrow smaller microwave absorption
- Increasing H_{res} shift at low temperature
- Less damping in Bi₂Se₃/YIG below 50 K

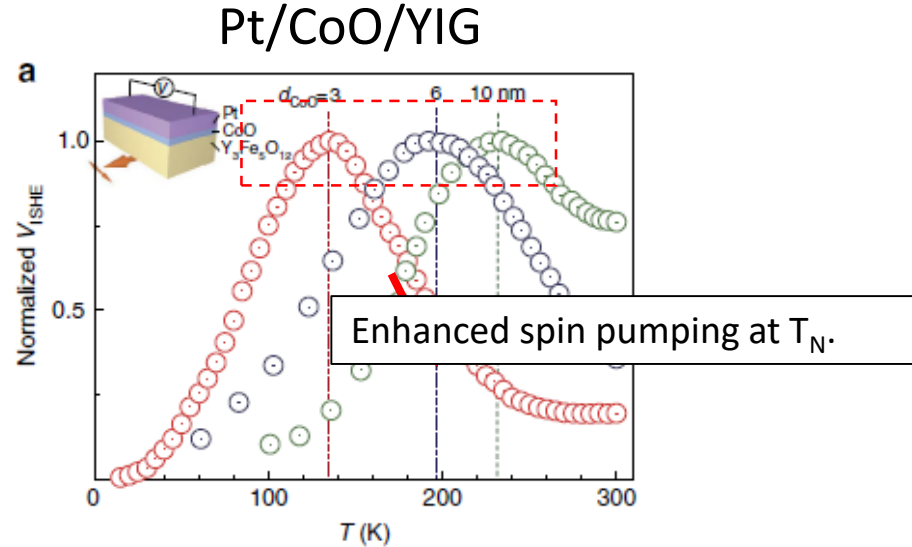
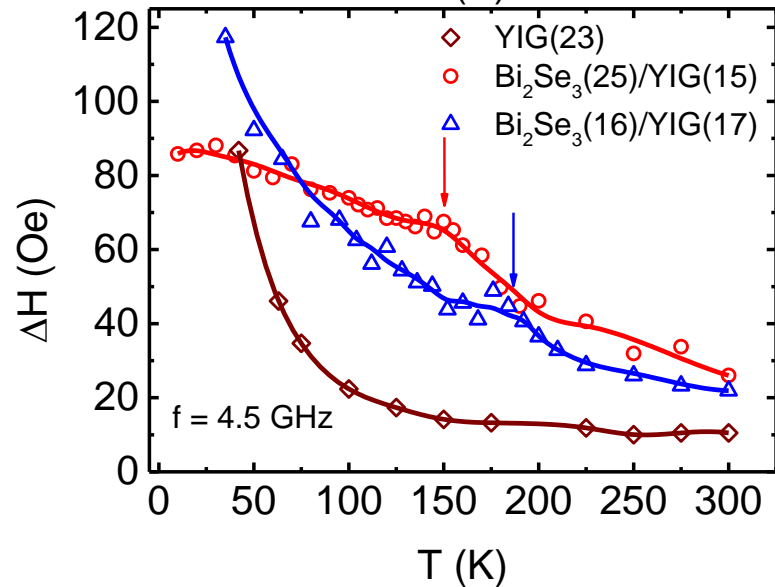
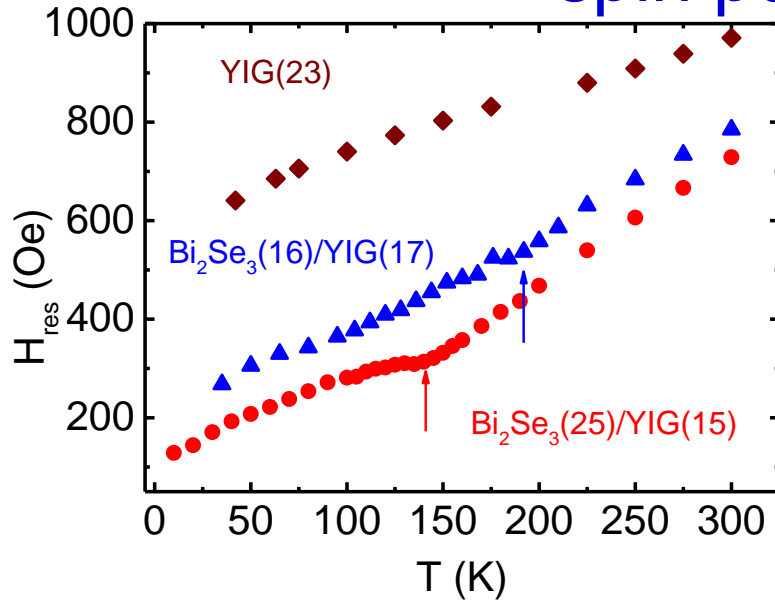
Temperature-dependent FMR of YIG and Bi₂Se₃/YIG



An effective field H_{eff} is necessary to fit the data.

$$f = \frac{\gamma}{2\pi} \sqrt{(H + H_{eff})(H + H_{eff} + 4\pi M_{eff})}$$

A possible indicator of MPE provided by spin pumping measurement



$$g_{\uparrow\downarrow} = \frac{8\pi J_{sd}^2 S_0^2 N_{int}}{\hbar^2 N_{SS}} \sum_k \frac{1}{\Omega_{rf}} \text{Im} \chi_k^R(\Omega_{rf})$$

χ_k^R : dynamical transverse spin susceptibility

Spin pumping is expected to enhance around T_C .
Magnetic proximity effect at 180 K?

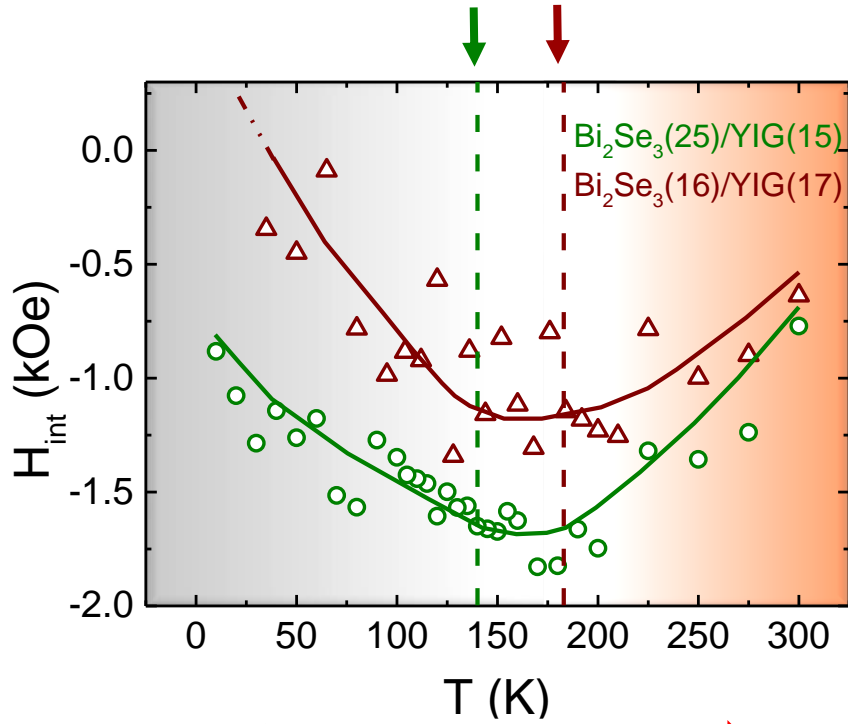
Ohnuma et al., PRB **89**, 174417 (2014).

Qiu et al., Nat. Comm. **7**, 12670 (2016).

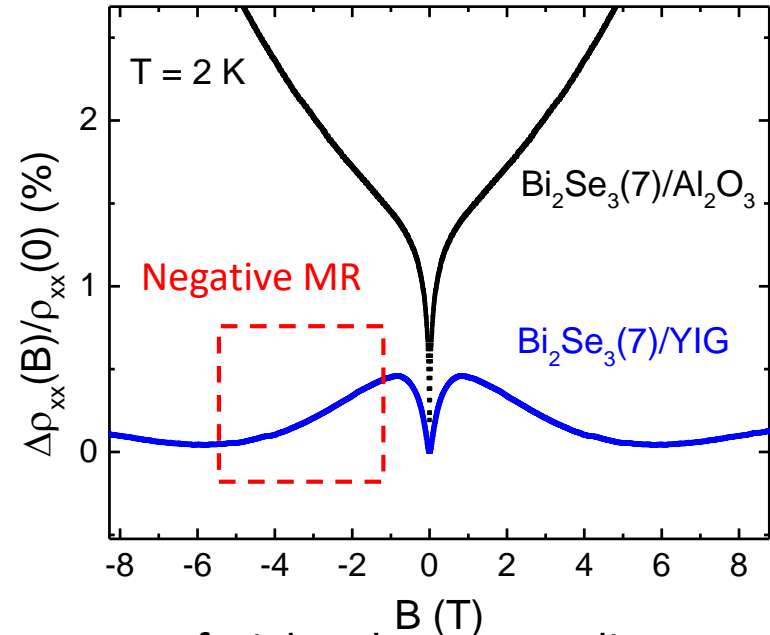
Frangou et al., PRL **116**, 077203 (2016).

Emerging low T PMA and negative magnetoresistance

"hump" temperature



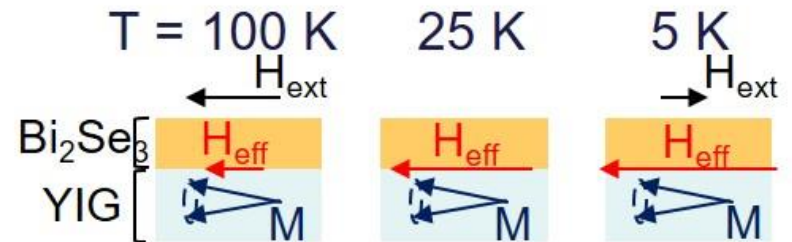
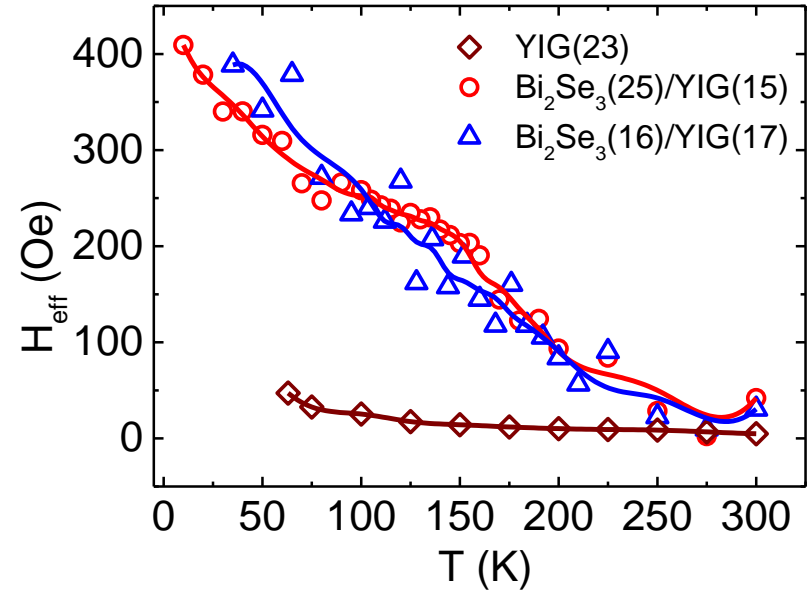
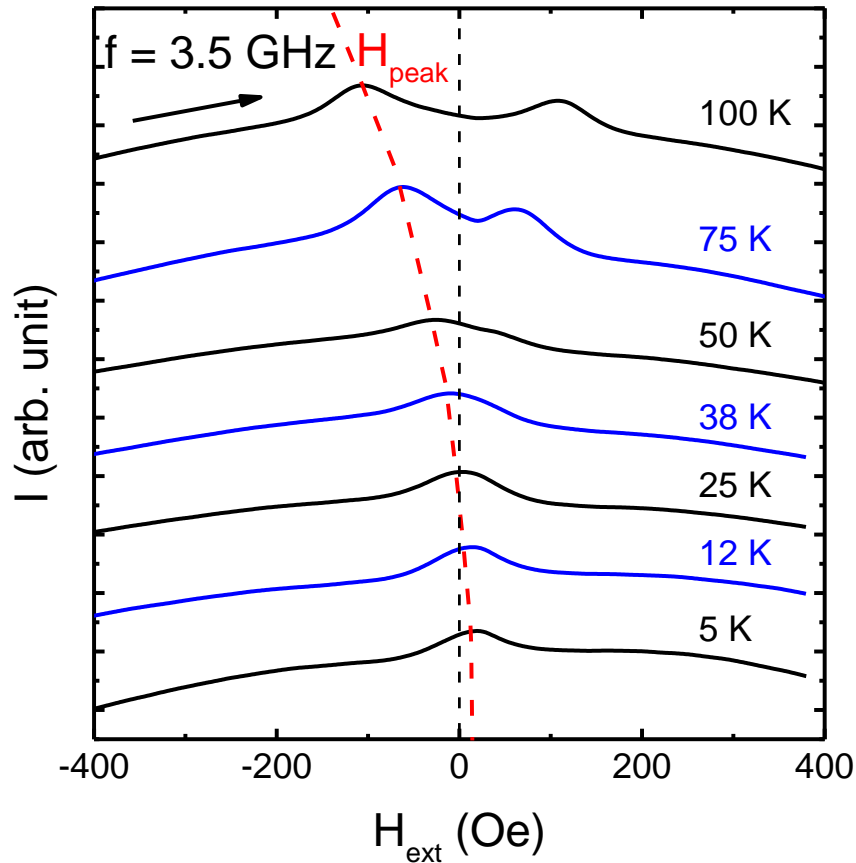
← IMA + competing PMA
→ High T IMA



- Interfacial exchange coupling
- Time-reversal-symmetry breaking
- Weak localization & Negative MR

Kim et al., PRL **119**, 027201 (2017).
 Lu et al., PRL **107**, 076801 (2011).

Internal effective field induced FMR without an applied field



- Internal effective field = $H_{\text{eff}} + H_{\text{an}} + 4\pi M_s$
- The exchange effective field H_{eff} becomes larger as T decreases.
- The strong H_{eff} has **great potential for spintronics application.**

Summary-1

- **Interfacial in-plane magnetic anisotropy** in $\text{Bi}_2\text{Se}_3/\text{YIG}$ is observed, and builds up as T decreases.
- **A unprecedentedly large spin mixing conductance ($2.2 \times 10^{19} \text{ m}^{-2}$)** for YIG systems was observed in $\text{Bi}_2\text{Se}_3/\text{YIG}$, implying an interface with **very efficient spin injection**.
- Temperature dependence of spin pumping in $\text{Bi}_2\text{Se}_3/\text{YIG}$ resembles that of antiferromagnetic CoO/YIG , suggesting **MPE with a T_c as high as 180 K**.